AWS TR 105-130

AIR WEATHER SERVICE TECHNICAL REPORT

A COMPENDIUM ON CIRRUS AND CIRRUS FORECASTING

Robert G. Stone

MARCH 1957

UNITED STATES AIR FORCE

AWS TR 105-130

AIR WEATHER SERVICE TECHNICAL REPORT

A COMPENDIUM ON CIRRUS AND CIRRUS FORECASTING

Robert G. Stone

MARCH 1957

UNITED STATES AIR FORCE

AWS TECHNICAL REPORT
No. 105-130

HEADQUARTERS
AIR WEATHER SERVICE
MILITARY AIR TRANSPORT SERVICE
UNITED STATES AIR FORCE
Washington 25, D. C.
March 1957

FOREWORD

1. Purpose. To provide a review of all available information on cirriform clouds ("High clouds") which should be useful from the operational, forecasting, and climatological points of view. At the same time, it is hoped this Report will create a greater awareness of the importance of the high-cloud problem and of some directions in which further investigation is especially needed to meet operational requirements.

2. Scope. This Report indicates the effects of cirrus on military operations, and notes the requirements for forecasting cirrus. Details are reviewed as to observing problems, forms of cirrus, physical constitution of cirrus, their modes of formation, thickness, distribution with height, season, area, and relation to various other meteorological conditions. Visibility values, optical and electrical phenomena, icing, and turbulence in cirrus are discussed. The various methods proposed for forecasting high clouds are reprinted from original sources, and opinions as to their probable practical value expressed. Considerable data of a climatological sort are included, including heretofore unpublished tabulations based on Project Cloud-Trail, which should be useful both in operational planning studies and in forecasting.

3. Acknowledgments. The Sandia Corporation has kindly granted permission for the reprinting herein of its report by Kendrick on a method of cirrus forecasting. Lt. Cdr. W. L. Somervell of Navy Project AROWA and Mr. Roy Endlich of AF Cambridge Research Center have generously furnished information from their yet unpublished studies.

4. Additional Copies. This Report is stocked at Headquarters MATS, Command Adjutant, Publishing Division. Additional copies may be requisitioned from Headquarters Air Weather Service, ATTN: AWSAD, in accordance with AWSR 5-3.

Approved:

HAZEN H. BEDKE
Colonel, USAF
Acting Director, Scientific Services

DISTRIBUTION:
"D" (less the 20% overage for stock)
plus "Z"

TABLE OF CONTENTS

		Page
1.0.	Operational Importance.	1
1.1.	Forecasting of Cirrus	1
2.0.	Nature of Cirrus.	2
2.1.0.	Forms, Classification	2
2.1.1.	Genera.	2
2.1.2.	Species	3
2.1.3.	Varieties	4
2.1.4.	States-of-Sky Code.	4
2.1.5.	Explanation of Forms.	5
2.1.6.	Surface vs Pilot Observations	5
2.1.7.	Stratification.	5
2.1.8.	Relation with Middle Clouds	6
2.1.9.	The Arrangement of Cirrus	6
2.2.0.	Physics of Formation.	7
2.2.1.	Ice-Nucleation Experiments.	7
2.2.2.	Observed Cloud Constitution	8
2.2.3.	Nuclei.	8
2.2.4.	Saturation Requirements	8
2.2.5.	Speed of Cooling.	9
2.2.6.	Crystal Types a. . Cirrus Types.	10
2.2.7.	The Concentration of Cirrus Particles . . .	10
2.2.8.	Persistence of Cirrus	11
2.2.9.	Fallstreaks and Shred-Clouds.	11
2.2.10.	Optical Phenomena	14
2.3.	Relations to Contrails.	15
2.4.	Turbulence in Cirrus.	15
2.5.	Icing in Cirrus	15
2.6.	Visibility in Cirrus.	16
2.7.	Electrical Effects.	16
2.8.	Nacreous Clouds	17
3.0.	Occurrence and Climatology of Cirrus.	17
3.1.0.	Heights	17
3.1.1.	International Cloud Year Data	18
3.1.2.	Potsdam Photogrammetry.	19
3.1.3.	British MWP Data.	19

TABLE OF CONTENTS (Cont'd)

		Page
3.1.4.	Project Wiback Data	21
3.1.5.	Project Cloud Trail	22
3.1.6.	RCAF Flight Data	24
3.1.7.	Estimates from Contrail-Formation Curves	27
3.2.	Thickness	29
3.3.0.	Frequency	33
3.3.1.	Ground Observations	33
3.3.2.	Observations from Aircraft	33
3.3.3.	Radar Observations	35
3.4.	Orographic Cirrus	36
3.5.	Tropical Cirrus	36
3.6.	Polar Cirrus	37
4.0.	The Cirrus Forecasting Problem	38
4.1.0.	Parameters Which Have Been Correlated with Cirrus Occurrence or Formation	38
4.1.1.	Surface-Pressure Pattern	40
4.1.2.	Fronts Aloft	42
4.1.3.	Contour or Flow-Direction Aloft	44
4.1.4.	Contour Patterns Aloft	45
4.1.5.	Vorticity Advection at 300 mb	46
4.1.6.	Pressure or Height Change Aloft	47
4.1.7.	Temperature Aloft	47
4.1.8.	Temperature Change Aloft	51
4.1.9.	Thickness	52
4.1.10.	Thickness Advection	54
4.1.11.0.	Tropopause	54
4.1.11.1.	Cirrus in the Stratosphere	60
4.1.12.	Wind Shear	61
4.1.13.	Lapse Rate	63
4.1.14.	Vertical Motion	67
4.1.15.	Humidity	67
4.1.16.	Jet Stream	70
4.2.0.	Forecasting High Clouds From High-Level Constant-Pressure Charts, by J. E. French and K. R. Johannessen	79
4.3.0.	A Method of Forecasting Cirrus Clouds, by Captain Hyko Gayikian	96

TABLE OF CONTENTS (Cont'd)

		Page
4.4.0.	An Approach to the Problem of Cirrus-Cloud Forecasting, by R. L. Hendrick.	105
4.5.0.	An Objective Method of Local Forecasting of Cirrostratus Clouds, by H. Appleman	120
4.6.	Suggestions for Further Study	131
5.0.	Summary and Conclusions	131
APPENDIX A	Study of Cirrus Climatology from Data Taken on Project Cloud Trail	136
REFERENCES	. . . . .	151

Guide for Using This Report

The paragraphs of this Report are written so that to a large extent they can be read and understood independently of one another; however, specific cross-references are made so that no information on a given topic will be overlooked. The following brief index will also provide a quick reference to material on any of the listed subjects:

Subject	Paragraph Numbers (Pages)
Summary and Conclusions of Report	5.0 (131).
Forecasting Methods (Complete):	4.0 (38), 4.2 (79), 4.3 (96), 4.4 (105), 4.5 (120).
Forecasting Aids or Rules for:	
Cirrus Height	3.1.6 (24), 3.1.7 (27), 4.1.11.0 (54), 4.1.13 (63), 4.1.16 (70), 4.3.3 (103).
Cirrus Density	2.6 (16), 4.3 (96).
Cirrus Occurrence	3.1.6 (24), 4.1 (38), 4.2 (79), 4.3 (96), 4.4 (105), 4.5 (120).
Visibility in Cirrus	2.6 (16).
Synoptic Factors in Cirrus Formation or Occurrence	3.4 (36), 3.5 (36), 3.6 (37), 4.0 (38), 4.1 (38).
Physical Factors in Cirrus Formation	2.2 (7).
Types and Forms of Cirrus	2.1 (2), 2.2.5 (9), 2.2.6 (10), 2.2.9 (11), 3.4 (36), 3.5 (36), 3.6 (37), 4.3 (96).
Cirrus in Tropical Regions	3.5 (36).
Cirrus in Polar Regions	3.6 (37).
Associated Phenomena	2.2.7 (10), 2.2.10 (14), 2.3 (15), 2.4 (15), 2.5 (15), 2.6 (16), 2.7 (16), 3.6 (37).
Observational Problems	2.1.1 (2), 2.1.2 (3), 2.1.3 (4), 2.1.4 (4), 2.1.6 (5), 2.2.10 (14), 3.1 (17), 3.3 (33), 3.5 (36), 3.6 (37).
Observational Data (Climatology)	2.1.4 (4), 2.1.8 (6), 2.6 (16), 3.1 (17), 3.2 (29), 3.3 (33), 4.1 (38), 4.2 (79), 4.5 (120), Appendix A (136).

A COMPENDIUM ON CIRRUS* AND CIRRUS FORECASTING

1.0. Operational Importance.

Until recent years cirrus* clouds were mostly a scientific curiosity and something of a mystery as well. As long as meteorologists could not reach them for direct observations, knowledge of cirrus clouds was confined to speculative inferences about the physical and synoptic processes involved. A practical interest was expressed only in the attempts to correlate occurrence of cirrus (or their haloes) with later surface weather, as an aid in local or single-station forecasting [11].

In World War II cirrus sometimes interfered with visual bombing and photo-reconnaissance from high altitudes [1] [2]. By 1945 it was evident that cirrus would be troublesome to jet, rocket, and guided-missle operations [2]. The horizontal visibility at high levels is frequently so poor in cirrus that aircraft cannot rendezvous or refuel there. Aircraft and guided missiles using celestial navigation may be hampered by cirrus obscuring sun, moon, or stars. High-level navigation when not impossible is generally precarious, in part due to cirrus. Pilots flying at cirrus levels in aircraft without navigational-weather radar or ground control risk collision with other aircraft or running into thunderstorms obscured by the cirrus. At proving grounds optical tracking of rockets or missiles fired vertically (for maximum height soundings) is prevented by a cirrus deck of sufficient thickness and extent. Use of day-fighters for high-level intercept may be greatly limited by extensive cirrus layers.

1.1. Forecasting of Cirrus. It is now expected of certain weather detachments that cirrus or cirrostratus coverage and heights be forecast. This poses difficulties owing to the lack of proven techniques of universal applicability and even more to inadequacies of synoptic cirrus observations and of upper-air soundings. The following sections will review such available knowledge about high clouds as may be of

---

* We will often use the term "cirrus" in this Report to designate all cirriform types collectively. However, in standard cloud-observation practice the term is used in the more restricted sense of detached fibrous clouds ("fine cirrus") as distinct from cirrostratus and cirrocumulus. The context in this Report will make it clear which sense is meant.

assistance to the forecaster, including results of some recent heretofore unpublished AWS studies. Information useful for climatological estimates is also included.

2.0. Nature of Cirrus.

2.1.0. Forms, Classification.

2.1.1. Genera. The broad grouping of cirrus into three "Genera" [33] [67]: cirrus, cirrostratus, and cirrocumulus, is of long standing (Luke Howard, 1803). It recognizes the main apparent distinctions as seen from the ground. Whether a sharp distinction between cirrus proper (detached filaments) and cirrostratus (fibrous veils) is justified on the basis of physical constitution, mode of formation, etc., is open to question. Some descriptions by pilots, for example, would indicate that the cirrostratus is often composed of large numbers of bands of the filamentous type of cirrus, overlapping in many layers or intertwining and extending through great and variable vertical distance. Thus, the uniform-stratiform aspect of much cirrostratus may be illusory, and at least some cirrostratus must be considered as a cloud of very variable density differing from cirrus only in the closer spacing of the filaments or layers. Frequently, the early stages of cirrostratus are merely detached cirrus which gradually "fills in" to make an extensive layer (see paragraph 2.2.5). In other cases, however, cirrostratus evolves from thickening of a widespread cirrus veil or haze.

Cirrocumulus is more distinct in character, often probably a water-droplet or "mixed cloud," lower than most Ci and Cs, and much like Ac in many respects, though (by definition [67]) it generally should be connected with other kinds of cirrus, except in the tropics. We need not be much concerned about it, for it is rather uncommon in most regions.

The difference between cirrostratus and altostratus is the most troublesome one for observers, forecasters, and cloud physicists alike. It will become apparent upon studying the information in ensuing paragraphs (especially paragraphs 2.1.8, 2.2, and 4.1.2) that in truth there exists in Nature every gradation from cirrostratus as a purely ice-crystal high-level stratiform deck to the purely water-cloud stratus of lower-middle levels. In middle and higher latitudes what is correctly reported as altostratus is frequently a predominantly ice

or snow*-and-graupel cloud, especially in its upper part [67] [50]. The instructions to observers [67] require that Cs be transparent to the sun or moon and whitish (except when sun is very low), whereas As is grayish or dark and denser than Cs, so that the position of the sun is only vaguely revealed in spots and often appears as through a ground glass even at high solar elevations. Evidently these criteria do not discriminate well between an ice-crystal and a water cloud. When halo is present, the observer must of course report Cs, but many true Cs do not show a halo; nor is there any opportunity to apply this criterion on moonless nights or with very low sun. (Likewise, many As clouds do not show a corona.) Because of this situation, a number of prominent meteorologists have questioned the value of the traditional observational distinction between these two cloud types. However, the WMO has upheld their continued use, at the same time recognizing their integradation in certain physical characteristics [67]. The distinction is practicable and perhaps useful as long as one does not concentrate on "splitting hairs" among the borderline cases. (See paragraph 2.1.8.)

2.1.2. Species. The latest classification of "Species" of clouds adopted by the WMO [67] recognizes the following as often applicable to cirrus or cirrostratus:

fibratus – fine, linear or irregular detached Ci filaments ("hair-like"), or thin striated veils (former filosus)

uncinus – upward-hooked Ci filaments often tufted at top (includes most cirrus "fallstreaks," see paragraph 2.2.9)

spissatus – dense white or gray Ci or Cs patches or entangled sheaves, may be fibrous at edges (including remains of thunderstorm tops, and "shred clouds"? – see paragraph 2.2.9) (former Ci densus, and Ci nothus)

nebulosus – nebulous Cs veil without fibers or patches ("cirrus haze").

* "Snow Crystals" are usually considered to be the types of ice crystals characteristic of precipitation reaching the ground. They are generally large and complexly dendritic in pattern, the result of growth by rapid sublimation in water or mixed clouds at temperatures in the 0° to -30°C range. "Ice Crystals" of the cirrus type are much smaller and simpler in form: prisms, plates, needles, and pillars; they are more apt to form and persist as such at temperatures below -30°C.

(Floccus, cirrillanus, stratiformis, and lenticularis may also occasionally apply.)

2.1.3. Varieties. For the minor "Varieties," [67] recognized as often applicable to cirrus or cirrostratus:

vertebratus – herringbone structure in Ci or Cs

radiatus – parallel broad bands, appearing to converge towards the horizon (Ci)

intortus – very chaotic or twisted Ci filaments (includes twisted fallstreaks)

duplicatus – double- or multi-layered (Ci or Cs)

undulatus – elongated parallel bands, like waves

2.1.4. States-of-Sky Code. Some of the above-mentioned "Species" are used in defining certain States of The Sky reported in International Synoptic Code for $C_H = 1$, $C_H = 2$, $C_H = 3$, and $C_H = 4$. This reflects a belief in the synoptic diagnostic significance of these Species, a belief which rests, however, on very subjective grounds (see paragraph 4.1.1). (Very little formal and conclusive investigation has been made of particular cirrus forms in relation to either synoptic or physical factors – see paragraph 2.1.5.) Since many cirrus species are commonly observed together in the same sky, it is not likely that any one individual form could be critically diagnostic of the large-scale synoptic processes aloft.

The WMO instructions for cloud observing [67] emphasize the importance of carefully watching the evolution of the cloudscape, because a knowledge of the genetic (sequential) interrelationships of the cloud forms is often necessary to correctly identify the species (and even some genera) in accordance with the WMO definitions. Many observers fail to do this properly. However, this deficiency is generally ignored in regions of ample upper-air soundings, where forecasters are seldom inclined to fully interpret the supposed genetic meaning of all the cloud distinctions reported. There is need for the development of special high-level "State of Sky" specifications which would be based on a study of time-lapse photos or motion-picture observations and aircraft operational criteria rather than on the totality of visual aspects, many of which are probably of no practical significance. Different combinations of certain cirrus varieties might be found thus to

have a useful correlation with synoptic and operational parameters.

Empirical models of the evolution of the state of sky in typical disturbances may also be useful as an aid in analysis or forecasting (see paragraphs 3.5 and 4.1.1) [11]. There is little incentive for their development except in regions lacking sufficient synoptic ground and upper-air reports.

2.1.5. Explanation of Forms. Schwerdtfeger, Weickmann, and Ludlam have pointed to some evidence of relations between the forms of cirrus, their microphysics (see paragraph 2.2), and synoptic processes (see paragraph 4.1). Such knowledge might be useful in single-station forecasting without soundings [11].

2.1.6. Surface vs Pilot Observations. Observations of cirrus made from the ground are subject to serious limitations. This is primarily because of obscuration by lower clouds, fog or haze, and at night when thin cirrus may be entirely overlooked. However, even under the best observing conditions the appearance of cirrus from the ground may give little indication of its character as seen by a pilot nearer to or in the cloud [46] [36] [23]. Frequently as the pilot climbs under "clear sky" the amount of visible cirrus seems to increase markedly, especially once he is on top of the low-level haze layer. The vertical visibility in cirrus is often quite good (ground visible) at the same time that horizontal visibility is less than a mile. To the pilot flying in cirrus it appears as a whitish haze. It may even be difficult for him to tell whether he is in cirrus or not, especially in the bases of the patches and filaments which, though appearing distinct from the ground, are actually very ill-defined where they thin out downward. On the otherhand, sometimes the pilot can see no evidence of cloud when he is flying in what appears from the ground as thin cirrus. Often, patches or bands seen as isolated from the ground are merely the denser portions of a widespread sheet of cirrostratus (cf. paragraph 2.1.1). The tops, which are usually denser than the bases, are more easily recognized. It is reported that the tops may be very smooth, rounded, or wave-like [37] [34], similar to tops of stratus or Ac; short non-persistent streaks and wisps may emerge from the tops here and there [37]. Some pilots have even noted that tops frequently coincide with bases of temperature inversions (tropopauses? -- see paragraph 4.1.12).

2.1.7. Stratification. Layering of the upper clouds (and haze)

is more pronounced than surmised from ground observations. Pilots note that the cirrus is often many-layered — aufm. Kampe [37] and Weickmann [65] found the most frequent thickness of individual layers (thin veils) was less than 200 or 300 m, (though a secondary maximum occurs around 2000-3000m). Project Cloud Trail data show a predominant thickness of around 500-2000 feet (see Appendix and paragraph 3.2). This layering becomes very sharp in mountain-wave situations [65]. Cirrus stratification is readily understood in light of the fine-structure in the vertical humidity distributions revealed by sensitive hygrometer soundings [6] [12] [17] [45] (see paragraph 4.1.15). The under-regions of cirrus anvils of Cb show little or no stratification, for here dense fallstreaks descending great vertical distances prevail [65].

2.1.8. Relation with Middle Clouds. The existence of all gradations between cirrostratus and altostratus (paragraphs 2.1.1, 2.2.2, 4.1.2) does not necessarily mean that altostratus generally evolves from cirrostratus, though this apparently can happen, possibly frequently. (Likewise, it is said that Cs may sometimes form from thinning of As [67].) The relationship is more likely or more often a spatial than a time-sequential one, the As evolving from Ac [50] simultaneously as associated Cs is evolving from Ci or Cc (see paragraph 2.1.1). Altostratus can, of course, exist without any Cs being associated in the same cloud system, and vice versa (as in high-level troughs or lows). In most warm-front situations the fine cirrus is largely detached from the middle clouds (see paragraph 4.1.2). Those cirrus or cirrostratus layers which extend down into and merge with middle-cloud decks are apt to be the densest and thickest type of cirrus [45]. Radar shows this is probably not a frequent situation [50], in middle latitudes at least; in the British MRF data it was noted in about 10% of the cirrus cases [45].

2.1.9. The Arrangement of Cirrus. Long parallel bands, stripes, or streaks and regular cross-bandings are frequently seen, suggesting a large-scale organization or system which must be related somehow to the processes of formation (see paragraph 2.2) and to the winds (see paragraph 3.5). It is claimed [26] [56] that the long bands move parallel to the wind, at least when the winds are strong [53]. Cross-banded patterns suggest effects of shear and instability, and parallel bands may indicate wave motion [11]. Very likely even the more chaotic and irregular-appearing cirrus would be seen to have a gross organization

plan if it could be viewed from a sufficiently high level (rocket photos?); the chaotic cirrus sky is probably an indication of marked and variable wind shears. But strong shear may inhibit fallstreaks [40: II Disc.].

2.2.0. Physics of Formation. The theory that all cirrus clouds are composed entirely or predominantly of ice crystals was originally derived from the frequent observations of haloes with such clouds and the known low temperatures at cirrus levels. This is now well verified by laboratory experiments and direct observations from aircraft.

2.2.1. Ice Nucleation Experiments. The microphysics of natural cirrus is not yet well understood. Most experiments on ice nucleation have used surface air samples; the results give a confusing and complex picture, which may not entirely apply at cirrus levels. The old idea that ice crystals form at high levels on "sublimation nuclei" has been abandoned. Experiments and theory indicate that there are various kinds of nuclei available, which vary in their capability of acting as "freezing nuclei," depending on the substance, its solubility and wettability, the temperature, and the rate of cooling. When samples of unsaturated but damp surface air are cooled steadily from a moderate temperature, the first condensation will be only as water droplets if it happens at temperatures down to -6°C; condensation starting at temperatures anywhere from -6° to -35° or -40°C shows an increasing proportion of ice crystals, in addition to the water droplets, as lower and lower condensation temperatures are tested. The warmest temperature at which ice first appears (which may be much colder than the initial condensation temperature) depends on the rate of cooling (see paragraph 2.2.5) and on the kind of nuclei present -- it may be as low as -30°C or -40° in fast coolings (i.e., much faster than usual outside of strong Cu or "thermal" convection).

The curve of the number of effective ice nuclei versus temperature is usually uneven, there being sudden increases in crystallizations at certain temperatures, such as near -10°, -20°, -30° (often around -32°); but these temperatures vary considerably with the air sample. Nevertheless, some investigators consider them to be true "critical temperatures." Many experimenters have found -40°C to be about the critical limit beyond which nearly all the water droplets formed immediately freeze; therefore, clouds below this temperature should be essentially ice clouds and always have the cirrus forms. A few droplets can be found to persist in some experiments down to about -72°C. At around -70°C it

appears that spontaneous crystallization or freezing of water takes place without any nuclei (so-called homogeneous nucleation), leading to many extremely fine crystals that are hardly visible to the eye. (Cf. however, paragraph 2.7.)

2.2.2. Observed Cloud Constitution (Phases). It is observed in the free atmosphere [15] [65] that in the region from 0° to -40°C, water clouds, or mixed clouds of water and ice in various proportions, are the rule, in agreement with theory and experiment. It often happens, however, that clouds in the colder part of this range (-12° to -40°C) are actually entirely of ice [15]. This comes about either by ice crystals descending as cirrus fallstreaks from higher levels (these are clouds occurring at -30° to -40°C), or by the conversion of all the original water drops in a middle-level cloud (ones occurring at -12° to -40°C) to snow or graupel fallstreaks through sublimation [50] (see paragraph 2.2.10). The latter process proceeds actively in the temperature range where there is a marked difference between vapor pressure over ice and over water; the water evaporates from the drops and sublimes on the crystals. Observations from aircraft and indirect indications have abundantly verified as a fact that below -40° clouds are almost purely crystalline, though a few scattered and very small water drops are probably often present (see paragraph 2.5). Weickmann [65] observed occasional very thin "cirrus" hazes of water drops at -35° to -40°C (see paragraph 2.2.4).

2.2.3. Nuclei [60], [39], [32], [40], [41], [44], [65], [66], [51]. Questions as to nature and abundance of the upper-atmospheric nuclei are difficult to answer at present. It may be said that some nuclei serve only for water-drop condensation, some only for ice nucleation, and some for both. The "freezing nuclei" are thought to be dusts and salts. A nucleus is an agglomerate of particles of one or various substances including one or a limited number of very minute particles with ice-forming properties. These particles are insoluble though the agglomerate as a whole may be mostly soluble, or at least wetable. Ions and contaminants in the solutes may also play a modifying role. (See paragraphs 2.2.1, 2.2.4, and 2.2.5).

2.2.4. Saturation Requirements. An important consequence of the behavior of the freezing nuclei is that, for a cirrus cloud to form as such (i.e., to form in the range below -35° or -40°C), the cooling must proceed to, or nearly to, the saturation temperature with respect to

water. This represents a large super-saturation with respect to ice (up to 150% or more relative humidity). The degree of ice-supersaturation needed for cirrus formation varies with the rate of cooling and with the kind and abundance of freezing nuclei present; unfortunately, we have little knowledge about this aspect, one which may prove to be very significant in determining the occurrence of cirrus and its different forms. The few observations made of freezing nuclei at high levels suggest that they may be much less abundant there than in surface air [49] [65] and subject to marked variations in kind and effectiveness, though perhaps not as great as the variations at sea level where the sources are more diverse and localized. Weickmann could find many droplets but few crystals in some thin "cirrus hazes" (temperatures around -35° to -40°C). He explains these hazes as forming where there are insufficient freezing nuclei, so that water condensation on soluble nuclei predominates (analogous to fumulus [63] in lower levels?).

2.2.5. Speed of Cooling. For determining the type of cirrus clouds formed, the speed of adiabatic expansion in rising air may have an important role. Various laboratory experiments show that [40]: "With extremely small rates of expansion of damp air, small numbers of ice crystals may arise on specially favorable nuclei at humidities substantially below that representing saturation with respect to water. With moderate and vigorous rates of expansion, the first visible product is always a water cloud or a mixed cloud, depending on the temperature." Fast (slow) cooling leads to a large (small) number of small (large) crystals.

Cirrus which forms in gentle, upgliding currents (vertical motions of 1-5 cm/sec) should correspond to the case of slow adiabatic expansion — Schwerdtfeger's "cirrostratus." (Weickmann [65] seems to imply that over Germany this is not a very common type; Schwerdtfeger [57] notes that it is less persistent there than other kinds of cirrus too.)

Cirrus formed in more-rapidly-rising air presumably corresponds to anvil cirrus and to what Schwerdtfeger called "pure cirrus" or "convective cirrus" (rapid convection in shallow layers due to advection of colder air at top of a shear layer); this process should account for much or most non-anvil dense cirrus (spissatus), cirrus uncinus, cirrus fibratus, and cirrocumulus. It is probably analogous to Kimachi's [38] idea that all cirrus over Japan forms in the steep-lapse-rate transition zone between air masses, one over-running the other; but he analyzed only a few cases. Lullam's "shred clouds" (paragraph 2.2.9) must also

be of this "convective" type.

The Schwerdtfeger "pure-cirrus" process [57] is one that apparently does frequently occur in northerly or northwesterly currents aloft over western Europe (see paragraph 4.1.3) and may account for much of the fine and patchy cirrus there. It is very doubtful, however, that all fine cirrus can be explained this way; over eastern North America, for example, the subsidence in northwesterly currents aloft is usually so strong as to inhibit cloud formation. There is, moreover, no reason to believe that fine cirrus is not also produced in the upglide situations leading to cirrostratus (see paragraphs 2.1.1 and 2.1.6). Often cirrostratus appears to result from the merging of fine-cirrus streamers. Indeed, Schwerdtfeger [57] found in Europe that the coexistence of cirrus and cirrostratus was a common situation, which he explained as due to wave motions and local instability within the general upglide regions.

2.2.6. Crystal Types and Cirrus Types. Weickmann [65] feels that a physical distinction between Schwerdtfeger's "pure" or "convective cirrus" and cirrostratus is justified because markedly different crystal shapes are observed in them. He writes: "In cirrocumulus, cirrus densus [spissatus], cirrus filosus [fibratus] and cirrus nothus [spissatus] we find mainly hollow [prismatic] crystals . . ." generally joined into twins or into clusters of many crystals. Whereas in cirrostratus . . ."we have individual shapes which do not go beyond twin formations [no tufts] . . .;" also, ". . . in addition to thick plate-shaped crystals and very clear and neatly-grown short or long pillar crystals, we note [in cirrostratus] . . . numerous very irregular shapes . . . a large number of different crystal types, all shapes from plates to every type of prism . . ." Crystals of this cirrostratus cloud-type grow with less ice-supersaturation than those in "pure" or "convective cirrus," indicating a steady slow lifting process, in which the "best" freezing nuclei are selected, ones on which water-vapor condenses before water-saturation is reached.

Cirrus of a mixed or intermediate type having form and crystal characteristics of both the Schwerdtfeger-Weickmann types is also frequently found [57] [65] (see paragraph 2.2.5).

2.2.7. The concentration of cirrus particles is very much smaller than for droplets in water clouds — Weickmann estimates 170,000 to 500,000 crystals per cubic meter [65]. The equivalent-water content is correspondingly low (0.1 g/m^3 for "pure cirrus," 0.4 for cirrostratus [65]).

2.2.8. Persistence of Cirrus. It is important for the forecaster to realize that ice clouds do not have the mercurial existence of water clouds, which respond instantly to the processes causing saturation and evaporation. The ice cloud may persist passively for many hours (even days?) [67] after being formed, for the ice particles evaporate but slowly when in nearly ice-saturated air [65]. (Schwerdtfeger [57] found the day-to-day apparent or statistical persistence of cirrus observations was around 60-80%; see also paragraph 4.5.4.) The ice crystals, falling at only a few cm per sec (for larger crystals, up to 1m/sec), usually find below their initial level a considerable layer (100's of meters or more) saturated with respect to ice. (See paragraph 4.1.16).

2.2.9. Fallstreaks and Shred-Clouds. Weather observers are often confused by seeing isolated streaks and trails of fibrous structure looking like cirrus but falling from middle level or lower clouds [11]. These lower so-called "fallstreaks" (German: Fallstreifen) are strictly speaking virga consisting of snow, graupel (rimed ice or snow), or rain particles [50], rather than elementary ice crystals of the cirrus type. (See paragraph 2.2.6.) They fall from water-droplet or mixed water and ice clouds, usually Ac, and may coalesce into an As [50]. The individual parent clouds often completely evaporate while the fallstreaks are descending from them, their water content having been entirely converted to snow or rain. This leaves the fallstreaks "floating" independently and requires the observer to report them as cirrus of the fibratus or uncinus species.

Years ago (1920), Wegener [62] noted that cirrus uncinus generally appears to form as fallstreaks from small tufts of dense cirrus or from cirrocumuli, which disappear in the course of time leaving only the pure uncinus. Wegener then postulated (as Moeller [74] had already done in 1881) that probably all cirrus streamers, bands, and cirrostratus sheets form in this way as fallstreaks from patches of dense cirrus or Cc parent clouds [62]. This view was never generally accepted, but has been re-examined recently by Ludlam in light of modern cloud physics research (see paragraph 2.2). At first Ludlam concluded that the initial stages of cirrus formation are probably always glaciated in form like Cc, rather than fibrous; from these, he thought, the fibrous clouds generate as fallstreaks [40 (I)]. However, more recently [40 (II)] he has found that actually the sequence is the reverse,

the cirrus fallstreak being the initial cloud, which then produces an updraft (from release of latent heat of sublimation as the crystals grow while falling through the ice-saturated air). (Findeisen [72] had made the same observation years ago but it had been ignored.) At top of the updraft a dense patch or "shred-cloud" (Ci spissatus?) often develops. The shred cloud is convective in nature, probably composed, at first at least, of both water and ice (corona iridescence seen). It may in turn dissipate into a trail of ice which regenerates the original fallstreak, – a process possibly accounting for much of the long apparent persistence of cirrus. According to Ludlam, the difference between the cirrus fallstreaks and those of middle levels is that the former develop spontaneously without a mother cloud, whereas the lower fallstreaks precipitate from water-droplet clouds (Ac, etc.) [50] – temperature being the critical factor in this distinction (see paragraph 2.2.2). Ludlam does not report any exceptions to his cirrus fallstreak-shred-cloud theory, but its universality and typicality cannot be accepted until it is checked by extensive observations in many regions. Moreover, it leaves the origin of fallstreaks still unexplained.

Ludlam [40] has also offered an explanation for the shape of cirrus-uncinus fallstreaks, in terms of the wind shear and falling speed of the ice particles. The upper part of the streak is generally almost vertical, whereas the lower end becomes almost horizontal; this being due to the decrease in wind speed downward and the decrease in falling speed of the particles as they evaporate in descending into drier air (Figure 1a). Changes in wind, or growth of the crystals in ice-supersaturated layers, may explain secondary bends often observed in the trails (Figure 1b). Filaments appear to taper downward because the outer crystals evaporate first.

A suggestion of a mammatus structure in the lower ends of cirrus fallstreaks is often noted, due to the chilling of the air in which the crystals evaporate [40] [81]. (Similar mammatus forms are sometimes observed in contrails.)

A question of interest to the forecaster is why so much cirrus formation is only in scattered fallstreaks and patches if the ascent of the air is as uniform and slow as we generally assume it to be at high levels? With the aid of Ludlam's ideas, this could be explained as follows: around -40°C fallstreaks are the typical initial form of cirrus; they form on special rare ice nuclei at temperatures near or

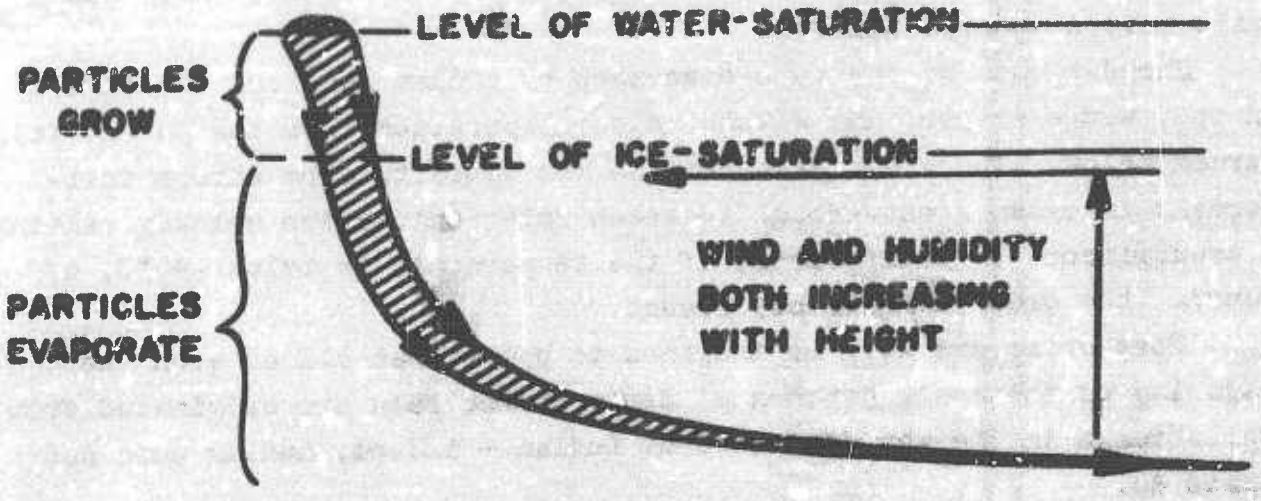

Figure 1a. Typical Shape of Fallstreak (vertical section) (Ludlam [40]).

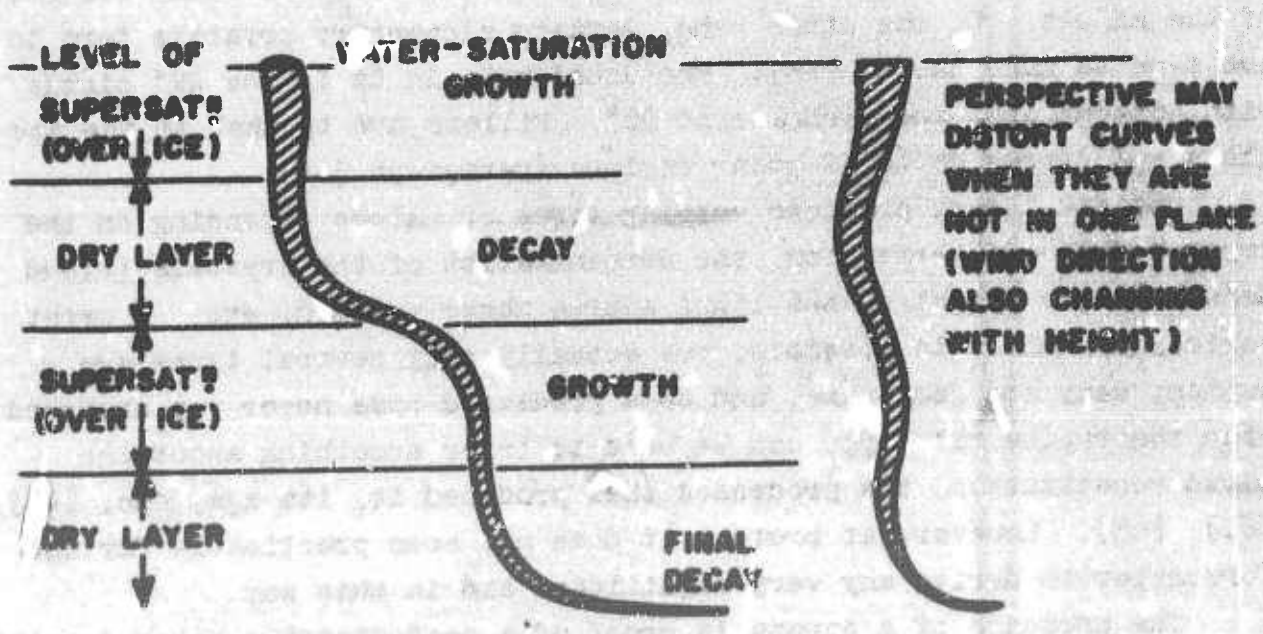

Figure 1b. Formation of Bands in Fallstreaks by Fall Through a Subsidiary Damp Layer (Ludlam [40]).

somewhat below saturation with respect to water. These nuclei are irregularly distributed. Also, there are small disturbances of the general air flow, and the humidity distribution is irregular. Crystallization is first reached at scattered points where the conditions of

favorable nuclei, locally greater ascent of air, and higher humidity happen to coincide. At temperatures much lower than -40°C the fall-streak and shred cloud are not the typical cirrus forms (-- nebulous veils more characteristic?).

Shred-clouds of the type discussed by Ludlam [40] are cumuliform on top, wedge-shaped, and without clear separation from the parent fall-streak below. The speed of ascent in the updrafts from cirrus fall-streaks is often great enough to reach water saturation quickly, causing a predominance of water drops; if the temperature is below -40°C, of course the drops immediately freeze.

Most observers will be inclined to doubt that all or even the majority of the small patches of dense cirrus seen are originated from fallstreaks in the way described by Ludlam -- indeed, Ludlam does not claim so.

2.2.10. Optical Phenomena. Solar and lunar haloes are characteristic of cirrus clouds and not of any other clouds. However, only a relatively small proportion of cirrus produces haloes. Freshly-formed prismatic crystals in not-too-thick cirrostratus veils account for most of the haloes. On the other hand, certain elementary crystals form to not seem to make haloes [65]. The usual halo in Cs is the 22° circle with tangent arcs and parhelia of 22°. Pillars are typical in the ice mists and cirrus hazes of polar regions (paragraph 3.6).

Optical theory predicts varying forms of haloes depending on the crystal type and perfection, the concentration of the crystals (cloud density), the height of the light source above horizon, etc. A great variety of haloes is possible, but actually only several types are common; many are very rare, and some predicted ones never yet observed. From theory, the halo type can be used to infer something about the cloud constitution, the processes that produced it, its age, etc. [40] [61] [65]. However, at present it does not seem practicable for the forecaster to derive any very significant aid in this way.

The presence of a corona is proof of a predominantly water droplet cloud. Corona is reported sometimes in cirrocumulus and fallstreaks (see paragraph 2.2.9). The corona-vs-halo criterion often distinguishes for the weather observer what is altostratus and what is cirrostratus [67], but even more often the crystal types [65] or cloud thickness are not conducive to these optical phenomena.

Even thin cirrus markedly reduces the transmission of solar radiation [30], though cirrostratus is not supposed (by definition) to

prevent the appearance of shadows in sunlight [67].

2.3. Relations to Contrails. Contrails may be considered as artificial cirrus clouds. (Reports from some ground observers indicate that occasionally a contrail gradually spreads out to cover the whole sky; contrails from aircraft circling around to rendezvous may soon fill their area with contrail-cirrus.) They can form at the same levels, and once formed they are governed by the same processes as cirrus. If temperature and humidity conditions are favorable for cirrus, they are very probably favorable for contrails, though the inverse is not so probable because contrails can occur with more humidity if the temperature is cold enough. In the region where some cirrus is already present any contrails formed will be very persistent, as a rule. Vice versa, where no cirrus is present contrails are not so likely to form, and if formed are generally non-persistent [45]. Very persistent contrails are more readily visible from the ground than thin cirrus. Thus, it can be assumed that when persistent trails occur extensive thin layers of very nebulous cirrus are present even though they can not be seen from the ground.

2.4. Turbulence in Cirrus. There are many pilot reports of turbulence encountered while flying in cirrus, as well as in clear air. However, no studies are yet available to indicate whether the probability of turbulence at cirrus levels is greater or less in the clouds than out of them. Since the conditions of vertical motion favorable for cirrus in the vicinity of the jet stream (see discussion in paragraph 4.1.17) are believed to be also favorable for turbulence, (and vice versa, for no-cirrus and no-turbulence), some relation between the two phenomena might be expected. Perhaps Ci uncinus and the chaotic (intortus) variety of cirrus will indicate turbulence (see paragraphs 2.1.9 and 2.2.9).

2.5. Icing in Cirrus. Inasmuch as experiments in the laboratory show it is possible to have supercooled drops down to -60°C or -70°C even though the clouds are predominantly ice below -40°C, a possibility of some icing of aircraft in cirrus must be reckoned. There are a few cases reported of icing in contrails at temperatures below -40°C and also of very light riming on aircraft in cirrus around -50°C [9]. At temperatures above -40°C cirrus clouds may have a considerable amount

of water, and icing is more frequently noted in them, especially in anvils. However, a B-47 at 36,000 feet and -51°C over Alabama in March 1953 reported ¼ inch accretion, apparently from an anvil [70].

2.6. Visibility in Cirrus. Visibilities in extensive cirrus are often over a mile and rarely less than 300 feet, the average being probably about a mile. But sometimes the cloud is so thin that the pilot is unaware he is in it (see paragraph 2.1.6). Vertical visibility is apt to be much better than horizontal. For lack of a background for depth perception, it is very difficult for the pilot in cirrus to accurately judge the horizontal visual range, whether it is small or great. From 40 RCAF aircraft observations over Canada [12], Clodman obtained the following percentage frequencies of visibilities in cirrus: < 1 mile 70%, < ½ mile 60%, < ¼ mile 30%. The last two percents seem rather too high, however. Clodman suggests that these probabilities can be multiplied to the probabilities of cirrus occurrence to obtain estimated probabilities of encountering given visibilities in flight at cirrus levels.

Captain M. W. Burton of AWS devised a rule of thumb for forecasting or estimating the visibility of one aircraft from another in thin cirrus or other high cloud (temperature below -30°C): V = ½ miles × dewpoint depression in degrees C. As an example: T = -35°C, T_d = -38°C, visibility = ½ × 3 = 1½ miles. Burton's Rule has been used with good success in the Arctic where poor visibilities in apparently cloud-free air are often encountered. Its applicability elsewhere remains to be tested.

2.7. Electrical Effects. There are a few reports of visible corona ("St. Elmo's Fire") on aircraft flying in cirrus at altitudes of 30,000-40,000 feet. This may be expected since it is well-known that ice particles hitting a fast moving aircraft can build up a charge with resultant corona. The charging rate increases as the cube of the air speed. That visible corona does not result more often on jet aircraft in cirrus is probably owing to the relatively low concentration of ice crystals, their small size, and the fact that at low barometric pressures the charge bleeds off the aircraft more readily so that very intense electric fields from frictional charging alone are not reached. On the other hand the "precipitation static" in aircraft radios while flying in cirrus often blanks out ordinary HF radio communication in spite of anti-static devices. On VHF and UHF the interference is not so serious. A case of lightning striking a jet aircraft in an anvil at

39,000 feet has been reported [78].

2.8. Nacreous Clouds. These luminous, beautifully iridescent ("mother-of-pearl") clouds, something like lenticular cirrostratus in form, are occasionally seen in winter in high latitudes before sunrise or after sunset when they are illuminated by the sun but the ground is in the earth's shadow. They occur between 21 and 30 km, and are not to be confused with the similar appearing noctilucent clouds at 82 km, nor with true cirrus.

Nacreous clouds are thought to be composed of water droplets of 1 to 3 microns diameter, which would explain the rapid dissolving and reformation of the clouds and their brilliant diffraction colors [65]. According to theoretical considerations [76] such condensation could occur under nuclei-free ozone-rich water saturation conditions at temperatures near -70°C when the air is cooled slightly by lifting or by radiation. The clouds usually form over the high mountain regions of Alaska and Scandinavia on the east side of a tropospheric ridge of high pressure (northwesterly wind in the stratosphere?).

3.0. Occurrence and Climatology of Cirrus.

3.1.0. Heights. There are a number of special series of observations of the heights of cirrus made by theodolite or from pilot reports. These methods of measurement, though much more accurate than ground observers, are not without some limitations. The theodolites can only fix on the cloud bases having "hard" and well-defined outlines; sometimes it is not easy to judge what is the "base." Aircraft can report the height of penetration of a definitely-visible cloud base to the accuracy of the altimeter. But ill-defined hazy cirrus bases are likely to be missed, especially at night. Moreover, aircraft observers have the same difficulty in judging height of clouds above or below the aircraft as does a ground observer. The aircraft observers' determinations of the cloud type are often questionable, partly because of lack of proper instruction and partly because of inherent difficulties in judging from an aircraft. For this reason it is preferable to refer to the aircraft data above 25,000 feet as simply "high cloud;" the distinctions between "Ci," "Cs," and "As" are not generally reliably made in the regions where either could occur. Though limited in coverage, data from these sources provide the only representative samples of the height distribution which are available.

3.1.1. International-Cloud-Year Data. During the International Clo' Year of 1896-7, double-theodolite measures of clouds were made daily at various observatories. The mean heights for cirrus and cirro-stratus are summarized in the following table [63]:

TABLE I

Mean Heights of Cirrus Bases for International Cloud Year 1896-7.

Latitude	Places	Northern Summer (km)	Northern Summer (km)
78.50°N	Cape Thordsen	7.32	----
70°N	Bossekop (Sweden)	7.46	----
60°N	Pavlovsk plus Uppsala	7.86	7.07
50.75°N	(Average of) Potsdam plus Trappes	8.70	7.68
40.5°N	(Average of) Blue Hill plus Washington	10.15	9.14
35°N	Mera (Japan)	11.02	9.13
14.5°N	Manila	12.05	11.14
7°S	Batavia	11.04	----
35.5°S	Melbourne	8.5	9.6

The maximum heights observed in these series were:

TABLE II

Maximum Heights of Cirrus Bases for International Cloud Year 1896-7.

Latitude	Places	Northern Summer (km)	Northern Summer (km)
78.5°N	Cape Thordsen	8.59	----
70°N	Bossekop (Sweden)	11.79	10.39
60°N	Pavlovsk plus Uppsala	11.69	10.12
50.75°N	(Average of) Potsdam plus Trappes	12.68	11.91
40.5°N	(Average of) Blue Hill plus Washington	15.01	13.60
35°N	Mera (Japan)	16.79	15.48
14.5°N	Manila	20.45	17.14
7°S	Batavia	18.60	14.21
37.5°S	Melbourne	----	----

Heights of cirrus bases estimated from pilot-balloon ascents (generally about 1 km below photogrammetrically-determined heights) are averaged for several stations in India [63] [75]:

TABLE III

Mean Heights of Cirrus Bases Over India.

Latitude; Elevation	Places	Nov - Feb	Mar - Jun	Jul - Oct
31°N; 1.9 km	Quetta plus Simla	9.7 km	9.7 km	9.4 km
27.2°; .17 km	Agra	9.3	9.1	10.6
18.5°; .56 km	Poona	8.9	9.9	9.9
20°	Akyab	9.0	9.2	9.3
13°	Madras	9.1	8.9	8.8

3.1.2. Potsdam Photogrammetry. Photogrammetric observations made at Potsdam during 1900-1920 [62] [63] suggest that cirrus heights tend to cluster at three or four levels, according to form:

very delicate veils	11 km
typical detached ci	8.67 km
cirrostratus	8.54 km
cirrocumulus	6.37 km

Analogous statistical height-groupings (without regard to form of cloud) are apparent in the data from all the stations of Table I [63]. There is some question whether this is a real or a sampling phenomenon.

3.1.2.1. Süring [63] found that at Potsdam the mean slope of the base of cirrus decks in the direction away from centers of depressions is about 6° (18° max), and for cirrocumulus (also Ac) only 3°; but in some cases the slope was in the opposite direction.

3.1.2.2. He found no evidence of a diurnal variation in height of a thermal nature. However, the cirrus bases of a given system tended to lower with time at a rate of about 200m/12 hours [63].

3.1.3. British MRF Data. From the observations of the British Meteorological Research Flights from South Farnborough during 1949-52, Murgatroyd and Goldsmith [46] prepared data on height of cirrus bases and tops. (Only cases where the observer was certain the plane was in cirrus are included; at the bases there was often a "region of doubt"

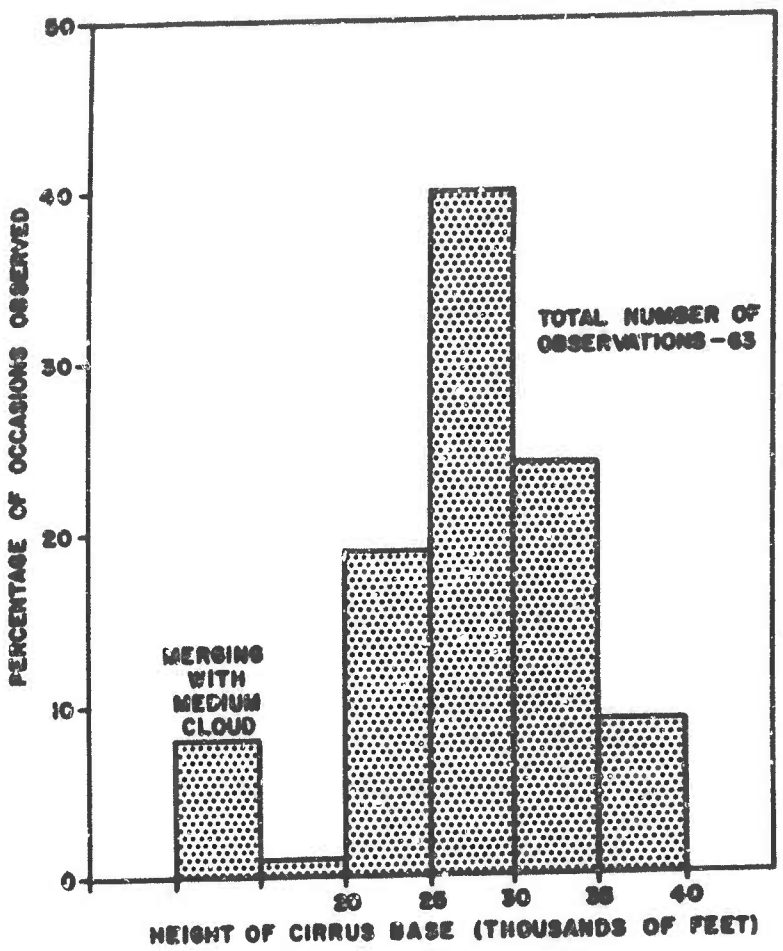

Figure 2. Frequency Distribution of Heights of Cirrus Bases Observed on British MR Flights from South Farnborough, 1949-52 [45].

which sometimes extended through several thousand feet.) Figure 2 shows the frequency distribution of the base heights. The tops were most frequently less than 2,000 feet below the tropopause, though 30% of the cases were in the range 3,000 to 11,000 feet below. About 7.5% of cases had tops in the stratosphere and several cases even with bases in the stratosphere (45,000-46,500 feet) were noted. (See paragraph 4.1.11 for discussion of cirrus and tropopause.) James [36] in summarizing the 1950-54 MR Flights found similar results (Figure 3), though the tops tended to range a somewhat greater distance below the tropopause than on the 1949-52 flights. Again the base was above the tropopause in a few cases. Whether the peaks in the frequency of bases at 20,000, 25,000, and 30,000 feet are real or caused by observer preference

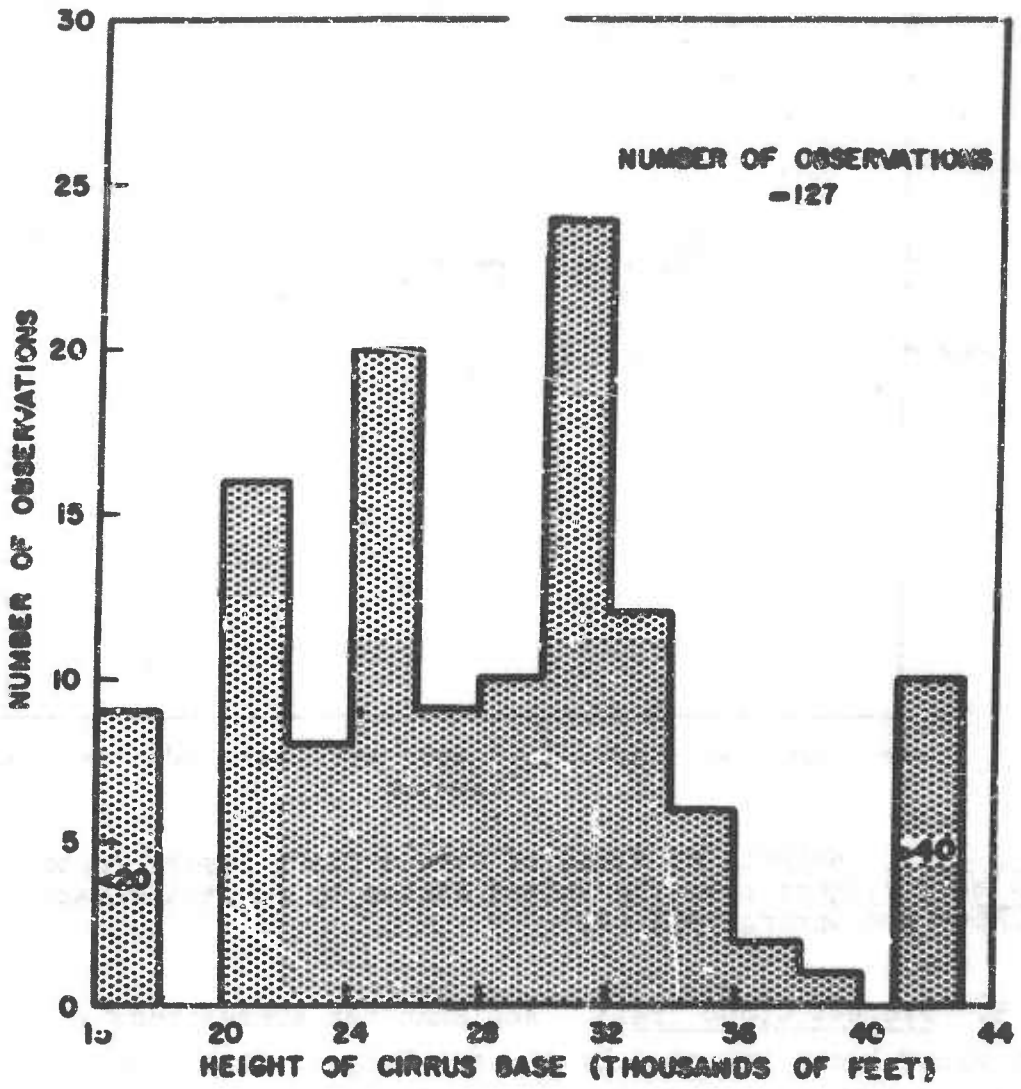

Figure 3. Frequency Distribution of Heights of Cirrus Bases from British MR Flights, 1952-54 [36].

for estimates to nearest 5,000 feet cannot be said.

3.1.4. Project Wiback Data. On Project Wiback during the winter and spring of 1951, B-47 flights over central and western United States recorded cirrus heights [22] [23]. The data on heights of the tops are shown and discussed in connection with the tropopause in paragraph 4.1.12. The data on heights of the bases of the lowest cirrus layers observed in each case are plotted against latitude in Figure 4. There is a tendency for the mean height to increase from 48°N to 30°N though the lowest values were around 20,000 feet over this whole range of latitude.

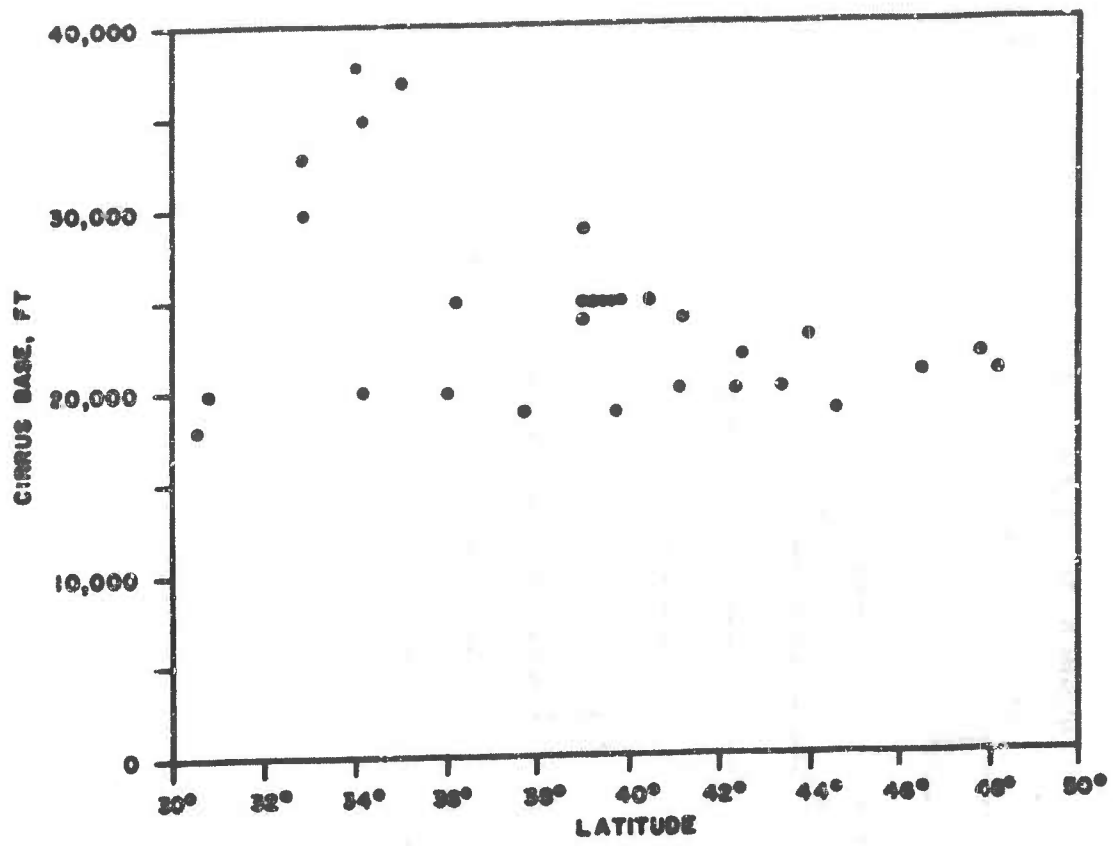

Figure 4. Heights of Bases of Cirrus Cloud Layers Observed on B-47 Flights over the United States by Project Wiback, Winter and Spring 1951 [22].

3.1.5. Project Cloud Trail. Appleman has summarized heights of all high-cloud bases reported by ADC-AWS Project Cloud Trail during the year December 1954-November 1955 (see AWS TR 105-132). The data are from daily jet-interceptor flights over certain U.S. radiosonde stations, at 1500Z. The aircraft reported heights of bases and tops of all high cloud penetrated above 25,000 feet MSL. There was probably a large proportion of water-drop clouds (As) included in the 25,000-30,000-ft region during spring, summer, and autumn. Average heights of the cloud bases were tabulated by seasons and the year, for northern and southwestern and all of the United States, and for scattered and broken coverages. (See Tables in Appendix.) No significant differences between broken and scattered decks were found; therefore, these categories were combined. The Tables show that in northern United States (above 39°N) there is a slight seasonal trend in base height, lowest in winter and highest in summer, ranging around an annual mean of 30,000

feet. The data for southwestern United States were too few to establish a significant seasonal trend. For the year, in general, the southwestern U.S. cirrus appear to occur at slightly greater heights than do the northern. Very few cases with bases above 36,000 feet were reported.

The standard and mean deviations of the cloud-base heights observed on this Project have also been computed (see AWS TR 105-110A for details); the standard deviation ranged from 3,580 feet in autumn to 5,099 feet in summer. The corresponding mean deviations are 2,864 to 4,079 feet, respectively. A recomputation eliminating cases probably not true cirrus did not significantly alter these figures.

A further summary was made showing by seasons and regions the frequency of cloud reported at each 1000-foot interval from 25,000 feet up (see Tables A10-12 in Appendix). There is some sampling bias in the results owing to the number of flights decreasing with height. Also, the local time of the flights (morning) and the lack of stations in central and southeastern sections of the United States, probably eliminated much cirrus of the anvil type. In the warmer seasons and regions this type of cirrus would be expected to occur more frequently at heights of 35,000-55,000 feet than these statistics reveal. In general, the percentage frequency of cloud encountered by the Project increased with height from 25,000 feet up to a maximum around 27,000-35,000 feet depending on season and region and decreased to zero above 40,000-50,000 feet. The annual percentage frequencies at modal height are about 14% for northeastern United States, 13% for northwestern United States, and 8% for southwestern United States — these are rather lower values than those computed for the RCAF data over Canada (see Figure 5, and paragraph 3.1.6) which give 18-19%, though the height of maximum frequency for the two sets of data is about the same. The seasonal variation in modal frequency was quite marked, as Cledman also found over Canada (see paragraph 3.1.6), about 10-11% difference between the extreme seasons — the greatest modal frequency was in winter in the west and in spring and summer in the east (in this respect the year 1955 may not have been typical). The height of the maximum frequency was generally 2,000-7,000 feet lower in winter than summer, as would be expected. It will be recalled that the mean height of the cloud bases was 30,000 feet, i.e., several thousand feet lower than the height of maximum frequency of cloud — this is a reasonable difference considering the average thickness of the clouds. However, the seasonal range

in modal height was almost insignificant in the northwestern region, even though the frequency was much greater in winter, which can be explained in terms of the maritime west-coast climate.

3.1.6. RCAF Flight Data. A report by Clodman [12] analyzes 2000 cirrus observations from RCAF aircraft flights distributed over bases in the prairie provinces, eastern Canada, and at North Bay. These flights observed the percent of time the aircraft was in cirrus at specified altitudes: 30,000, 35,000, and 40,000 feet (only one case reported at 50,000 feet). The observers also estimated the percent of the sky covered with cirrus regardless of altitude or number of layers (called by Clodman "total cirrus"). This observational series is considered by Clodman to be random and representative of the region (– some cases where the height was not reported were eliminated). There is very little geographical and seasonal variation in cirrus frequency shown in the data. The distribution with height, however, shows a marked difference between summer and winter. Clodman, with the aid of certain assumptions, derives from the data a set of curves of climatological probability of cirrus occurrence as a function of height, for several ranges of climate, along with modifying factors to allow for differences in predominance of cyclonic or anticyclonic situations in the climate. In doing this, the assumption is first made that the shapes of the curves should be the same for all seasons. Thus, values can be interpolated for other heights than reported by the aircraft. It is also assumed that amounts of cirrus occurring below the height of maximum cirrus frequency are equal to the amount occurring above the maximum. The "total cirrus" values are multiplied by thickness (i.e., heights) to obtain the areas under the curves. Heights of the maximum frequencies are now adjusted to give areas equal to the calculated values. The resulting height-vs-frequency curves are shown in Figure 5. Curves 2, 3, and 4 are for the cold, intermediate, and warm months over southern Canada, respectively. The mean-upper-air temperatures for Canada associated with these curves are:

	Curve Number				
	1	2	3	4	5
500 mb	-38°C	-30°	-23°	-15°	-8°
400 mb	-47°C	-42°	-36°	-27°	-19°

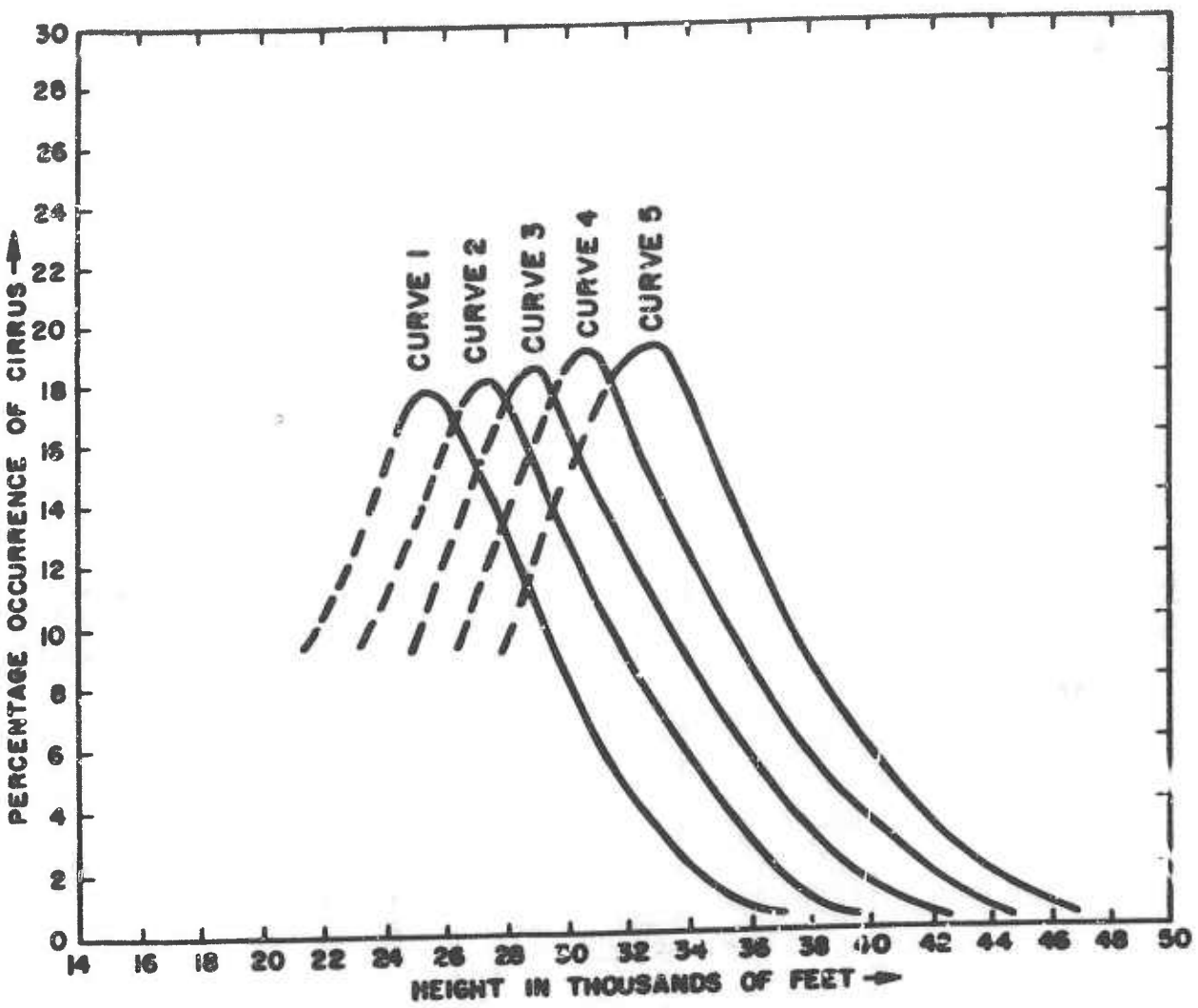

Figure 5. Mean Frequency-Height Distribution Curves for Cirrus Clouds (after Clodman [12]) Applicable to Areas in Figures 6, 7, and 8.

The curves 1 and 5 are estimates for more extreme climates than southern Canada, assuming parallelism of the curves and linear dependence of mean cirrus frequency upon mean 400- and 500-mb temperatures. Thus, the curves can be used to estimate climatological cirrus-height distributions for a wider geographical area than southern Canada — but the validity of such a procedure cannot easily be tested at present except over northern United States (cf. paragraph 3.1.5), and its justification rests largely on the a priori reasonableness of the assumptions made. To facilitate such use, Clodman presents three maps (Figures 6, 7, and 8) to mark off the zones of the Northern Hemisphere (150°W to 30°E) where each curve should apply, judging by the mean temperatures. Estimates for other regions can be improved by multiplying the curve

431736 O - 57 - 3

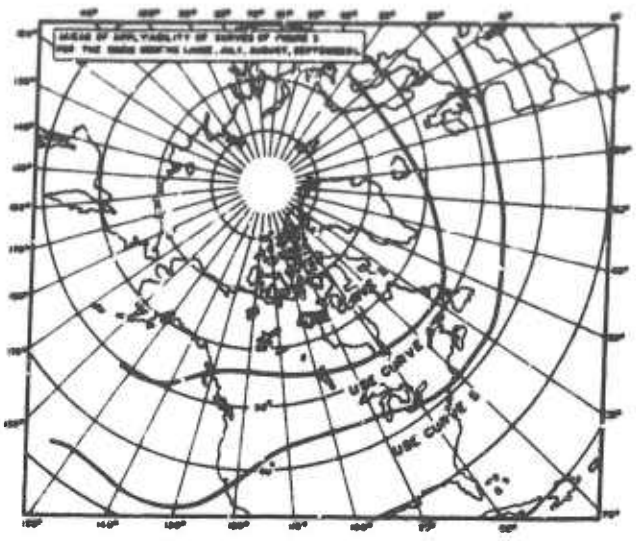

Figure 6. Areas of Applicability for Mean Cirrus Frequency-Height Curves of Figure 5, in the Warm Months (after Clodman [12]).

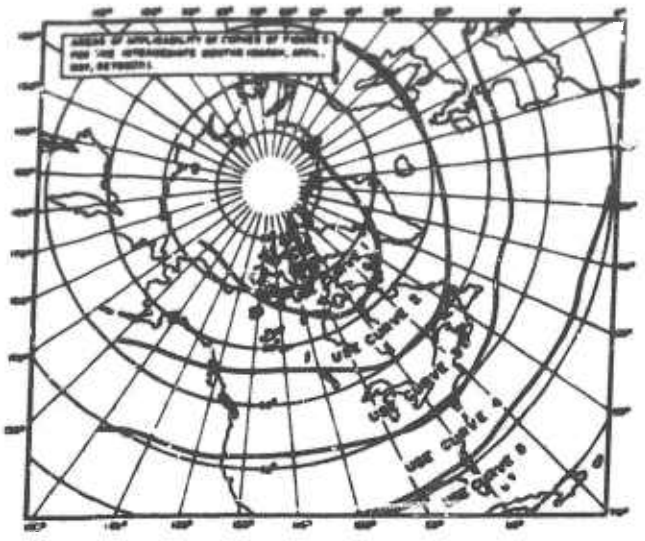

Figure 7. Areas of Applicability for Mean Cirrus Frequency-Height Curves of Figure 5, in the Intermediate Months (after Clodman [12]).

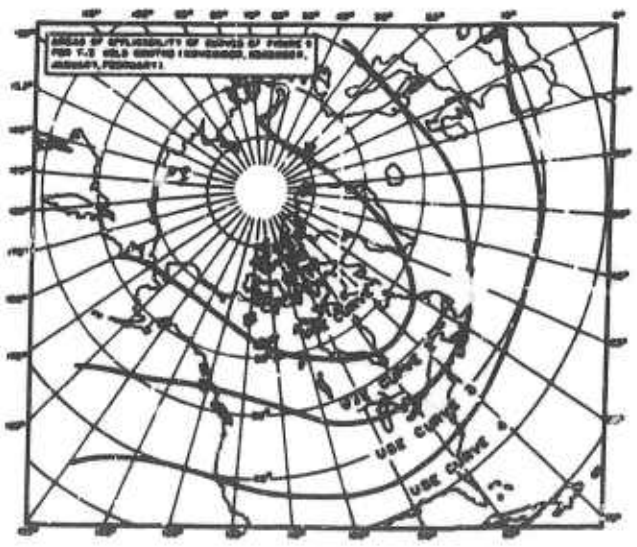

Figure 8. Areas of Applicability for Mean Cirrus Frequency-Height Curves of Figure 5, in the Cold Months (after Clodman [12]).

readings with factors to compensate for effects of having less or more cyclonic activity than typical of southern Canada. The following values for such factors are suggested by Clodman, based on the relation he found between cirrus frequency and undercasts or precipitation (see paragraph 4.1.2):

Active Storm Area	x1.8
Light to Moderate Cyclonic Activity	x1.4
South Sides of Jet Streams	x1.4
High-level Lows	x1.4
Anticyclonic Area	x0.7
Semi-permanent Low	x1.2
Semi-permanent High	x0.8

It should be noted that Clodman's curves are extrapolated to almost zero frequency of cirrus at low levels – the forecaster or climatologist concerned with operational problems must remember that actually the occurrence of middle clouds overlaps the lower cirrus region so that these curves may be more or less meaningless for many practical purposes in the region below 30,000 feet.

A method for estimating the height of cirrus bases in individual situations is also proposed by Clodman, derived as follows: The mean base height is taken as ½ the mean thickness minus the mean height of maximum occurrence. The mean temperatures for the mean base heights were found from mean upper-air data for each season. When plotted on a Canadian Meteorological Service tephigram, these temperatures form a straight line passing through -43°C at 400 mb and -37°C at 300 mb. This line agrees with the general critical temperature for cirrus formation, around -40°C, but implies that the critical temperature is a little warmer in warmer air masses. Where the current sounding intersects this line, should be the height of any cirrus then occurring. Clodman fails to point out that there is an inconsistency between this empirical line and data from other investigations which would call for frequent cirrus occurrence at temperatures much warmer than -40°C. The explanation for this is that Clodman used the height of maximum occurrence in deriving his critical line, which thus excludes the half of the cases that occur below the height of maximum frequency. His critical line should probably be shifted about +10°C to include these cases. (Cf. paragraph 3.1.7.) No test of Clodman's method as a forecast aid has been reported.

3.1.7. Estimates From Contrail-Formation Curves. Estimates of the height of cirrus and cirrostratus bases made by ground weather observers without aid of radio-soundings, aircraft, theodolite, or radar, can be grossly in error. Appleman (AWS TR 105-110 and 105-132) compared ground-observer estimates with aircraft-observer estimates, finding the

former were 9,600 feet too low on the average. Because cirrus is generally observed when contrails are reported (paragraph 2.3), he proposed using his contrail-formation curves to estimate the probable height of observed cirrostratus clouds. Tests showed this would reduce the average error of cirrus-height estimates to within 3000 feet. However, Clodman's [12] empirical cirrus-base vs temperature criterion gives values 2000 feet higher than Appleman's on the average for the warm months and 1000 feet lower in the cold months (see paragraph 3.1.6). Recently, Appleman has made a test of contrail-formation-curve estimates on high clouds whose heights were reported by Project Cloud Trail (AWS TR 105-132). He found the method gives good estimates for clouds at -40°C or colder (about 900-1500 feet too low on the average), but increasingly inaccurate results as the clouds become warmer, the estimates being systematically 5000 to 9000 feet higher than the actual heights. For the year as a whole and on all clouds above 25,000 feet the results were (using the 90% humidity-contrail curve in AWSM 105-100):

Error (feet)	Overcast and Broken Layers (>.6)		Scattered Layers (<.5)	
0 - 2000 feet	78 cases	(35%)	166 cases	(37%)
2100 - 4000	64	(63)	122	(64)
4100 - 6000	37	(80)	68	(79)
6100 - 8000	28	(92)	53	(91)
8100 - 10,000	12	(98)	24	(97)
>10,000	4	(100)	12	(100)
Total	223		445	
Aver. Absolute Error	3870 feet		4120 feet	
Aver. Algebraic Error (Est. Ht. minus actual)	+1620 feet		+3160 feet	

There was little difference between seasons. The results grouped by cloud-base temperatures were as follows:

Temp. Groups (°C)	No Cases	Average Absolute Error (feet)		Average Algebraic Error (feet)	
		Overcast and Broken	Scattered	Overcast and Broken	Scattered
-20/-29°	30	7600	9100	+7600	+9100
-30/-39°	175	5100	5500	+5100	+5500
> -40°	430	1900	2900	-900	-1500

This study is fully reported in AWS TR 105-110A.

It has been questioned whether this use of the contrail curve gives any better improvement than could be obtained by using the climatological height as an estimate, assuming the climatology were available. A test of this idea was made on the Project Cloud Trail data. The results suggest that very probably climatology would give estimates of an accuracy comparable to those from the contrail curve (see AWS TR 105-110A). Lack of suitable climatological data on cirrus heights prevents general operational use of this simple method.

H. Appleman (at Hqs, 2d Air Weather Wing) noted that the hypothesis of Krebs and Doege [39] (see paragraph 4.1.13) can probably be used to estimate the base heights of observed cirrus with an improvement in accuracy over eye estimates equivalent to that obtained by use of the 90% contrail curve. No test of this method has yet been made on independent data.

3.2. Thickness. Aufm. Kampe [37] and Weickmann [65] measured thicknesses of cirrus layers (individually) on 46 research flights to 10,000 m, at Ainring. They obtained a maximum frequency at less than 200 m, and secondary maxima at 1000 and 2600 m. The greatest thickness was over 5000 m. (See Figure 9.) During Project Wiback (see paragraph 3.1.4) about 25 cases of cirrus base and top observations from B-47 flights were obtained from which thicknesses could be computed [22] [23]. These results are illustrated in Figure 10. The majority of cases were less than 1000 feet thick, but one (multiple-layered probably) reached 10,000 feet, another 17,000 feet.

The British Meteorological Research Flights of 1949-52 obtained 63 measures of cirrus thickness (Figure 11) [38]. The most frequent values fell in the 3000-5000-foot range though several cases exceeded

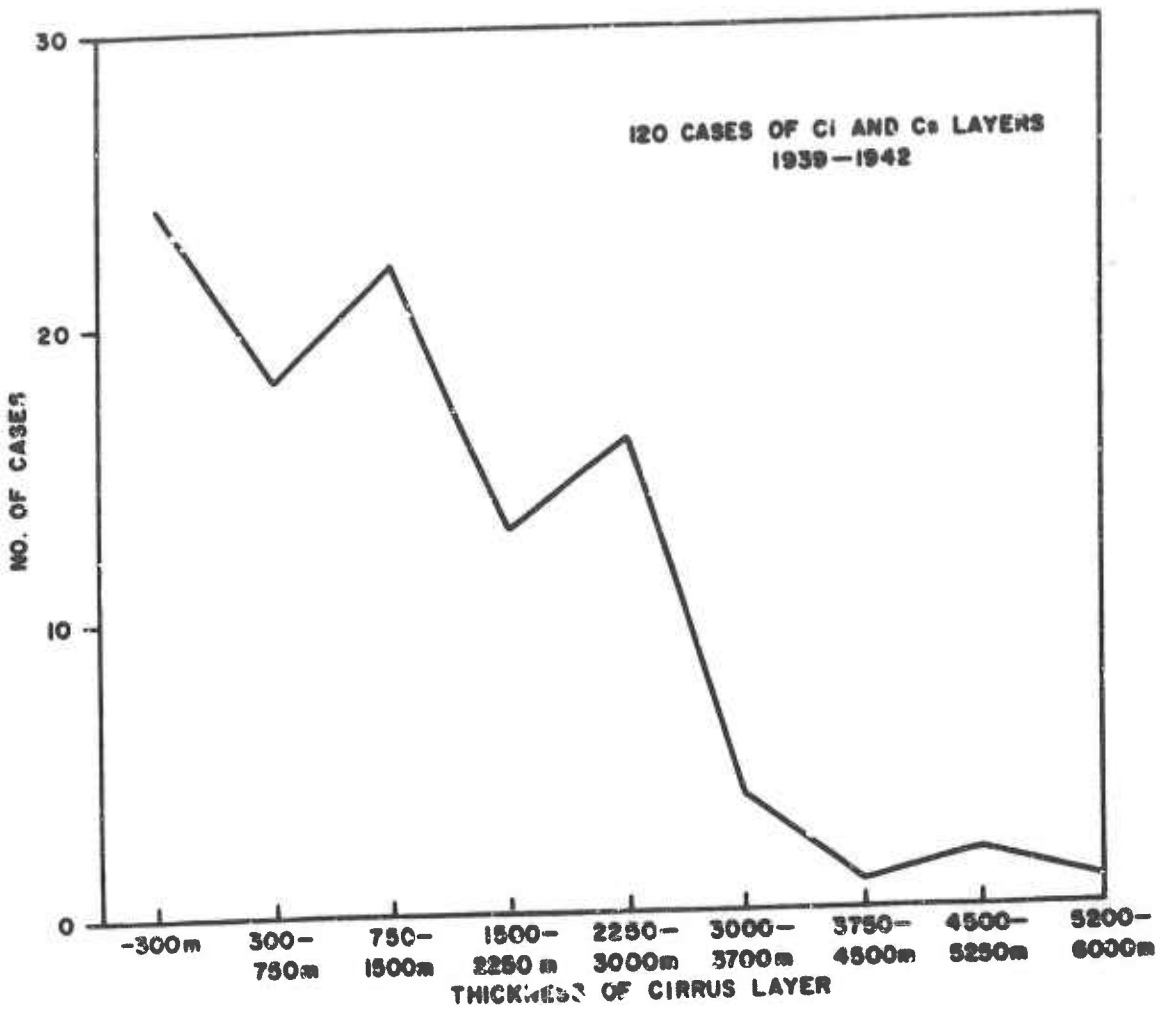

Figure 9. Frequency Distribution of Thicknesses of Individual Cirrus Layers Observed on Research Flights from Ainring, Bavaria, 1939-42 [65].

11,000 feet, and 10 cases were merged with middle-level clouds. When the thickness was great, the observers noted a tendency to layering (cf. paragraph 2.1.7) or to stratification in the density (difficult to tell which). The results for 113 cases from the 1952-54 MRF's [36] are shown in Figure 12. About 70% of the cases were in the range from several hundred feet to 6000 feet, with greatest frequency at 4000-6000 feet. Some cases reached 17,000 feet.

The Project Cloud-Trail data [AWS TR 105-132] (see Appendix) indicate the patchy ("scattered") cirrus were predominately less than 2000 feet thick, whereas cases of .6 sky cover or overcast cirrus tended to be thicker (mostly less than 5000 feet). There were many cases over

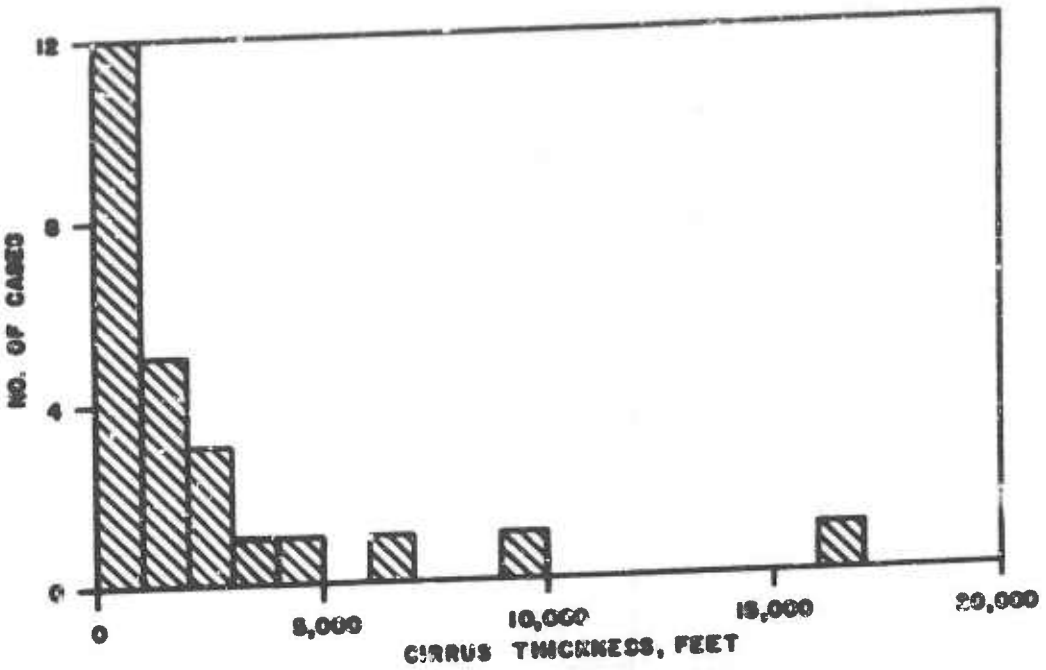

Figure 10. Frequency of Cirrus Thicknesses Observed on Project Wiback B-47 Flights over the United States, Winter-Spring 1951; Tabulated by 1000-ft Intervals [22].

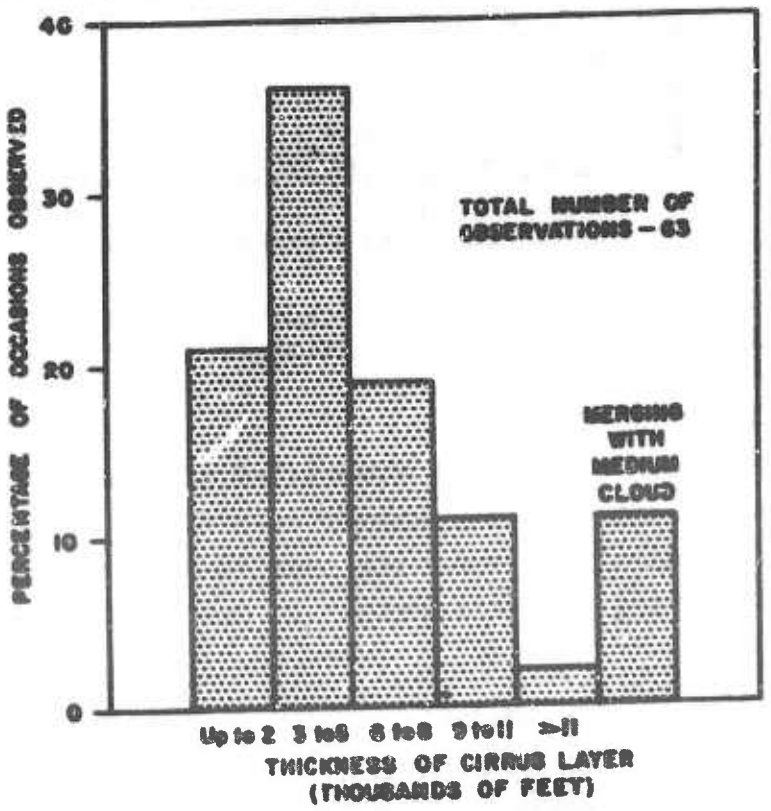

Figure 11. Frequency Distribution of Thicknesses of High Clouds Observed on British MR Flights from So. Farnborough, 1949-52 [45].

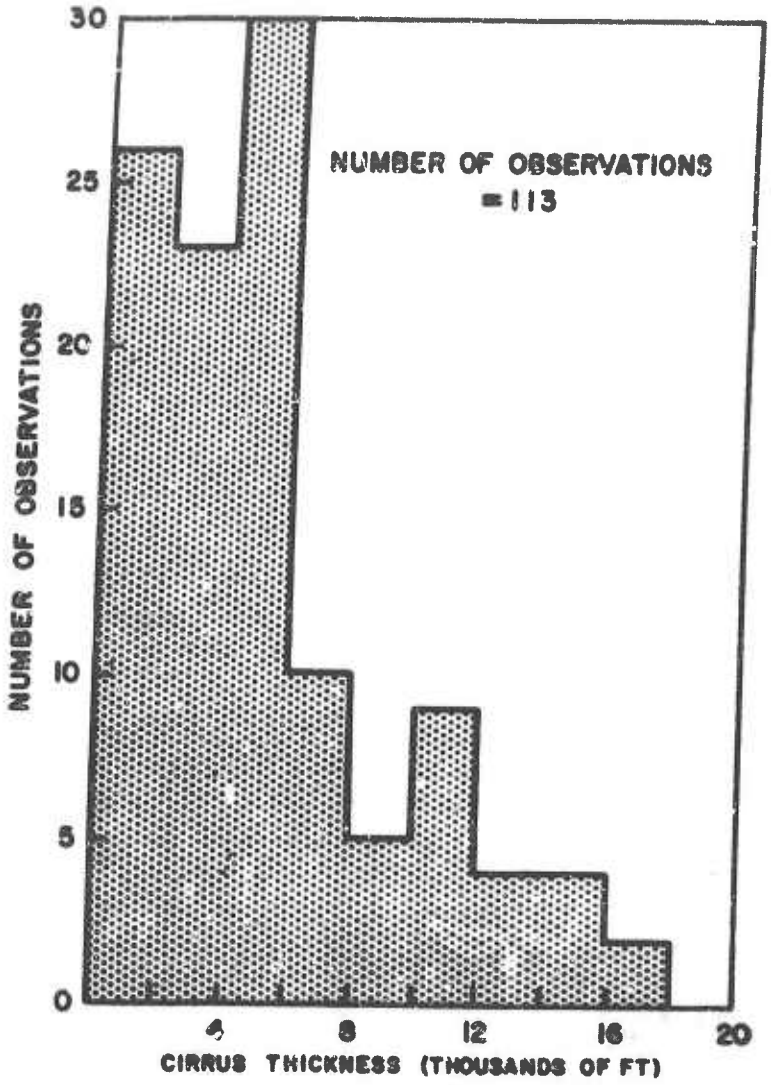

Figure 12. Frequency Distribution of Cirrus Thicknesses Observed on British MR Flights of 1952-54 [36].

7500 feet, most of which included associated altostratus. The average thickness was greater in the warmer season.

In the RCAF aircraft cirrus data over southern Canada [12] there were 400 reports citing the thickness. The means of these were:

warm months	6,700 feet
intermediate months	6,399 feet
cold months	6,000 feet
annual	6,300 feet

3.3.0. Frequency.

3.3.1. Ground Observations. A vast amount of data on frequency of cirrus could be compiled and summarized from standard surface synoptic or observatory reports and from ships observations. A considerable amount of such summaries can be found in the literature, but it is doubtful that they contain much information of value for the forecaster, owing to the inherent limitations of the observations. These limitations are also serious for the forecaster who may attempt to use them in nephanalysis or in any method for forecasting cirrus; therefore, a notice of them is not out of place here.

In the first place, the international instructions [67] for observing and reporting cirrus are complicated and not easy for the observers to apply. Especially the distinctions between cirrostratus and altostratus and between cirrocumulus and fine-grained altocumulus are confusing and often confused (see paragraph 2.1.1). The division between cirrus and cirrostratus is vague and arbitrary (see paragraph 2.1.1). At night, without moonlight, much cirrus passes totally unnoticed [68] or is grossly misjudged as to type and coverage; there is probably no real diurnal variation in cirrus except where airmass thunderstorms or orographic effects are important (see paragraph 3.4). Lower or middle clouds on the horizon may look like cirrus, or vice versa. The difficulties of judging the nature and extent of cirrus from the ground, even when there are no lower obscurations, has already been pointed out in paragraphs 2.1.2, 2.1.6, and 2.1.7. When lower and/or middle clouds are present, which in many climates is a large proportion of the time, the cirrus are partly or totally hidden from the ground observer, who can only guess what cirrus if any exists in the obscured area. The outcome is that data on coverage and frequency of cirrus always give values too low and their variations tend to reflect inversely the variations in the phenomena obscuring cirrus rather than in the cirrus itself. Finally, instructions have changed from time to time and varied from country to country. Stations report in different codes according to the type of report and purpose. Observations are consequently often inhomogeneous. In view of all these circumstances the climatology of ground observations of cirrus is probably of little intrinsic value for the air-operational weather forecaster.

3.3.2. Observations from Aircraft. These provide an opportunity

to correct some of the bias in the surface observations. Schwerdtfeger [57] compared the frequency of high clouds observed from airplane meteorograph flights at Königsberg with the simultaneous ground observations at the same place, over a period of two years (1934-36). The results were as follows:

Define: Σ as the total number of days in the period of investigation (731 = total); O as the number of days the report of "cirrus" was made by the ground observer (G) (111 = total), or by the aircraft observer (A) (228 = total); and C_H as the number of days when the report of "high cloud" was made by the ground observer G (208 = total), or by the aircraft observer A (377 = total). Then:

TABLE IV

Percentage of Time when it was Possible for the Ground Observer (G) and for the Aircraft Observer (A) to Determine whether Cirrus or "No-Cirrus" was Present. Königsberg, 0800Z, 1934-36.

$\frac{O+C_H}{\Sigma}$	Summer	Winter	Year
G	56.6%	30.7%	43.6%
A	88.9%	82.9%	85.9%

As seen from the table the aircraft failed to get a complete view of the upper sky only 14.1% of the time. This could be partly due to aborted missions, but it was mainly because the aircraft was still in cloud at its ceiling (about 500 mb). The ground observer on the other hand was unable 56.4% of the time to make any decision as to whether cirrus was present or not. The figures reveal quite strikingly the large number of occurrences of high cloud which ground observers will fail to see for one reason or another. Where low and middle clouds are frequent, the ground observations of cirrus probably record but 50% of the true frequency. This conclusion is supported also by French and Johannessen [24] and by Cole [13].

Murgatroyd and Goldsmith [45] had occasion to compare ground and aircraft cirrus observations in connection with the British MR Flights of 1949-52 from South Farnborough. The ground observations had a pronounced diurnal variation, the day hours reporting about twice as much as the night hours. Clear skies with no cirrus were reported 20% of

the time by day and 40% at night. More cirrus was observed in summer than winter. The diurnal and seasonal variations were similar at three stations in southern England (but ratios of cirrus to no-cirrus were greater towards western England). Cirrus sheets are often extensive and sometimes cover almost all the British Isles. Periods when the high clouds are obscured by lower ones occur 60% of the time in winter and 45% in summer, a maximum at dawn and a minimum at dusk. All this strongly suggests a large bias from darkness and lower clouds. The frequency of ground reports of C_H code numbers was greatest for $C_H = 2$ and $C_H = 1$, followed by $C_H = 3$, $C_H = 8$, $C_H = 6$, $C_H = 9$; the numbers $C_H = 0$, 7, 5, and 4 were seldom reported.

The <u>aircraft</u> observations gave:

high cloud in immediate vicinity	46%
high cloud visible in distance	27%
no high cloud	27%
	100%

Thus, about 50% of the time in daylight there is high cloud above southern England and only 25% of time is cirrus absent. There is a small seasonal variation in these frequencies, spring having fewer "cirrus" and more "no-cirrus" than other seasons. Summer and autumn have somewhat more cirrus than winter and spring, which is only roughly similar to the surface observations.

James [36] in discussing the 1952-54 MEF observations found that the aircraft reported "cirrus" about twice as often as "no-cirrus."

In the 2,000 RCAF flight observations of cirrus over southern Canada [12] (see paragraph 3.1.6), little or no significant geographical and seasonal variation in frequency was found. In analyzing this data Clodman computed the percent of the aircraft-reported cirrus sky-coverage ("total cirrus," see paragraph 3.1.6) which occurred with an undercast (45%), without an undercast (21%), with precipitation (60%), and "unspecified" (33%). One may readily infer from these figures that a large proportion of the cirrus, probably well over 50%, is obscured from ground observers. Clodman further estimates that even 40% of the "total cirrus" coverage was with an undercast but without precipitation (see also paragraph 4.1.2). Additional thickness data are given in [80].

3.3.3. <u>Radar Observations</u>. Observations by an experimental Radar Cloud Detector developed by the Signal Corps Engineering Laboratories [64] [50] indicate such a device can detect much cirrus that a ground

observer does not see. In a year's test at Belmar, New Jersey, during 1951-52, this .87-cm radar-observed high clouds 51.5% of the time, the radar and ground observer alone but 14.5% of the time [64]. There were only a few cases when the radar missed cirrus reported by the ground observer. Aufm. Kampe and Weickmann [73] reported they obtained continuous echoes on a 1.25-cm model of this radar from regions where large ice crystals (snow?) were present but no obstructions to visibility were observed! It was estimated for a 1.25-cm radar of less peak power than the above set that it can detect 40% of thick but no thin Ci fibratus, 20% of Cc, no thin Cs, and 70% of thick Cs [50].

3.4. Orographic Cirrus. Over the Alps and the Sierra Nevada, pilots have reported standing lenticular ("Moazagotl," "Bishop Wave") clouds which were high (i.e., cold) enough to produce plumes of cirrus streaming from them. These must be cases where the temperature at cloud level is below -35°C. Then, although the lenticular cloud is forming and evaporating continually as a cloud of water drops, a certain proportion of the droplets freeze before they reach the evaporating lee edge of the cloud. The ice crystals drift away with the wind as a long band or as successive patches of cirrus [42].

Ludlam [42] has observed this process in high lenticular clouds caused by low hills in southern England, for even hills can disturb the flow up to 30,000 feet or more under certain conditions. These conditions are more frequent at night when the lower air is stable, and this may partly explain a peculiar ground-observed diurnal variation in cirrus over southern England.

3.5. Tropical Cirrus. The cirrus of the subtropics over land is mainly from anvils; at sea it is mostly Ci or Cs spissatus and fibratus associated with general convergence in easterly waves, in high-level disturbances, or in the tropical exensions of mid-latitude troughs of the westerlies. The Cb is not a common cloud over the open tropical oceans. Cirrocumulus is rare but appears to be unassociated with other cirrus and is easily confused with altocumulus. A characteristic situation in the trades is for one isolated tall Cb cloud moving westward with the lower winds to produce an enormous extent of cirrus spissatus or Cs in a few hours because the anvil is continually sheared off in the oppositely-directed flow aloft (antitrades) [43].

The equatorial zone of general convergence between the Northern and Southern Hemisphere trades has rather persistent multi-layered

cirrostratus overcasts or dense cirrus patches, with bases above 40,000 feet. Pilots in Africa [18] report this cloud is common over a distance of 1600 n.m. on the Cape-Cairo route. It is apparently formed and carried polewards in the general rising outflow from the intertropical convergence, and is not necessarily from anvils (see AWSM 105-48).

The height of tropical cirrus is deceiving to ground observers, who often estimate it at 30,000 feet, whereas pilots find it looks almost as high above them from 30,000 feet as from the surface.

The radiating cirrus stripes from tropical cyclones were formerly considered useful indicators of the location and approach of the storm, assuming the bands point in the direction of the storm center and outflow. This is valid only with severe limitations, because stripes are also produced by scattered anvils not associated with storms and because only certain sectors of the storms seem to produce stripes [16] [53].

Palmer [43] has analyzed the successions of skies associated with the slow passage of high-level cyclones ("distal cyclones") over stations in the equatorial mid-Pacific; the usual case was as follows:

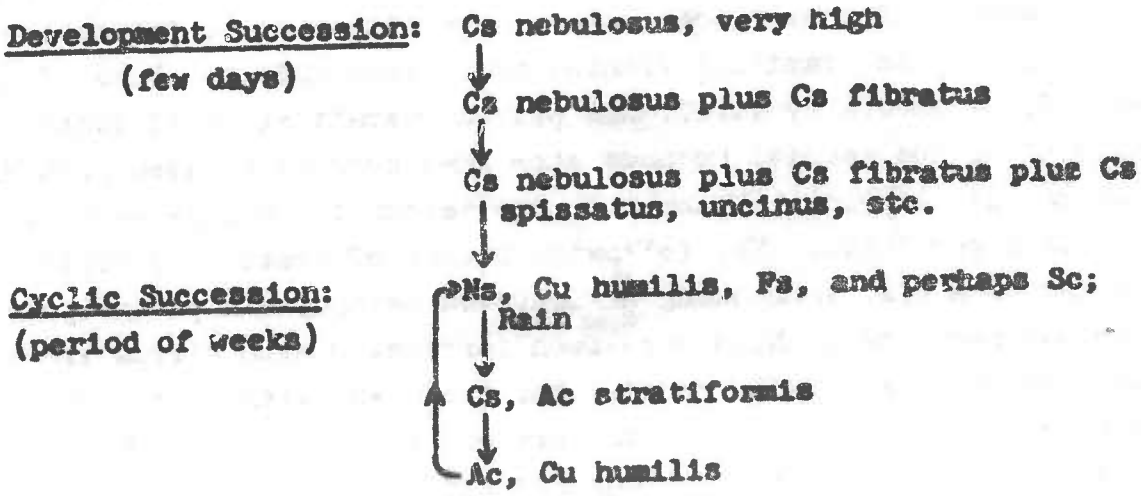

This sort of "model" when based on sufficient data may prove valuable as an indirect aerological aid, for example, in forecasting the approach of such disturbances. Palmer suggests several models [43] for the mid-Pacific.

3.6. Polar Cirrus. In high latitudes in winter the lower air masses often cool by radiation to temperatures well below -30° or -40°C and even to -70°C, which persist for weeks or months. It is possible under such conditions for ice-crystal clouds formed in middle or high levels to descend to low levels, or even to form there, and this is sometimes

observed. In addition, ice-crystal fogs and hazes form near the ground. Over the Arctic basin in winter a thin ice "mist" prevails, which can be considered a cirrus cloud at the surface. However, the "ice fogs" occurring around airfields and settlements are artificial clouds, like contrails, resulting from addition of moisture to the air by combustion of hydrocarbon fuels (see AWSM 105-44). An optical phenomenon known as "diamond dust," due to fine widely scattered ice crystals floating throughout a large body of air, is also commonly seen in high latitudes in winter when the sun or moon is up. In this case the concentration of crystals is too slight to noticeably reduce visibility or to be called a "mist." These thin cirrus types of the polar regions frequently produce the characteristic pillar form of halo.

High-level cirrus hazes, invisible from the ground but seriously reducing visibility aloft, are frequently reported by pilots in the Arctic. While this sort of thing is also common elsewhere, the illumination conditions in the Arctic probably aggravate the problem.

4.0. The Cirrus Forecasting Problem.

Only four special methods of forecasting cirrus have been published. Also, undoubtedly many forecasters have attempted to forecast cirrus or high-cloud using familiar frontal or cyclone models. None of these methods or models by itself has proven operationally adequate though several of the special methods show some success or seem promising for further development. Meanwhile, the search for a more satisfactory solution continues. The following review of previous studies is intended to assist in seeking an improved method. In paragraph 4.1, various parameters which have been correlated with cirrus are listed and the results briefly noted. For those who wish to try the special methods already proposed, these are outlined in paragraphs 4.2, 4.3, 4.4, and 4.5. Some suggestions for further experiment are mentioned in 4.6.

4.1.0. Parameters Which Have Been Correlated with Cirrus Occurrence or Formation. From a survey of the more accessible literature, various attempts to relate cirrus to certain meteorological parameters or synoptic conditions were noted. Such correlations are of interest in that they may suggest the bases for forecasting methods [22]. However, some of this work is of only negative or historical value. Additional parameters, not yet adequately analyzed in relation to cirrus but which might well be tested, are mentioned in paragraph 4.6. There are 16

parameters discussed in the following paragraphs. The order of treatment corresponds to the sequence in which a forecaster might consider these parameters while preparing a general surface and upper-air forecast. However, each parameter is discussed independently so that the whole sequence need not be read to understand any part of it.

The parameters and types of charts required to evaluate them are as follows:

Parameter	Paragraph No.	Chart(s) Required
Surface-Pressure Pattern	4.1.1.	Surface-Synoptic Chart
Fronts Aloft	4.1.2.	Surface and Contour Charts, or X-Sections
Contour- or Flow-Direction Aloft	4.1.3.	Constant-Pressure Charts
Contour Patterns Aloft	4.1.4.	Constant-Pressure Charts
Vorticity Advection, 300 mb	4.1.5.	300-mb Chart, With or Without Vorticity Lines Added
Pressure- or Height-Change Aloft	4.1.6.	ΔP or ΔH Chart, or Raobs on AWS Form 72
Temperature Aloft	4.1.7.	Constant-Pressure Charts, or Raobs
Temperature Change Aloft	4.1.8.	Constant-Pressure Charts, or Raobs
Thickness	4.1.9.	Thickness Charts
Thickness Advection	4.1.10.	Surface or Contour Chart With Thickness Lines Added
Tropopause	4.1.11.	Tropopause Chart, Raobs or X-Sections
Wind Shear	4.1.12.	Constant-Pressure Charts, or Winds-Aloft Charts, or Wind Profiles, or Max-Wind Shear Charts
Lapse Rate	4.1.13.	Raobs, or Thickness Charts
Vertical Motion	4.1.14.	Vertical-Motion Charts, or Thickness-Vorticity Charts
Humidity	4.1.15.	Raobs, Constant-Pressure Charts With a Moisture Index Added
Jet Stream	4.1.16.	Isotach Charts, Winds-Aloft Charts

4.1.1. Surface-Pressure Pattern. During the era when weather forecasting was based solely on surface-isobaric analysis many meteorologists [11] [63] attempted to find an empirical-statistical relation between the directions and speeds of cirrus in advance of depressions and the subsequent weather (– a primitive sort of indirect aerology). With the advent of the Norwegian School of synoptic meteorology, this idea took on a more rational expression in the form of cyclone and frontal models which embodied the associated idealized cloud distributions. In these models the cirrus thickening and lowering into altostratus is taken as the characteristic sequence in an advancing warm front. The cirrus of fair weather, i.e., outside the cyclone cloud-shields, was not clearly identified nor accounted for in the Norwegian models. However, the empirical cloud-distribution model for an occluded cyclone developed by Schereschewsky and Wherlé in 1923 and later incorporated in the International Cloud Atlas (editions of 1931 and 1939), does recognize a typical cirrus distribution outside the frontal shields (Figure 13). Also the International (Copenhagen) Synoptic Code for States of the Sky was designed in a way which attempts to distinguish between pre-warm-frontal cirrus and other formations of cirrus, mainly accordin to the synoptic experience of Bergeron in western Europe. Useful as these models have been in general weather analysis and forecasting since 1923, experienced forecasters are well aware that using these aids alone one cannot or could not satisfactorily forecast the occurrence of cirrus as a distinct entity nor as to the criteria affecting military operations [1] [2]. The gross oversimplification in these models is well brought out in the detailed nephanalytic study of a winter situation over the United States by Conover and Wollaston [14]. It is well-known that much cirrus is observed which has no obvious causal relation to any features analyzed on the surface synoptic charts. A statistical analysis [36] of the cirrus observations from British MR Flights 1952-54 in terms of distance from the surface-pressure centers and frontal positions showed about ¼ of the cirrus occurred remote from any marked front, whereas about ½ of the "no-cirrus" was reported within 400 miles of the fronts (see Tables below). (Note also paragraph 4.1.4, Wolff and Somervell's rules.)

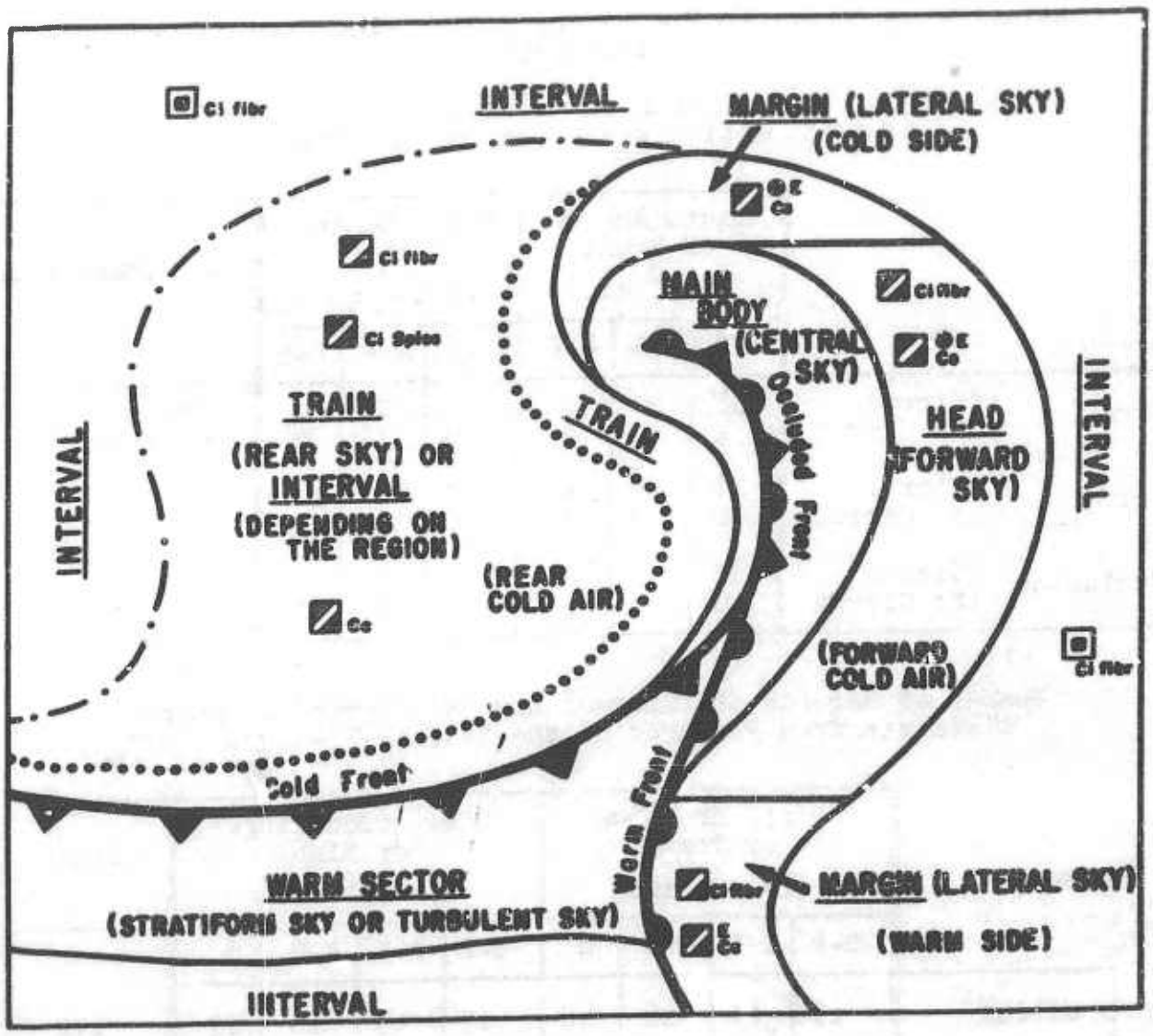

Figure 13. Distribution of States of Sky with Respect to an Idealized Extratropical Cyclone. (After Viaut, in preliminary draft for WMO "Atlas of Clouds," Paris, 1952.) The square symbols are meant to be representative of the entire zone in which they are located; only symbols for high-cloud are shown. High cloud is not shown in the Main Body as it is normally obscured by lower and middle cloud.

433730 O - 57 - 4

Relation of Cirrus to Fronts and Surface-Pressure Patterns
(from [36])

Number of Observations of "Cirrus" and "No Cirrus"
at Various Distances from Surface Fronts

		Dist. Ahead of Front ($\times 10^2$ mi.)			Dist. Behind Front ($\times 10^2$ mi.)			No Marked Front	
		0-2	2-4	4-6	0-2	2-4	4-6		
Warm	Cirrus	33	21	8	13	2	1	Cirrus	38
	No Cirrus	2	7	8	0	3	3	No Cirrus	33
Cold	Cirrus	18	12	4	10	3	1		
	No Cirrus	6	3	0	6	2	0		
Occlusion	Cirrus	12	3	0	3	5	1		
	No Cirrus	0	5	1	1	3	2		

Number of Reports of "Cirrus" and "No Cirrus" at Specified
Distances from Features of the Surface-Pressure Chart

	Dist. from Low or Trough ($\times 10^2$ mi.)				Dist. from Ridge or High ($\times$ [illegible] ^{2} mi.)				Totals
	0-2	2-4	4-6	6	0-2	2-4	4-6	6	
Cirrus	11	24	28	48	17	13	18	13	172
No Cirrus	4	8	3	18	9	12	4	11	69

4.1.2. Fronts Aloft. Above 500 mb the usual concepts of air masses and fronts have little application. It is difficult to find many clear-cut cases where the warm-frontal surface extends to the tropopause, except perhaps in winter in high latitudes. Most of the fine cirrus seen ahead of (and above) warm fronts or lows initially forms detached from the frontal middle-cloud shield, though later some of it may trail downward to join with Ac-As (see paragraphs 2.1.1 and 3.2). The flow processes (troughs, jet streams, etc.) causing this upper detached cirrus and those causing the warm-front clouds are of course often dynamically closely coupled, and in this way an apparent connection of the high- and middle-cloud can result (see paragraph

4.1.16). However, it has been suggested that cirrus fallstreaks may also play a trigger role in the development of the middle clouds and precipitation through the effect of the ice crystals in cooling, moistening and "seeding" the regions into which they descend [10] [50] [81]; others [40] [79] doubt this and point out cases where the cirrus seeding Ac causes it to dissipate, as also happens in many artificial cloud-seeding experiments with dry ice ("overseeding").

Clodman's [12] analysis of the RCAF flight observations of cirrus over southern Canada contains a table of percent of cirrus cases at 30,000 feet, at 35,000 feet, and at 40,000 feet, and the "total cirrus" coverage (see paragraph 3.1.6), occurring with undercast, without undercast, and with precipitation:

	30,000 Feet	35,000 Feet	40,000 Feet	"Total Cirrus"
With Undercast	25.3%	9.6%	1.8%	45%
Without Undercast	8.7	4.4	1.8	21
With Precipitation	38.7	15.3	2.1	60
Unspecified	15.7	7.6	2.2	33
Mean of All Cases	15.2	6.7	1.9	31

The 60% of "total cirrus" with precipitation is cited by Clodman as justification for forecasting cirrus whenever an active warm-front is approaching. However, the fact that the cirrus frequencies fall off with height to about the same amounts at higher levels, in undercast and precipitation as well as in other unspecified conditions, strongly suggests that only the lowest cirrus is very noticeably connected with frontal activity. (Much of the cirrus with precipitation was probably anvil cirrus.)

In paragraph 2.1.1, it was pointed out that cirrostratus and altostratus may be spatially continuous; this is generally the case with the solid warm-front shield which appears as cirrostratus on its leading edge and gradually lowers to altostratus and nimbostratus towards the center of the disturbance. The solid shield, however, does not usually extend above 500 mb; and if the temperature at the edge of the shield is warmer than -30° or -35°C, the whole cloud system is probably really As even though ice or snow crystals may predominate (see

paragraph 2.1.1). The sharpness and manner of advance of the forward edge of the shield will differ according to whether it is of ice crystals or droplets, whether it is preceded by a pronounced ridge line (subsidence area), whether the moisture and effective nuclei are uniformly distributed, etc. Thus, patchy or wave-like formations may or may not precede the solid shield, or the shield may never become solid.

Conover and Wollaston's study [14] and the time-lapse photos taken by Mr. Larkin at Buffalo indicate that the cirrus appears to break away from the region of the warm-front shield in waves or surges which move faster than the shield as a whole owing to the increase in wind speed with height. This could be cirrus formed by over-running or by Cb of the front, or it may be independent detached cirrus of higher levels.

Cirrus observed with the cold-front cloud shield either originates from cumulonimbus along and behind the front or from convergence around an associated upper trough. In many cases there is no post cold-front cirrus, presumably owing to the marked subsidence aloft. Squall-lines can also produce much anvil cirrus which spreads out in advance and persists after the Cb dissipate.

4.1.3. Contour or Flow-Direction Aloft. Many early investigations [63], having very little or no direct aerological soundings available, made use of observations of cirrus motions to study the upper-level flow patterns, both synoptic and mean. In retrospect the results of these analyses appear, in their larger features at least, to be remarkably in agreement with recent direct observations. Studies [11] were also made to find a relation between cirrus motions and ensuing motions of associated surface lows or highs, leading to useful rules that were familiar to forecasters of a generation ago. Now the objective is the inverse, i.e., we now analyze the contour and wind fields to explain the origin of the cirrus and to perhaps forecast it.

Schwerdtfeger [57] tabulated the aircraft cirrus reports from Königsberg 1934-36, according to the meridional component of the 500-mb flow as measured by the height differences Königsberg-Hamburg, and Königsberg-Breslau. Considering only the cases of flow greater than 10 m/sec, he found that cirrostratus is more likely with southerly and "pure cirrus" with northerly components. Even including the cases of weak flow the same general picture results. However, if the data for both types of cirrus were combined, the relation to wind direction would presumably be very poor.

Murgatroyd and Goldsmith [45] compared South Farnborough hourly ground observations of cirrus with 300-mb wind directions from Larkhill (6-hourly) for 1950-51. The percentage of high cloud was greatest when the wind was from the southwest to west and least when from the northeast to east. "No-high-cloud" showed an inverse relation. "Sky obscured" cases were about evenly divided among the directions. When the ratio of high-cloud to no-high-cloud cases is considered, the result is that westerly winds at 300 mb are more likely to produce cirrus even allowing for the fact that westerly winds are much more frequent than easterlies. James [36] in discussing the 1952-54 cirrus data (South Farnborough) found similar results for wind directions at levels from 500 mb to 200 mb. No relation with wind-speed was evident.

The dependence, if any, of cirrus upon upper-wind direction must be bound up with other parameters to be discussed below, and should be given consideration in that light.

4.1.4. Contour-Patterns Aloft. The cirrus forecasting method of Gayikian, described in paragraph 4.3, is based upon empirical models of upper-level flow-patterns associated with cirrus. The method of French and Johannessen (paragraphs 4.1.5 and 4.2) and the method of Hendrick (paragraph 4.4) lead from physical considerations to certain conclusions on the relation of the upper-level patterns to cirrus or no-cirrus; however, they do not use the patterns explicitly as models or as an independent parameter or predictor. For relation to the jet stream see paragraph 4.1.16.

One of the forecasting rules widely used in the United States for several decades or more, states that the ridge line at 20,000 feet preceding a warm front marks the forward edge of the cirrus cloud sheet. This undoubtedly refers to the edge of the solid Cs-As overcast. It probably does not include the fine cirrus, which would either be higher and/or would not evaporate immediately in the lee of the ridge. (Cf. paragraph 4.1.2.)

Commanders Wolff and Somervell of the U. S. Navy Project AROWA devised a more sophisticated set of forecast rules of this sort in which both surface and 500-mb patterns are considered. For a typical 500-mb wave pattern, they state:

a. No extensive Cs will occur before the surface ridge-line arrives.

b. Extensive Cs follows the passage of the surface ridge-line.

c. No middle clouds appear before arrival of 500-mb ridge-line.

d. Middle clouds tend to obscure the cirrus after the 500-mb ridge-line passes.

When the 500-mb wave is rather flat the cirrus arrival is delayed and the cloud is thinner. The greater the 500-mb streamline convergence from trough to ridge, the more the cirrus between the surface and 500-mb ridge-lines. Some kinship between these rules and the models of Gayikian (paragraph 4.3) and the principles of French and Johannessen (paragraph 4.2) will be noted. The Wolff and Somervell rules worked well at Norfolk and they have been used over the North Atlantic allegedly with success.

James shows [36] a relation of the "cirrus/no cirrus" ratio to the idealized 300-mb contour wave (ridge and trough), the ridge having the maximum ratio (Figure 19).

4.1.5. Vorticity Advection at 300 mb. French and Johannessen [24] constructed their method of cirrus forecasting (see paragraph 4.2) on two premises: that at least the sheets of cirrostratus are produced by large-scale general ascent at high levels (300 mb), and that the relative vertical-motion field at such levels can be evaluated in practice with the vorticity equation and equation of continuity. The tropopause is assumed to be a reference level of no vertical motion. The favorable region for high clouds would thus be found where there is positive vorticity advection at 300 mb, and also in the lower stratosphere above the region of negative 300-mb vorticity advection. (A model of the vertical motion and cirrus distribution around a jet stream can be derived from the same considerations and is discussed in paragraph 4.1.16.) Using some cloud reports from B-47 flights, the frequencies of cloud cover above 25,000 feet were compared statistically and synoptically with the computed 300-mb vorticity advection term. The results were in good agreement with the theory, viz: The probability of overcast high cloud shows a very definite increase as the vorticity advection increases. Fourteen percent of the cases of high cloud were found with negative vorticity advection and 86% with positive vorticity advection. Areas of high cloud were generally centered on the areas with maximum vorticity-advection values.

James [36] has verified French and Johannessen's results in an analysis of the cirrus reports from British MR Flights for 1952-54

(anvil cirrus cases excluded) He found 77% of all "thick cirrus" reported was in areas with pos. ve 300-mb vorticity advection; 66% of the cases of "no cirrus" were in areas with negative vorticity advection. Bundgaard [69] also obtains a verification of French and Johannessen's method.

(An incidental observation of French and Johannessen is possibly of interest: there were four flights on which areas of negative absolute vorticity were encountered and in each case these areas contained overcast high-cloud decks. The interpretation to be put on this is not clear.)

French and Johannessen's work may be looked upon as providing a justification or rationale for Gayikian's empirical models (paragraphs 4.1.4 and 4.3).

4.1.6. Pressure or Height Change Aloft. In connection with his attempt to justify the division between "pure" or "convective" cirrus and cirrostratus, Schwerdtfeger [57] correlated the occurrence of these two types with the sign of the 24-hour height change of the 500-mb surface at Königsberg. He found a slight tendency for "pure cirrus" to follow more often a preceding 24-hour pressure decrease aloft and for cirrostratus to follow more often a pressure increase. The relation is somewhat more pronounced for the cases of newly-formed cirrus only. (He also noted incidentally, that the appearance of cirrostratus was followed by a pressure decrease.)

Appleman, in a study reported more fully in paragraph 4.5, chose, as one of the predictors for an objective cirrus-forecasting technique, the 24-hour change in height at 300-mb. This parameter was taken as a partial measure of vertical motion at cirrus levels. The scattergrams including this parameter (see paragraph 4.5) did not show any consistent predictive relation of ΔH_{24} by itself to cirrostratus occurrence. However, ΔH seemed to have some predictive value when combined with other parameters.

4.1.7. Temperature Aloft. The temperature limits for cirrus formation and persistence were discussed from the physical standpoint in paragraphs 2.2.1, 2.2.2, and 2.2.10. Data on temperatures measured in cirrus clouds indicate occurrences extending over the theoretical possible range; but for any given place and season there appears to be a characteristic, more or less symmetric distribution having a maximum somewhere between -30° and -50°C.

Aufm. Kampe [37] and Weickmann [65] took temperature measurements at bases and tops of cirrus on 120 fine-weather days during research flights from Ainring, 1939-42. The frequency curves (in 4° steps) for these are given in Figures 14 and 15. The cirrus-top temperatures are probably mostly controlled by the tropopause height (see paragraph

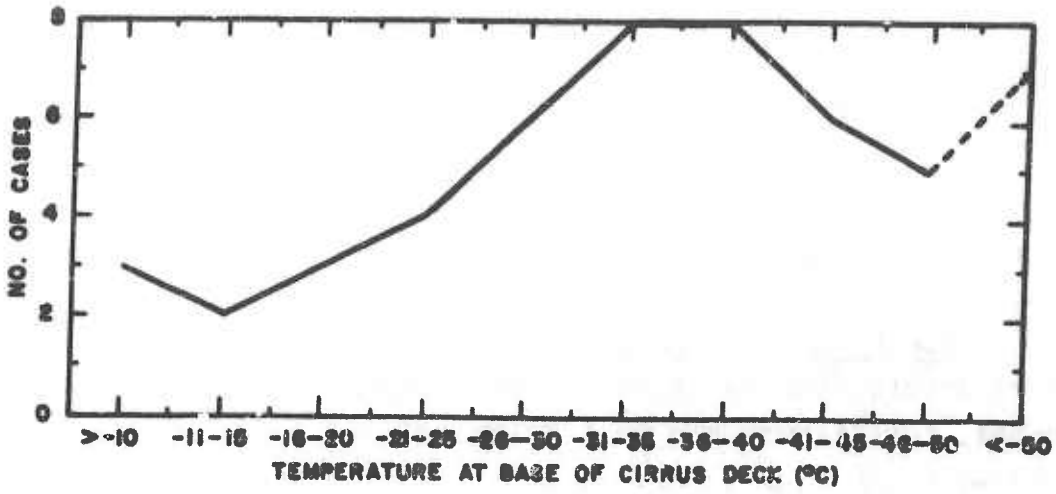

Figure 14. Frequency Distribution of Temperatures at Bases of Cirrus Decks Observed in Research Flights from Ainring, Bavaria, 1939-42 [65]. Data grouped by 4° intervals.

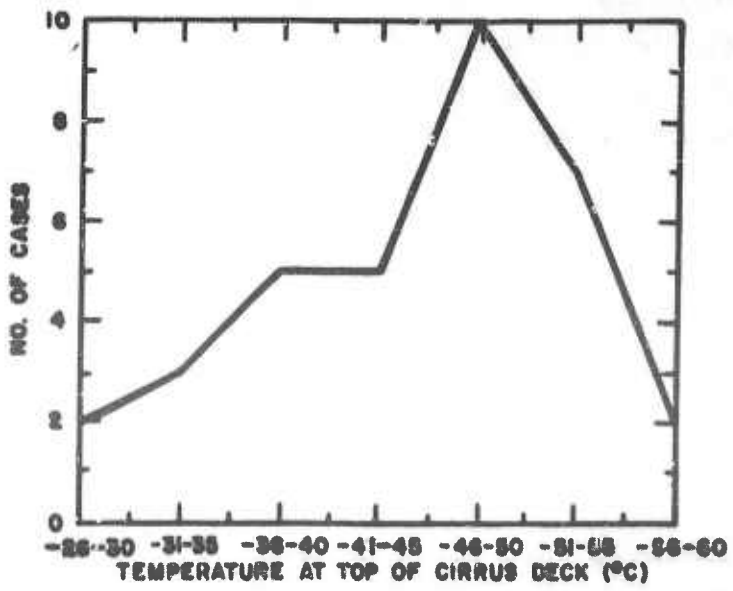

Figure 15. Frequency Distribution of Temperatures at Tops of Cirrus, Ainring Flights 1939-42 [65]. Data grouped by 4° intervals.

4.1.11). On the other hand, the wide frequency spectrum for the base temperatures is not so easy to explain. Weickmann suggests it may be indicative of the great range in the critical temperature at which freezing nuclei become active. The greater frequency is from -31° to -50°C. These cases probably represent mostly young cirrus not yet descended far down into warmer regions, whereas the cases from -10° to -30°C are either old cirrus much evaporated after long descent from higher levels or water clouds converted to ice by colloidal instability or by natural "seeding."

On Project Wiback (United States, winter-spring 1951) the temperatures recorded at cirrus-layer bases showed a maximum frequency at -20° to -25°C, the values ranging from -15° to -55°C [22]; some of these cases are obviously too warm to be true cirrus.

Murgatroyd and Goldsmith [45] in their study of the 1949-52 MR Flights from South Farnborough, compiled the frequency distribution of temperatures at base and top (Figures 16 and 17). The most frequent base temperatures are in the -40° to -46°C range, with cases spread from -23° to -62°C. The tops had a more extended double-maximum distribution ranging from -29° to -73°C, though very few cases were warmer than -40°C, which is the critical temperature for "spontaneous" cirrus formation. The double-maximum perhaps reflects the effect

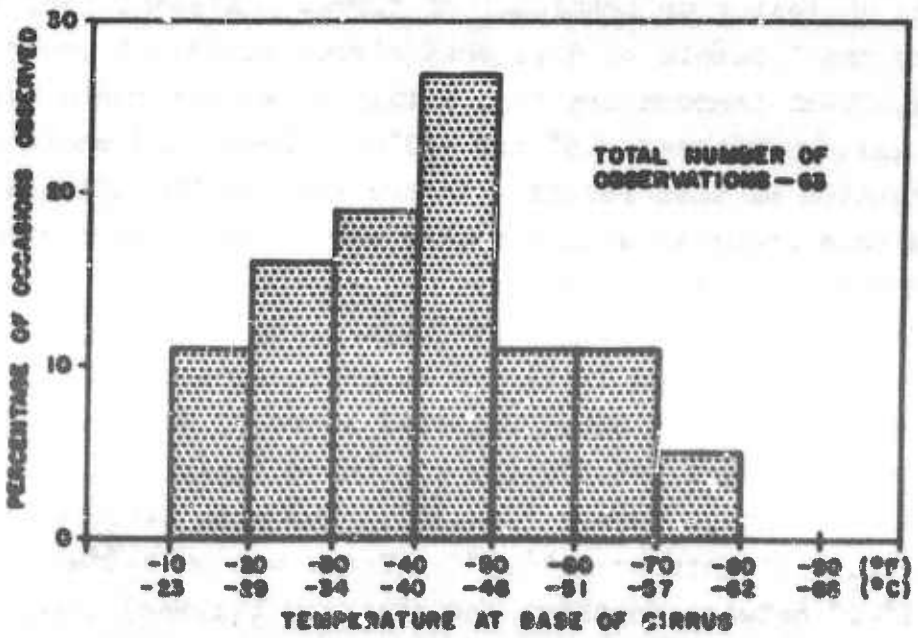

Figure 16. Frequency Distribution of Temperature (°F) at the Bases of Cirrus Clouds Observed on British MR Flights, South Farnborough, 1949-52 [45]. Data grouped by 10°F intervals.

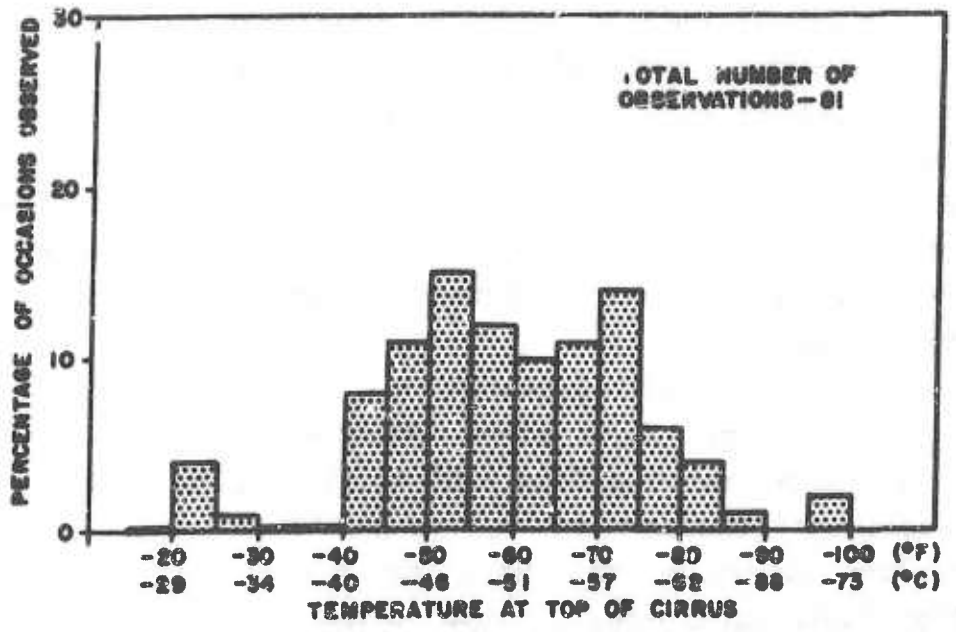

Figure 17. Frequency Distribution of Temperature (°F) at the Tops of Cirrus Clouds Observed on the British MR Flights, 1949-52 [45]. Data grouped by 10°F intervals.

of the two types of tropopause – polar and tropical.

Several investigators have considered using the 500-mb temperatures as an indicator or predictor of cirrus. Kimachi [38] concluded from a very small sample of data that cirrus would not occur over Japan unless the 500-mb temperature fell within a certain range having a frequency maximum between -18° and -29°C. James [36] could not find any verification of this relation in the British MRF 1952-54 data; also his cirrus data occurred with a rather warmer range of 500-mb temperatures than Kimachi's rule requires.

Statistics on temperatures at "high-cloud" bases (≥25,000 feet) observed on Project Cloud Trail are given in Appendix A. The mean temperature at all cloud bases reported above 25,000 feet (including some middle cloud) was -45.3°C for scattered layers (.1-.5) and -43.6°C for broken or overcast layers (.6-.10). The mean temperature for all the Cloud Trail flights was -48.5°C. There was an average difference of about 1°-2° between northern and southern (warmer) cases in the United States; however, the median values show a greater difference, as the distributions are somewhat skewed. Some seasonal variation is evident too. There were some cases reported down to the neighborhood

of -67°C, and some cases warmer than -30°C, which very probably were not true cirrus. Eliminating the latter would not greatly change the mean values.

Clodman [12] associated mean temperatures at 500 and 400 mb with mean cirrus-height distributions (see paragraph 3.1.6) over Canada.

.1.8. Temperature Change Aloft. Schwerdtfeger [57] analyzed the soundings and cirrus observations of three German balloon-sounding stations, separating the cases of "cirrus," "cirrus and cirrostratus reported coexisting" and "cirrostratus alone". The mean values of 24-hour temperature change at each kilometer level up to 12 km were tabulated for each of these cloud types. Figure 18 shows the results.

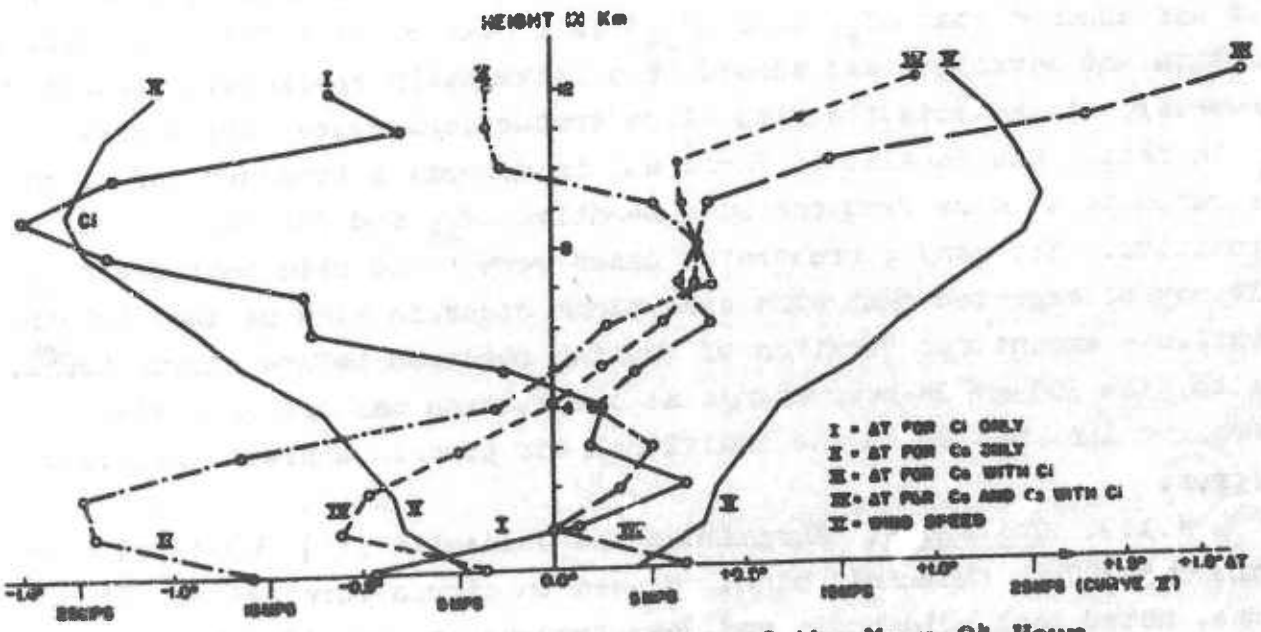

Figure 18. Distribution With Height of the Mean 24-Hour Temperature Change (at each km level), for Situations Reporting (over the sounding stations): "Cirrus Alone" (Curve I), "Cirrostratus Alone" (Curve II), "Cirrostratus and Cirrus Coexisting" (Curve III), "Cirrostratus, and Cirrostratus with Cirrus, Combined" (Curve IV), "Mean Wind Speed With Height" (Curve V). For Hamburg, Lindenberg, and Munich, 1932-35 [57].

Curve I, for cirrus alone, shows the prevalence of temperature falls at cirrus levels before the occurrence of the type; Curves II, III, and IV for "cirrostratus," "Ci + Cs," and "Cs" + "Cs + Ci," respectively, indicate temperature rises at cirrus levels before these types occur. Schwerdtfeger points to these figures as supporting his theory of the physical and synoptic distinction between "pure" or "convective" cirrus

and cirrostratus (see paragraph 2.2.5). The steepness of the slope of Curve I, he says, indicates a tendency for an increased lapse rate aloft owing to the strong wind shear (see wind profile plotted on Figure 18), to result in the formation of the shallow convective layers that produce "convective cirrus." The warming aloft with Cs and Ci + Cs is attributed to the upglide advance of warmer air that causes cirrostratus. This sort of correlation seems reasonable for western Europe but might not be expected over the eastern sides of the continents.

In his objective cirrostratus-forecasting study, Appleman (see paragraph 4.5) included the 24-hour change in 300-mb temperature as one of the predictors. Though he found it to be one of the best predictors of those tried, the results were anomalous and difficult to interpret. It was assumed that ΔT_{24} (and ΔH_{24}) is a measure of effects of vertical motion and advection and should be a universally applicable predictor. However, its association with cirrostratus occurrence varied greatly with season and locality. There was in general a tendency for cirrostratus to be more frequent with negative ΔT_{24} and for "no cirrus" with positive. Yet many cirrostratus cases were found with positive ΔT_{24}. It may be expected that such exceptions occur, in view of the certain variable amount and duration of cooling required before cirrus forms. Also, the 300-mb 24-hour change at one station may not accurately measure the changes in the individual air parcels wherein the cloud forms.

4.1.9. Thickness. Murgatroyd and Goldsmith [45] suggested that the 500-300-mb thickness might be used in cirrus forecasting, since they noted that cold pools and deep troughs on the 500-300-mb thickness chart are often accompanied by large areas of high cloud. They observed from the 1949-52 MRF data that the high cloud generally occurs to the east and southeast of troughs, often with warm advection in the south end of the trough. With cold pools the high cloud was more widespread. Their view is that the warm-front cirrus is merely a special case of the warm-advection effect in the 500-300-mb layer. Cold advection in the 500-300-mb layer appeared to be associated with "no-high-cloud." The association of high cloud with warm advection is also indicated by other studies, using wind shear as a parameter (see paragraph 4.1.12).

James [36] considered the relation of the 1000-500-mb thickness

values to "cirrus" and "no-cirrus" observed on the 1952-54 MR Flights. The mean thermal wind for cirrus was 21 kts and for no-cirrus 16 kts. He also related the position of cirrus in the 100-500-mb thickness pattern, by computing the ratio "Ci"/"no-Ci" in each section of an idealized trough-ridge wave. The ratio was greatest in and near the thermal ridge and least around the trough (see Figure 19), which James

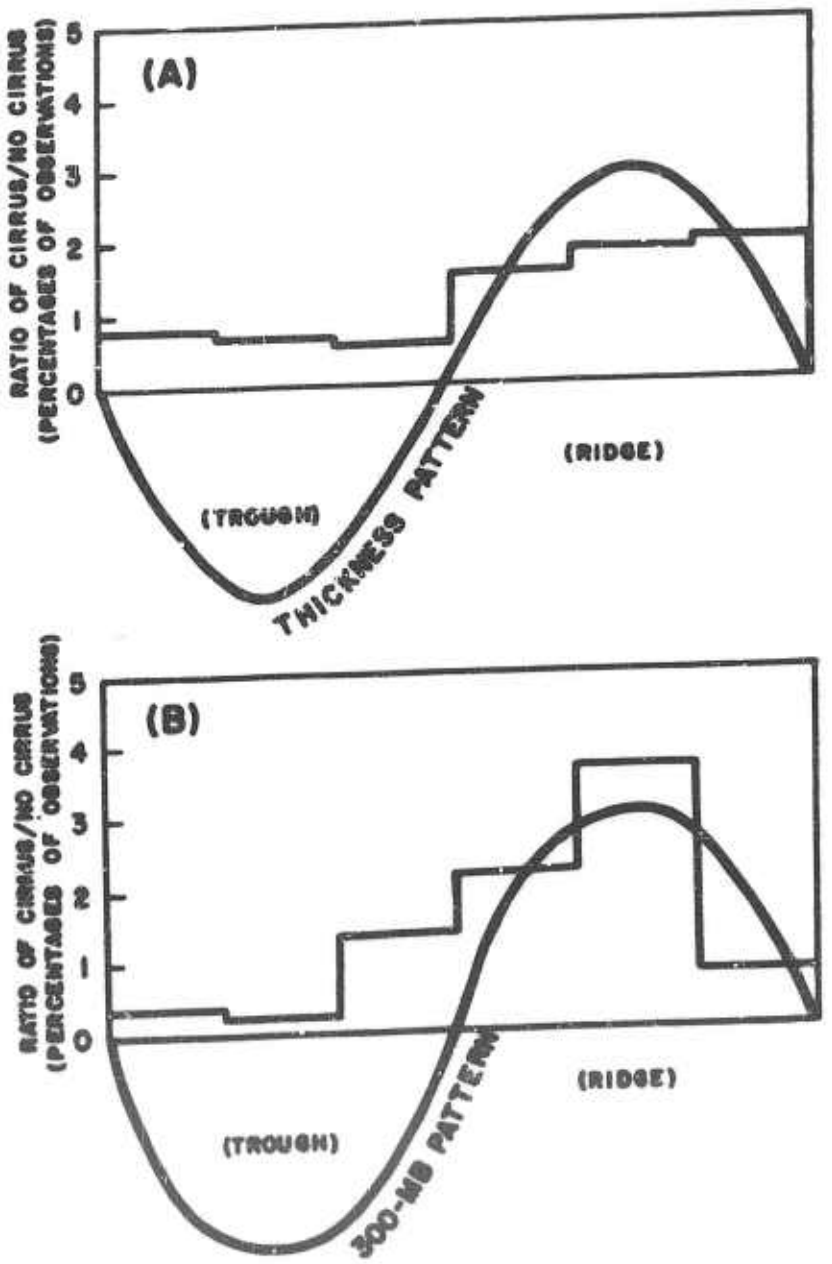

Figure 19. Ratios of Percentage of Number of Observations of "Cirrus" to "No-Cirrus" in Relation to: A, an Assumed Wave-Form in the Total 1000-500 mb Thickness, and B, in Relation to the 300-mb Contour Pattern [36]. Cloud data from British MR Flights 1952-54.

thinks is indication of the association of cirrus with warm fronts. Correlating the observations with the curvature of the thickness lines showed a tendency for cirrus to be almost equally frequent with anticyclonic, cyclonic, and straight isotherms, but there was definitely less of "no-cirrus" with anticyclonic than with cyclonic and straight isotherms.

4.1.10. Thickness Advection. Hendrick [31] used the sign of the 400-300-mb thickness advection, judged from the wind shear (see paragraph 4.1.12), as a parameter in his cirrus-forecasting method (see paragraph 4.4). This parameter was chosen as a measure of vertical motion. It was preferred for this purpose to the horizontal temperature advection because the effect of the latter on the local temperature change is more or less compensated by the vertical motion. The thickness advection combined with a moisture parameter was found to be correlated reasonably well with cirrus vs no-cirrus. It appeared that whereas with negative thickness advection no-cirrus is much more frequent than cirrus, with positive thickness advection cirrus is only slightly more likely than no-cirrus.

4.1.11. Tropopause. Early triangulated cloud-height data [63] revealed that cirrus and cirrostratus mean heights parallel the tropopause mean height, being higher toward the equator, lower near the pole (Figure 20). Until recent years, it has been generally assumed that the tropopause was the upper limit of cirrus occurrence. The experiences of high-flying-aircraft pilots have confirmed that the tops of most cirrus are at or below the tropopause, rather few cases having been reported within the lower stratosphere. Data from Project Wiback (1951) (Figure 21) showed this clearly [22] [23]. A larger sample is available from the British MR Flights. Murgatroyd and Goldsmith [45] in discussing the 1949-52 flights found the high clouds usually extended to or near the lowest tropopause (Figure 22), the majority to within 2000 feet of it. A few cases extended into the stratosphere a short distance. The relationship of the height of the tropopause to the base and top heights and thickness of the cirrus was examined (see Figure 23). There seemed to be some tendency in the mean for the cirrus not to extend as often to the tropopause when the latter was very high, and for the thickness to be greater under high tropopauses (an effect noted also in the Wiback data). As an explanation, it is suggested that the greater stability under high than under low tropopauses often limits the cirrus development in the former case to some

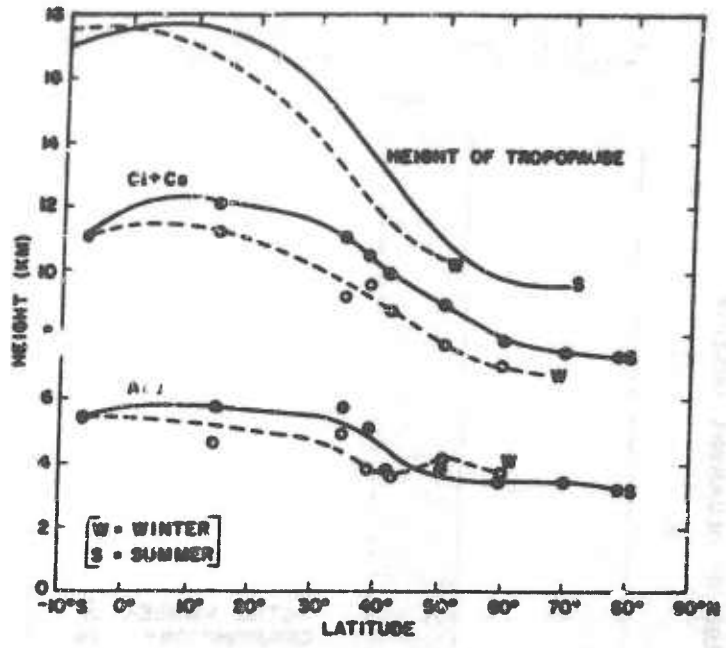

Figure 20. Variation with Latitude of Mean Cloud-Base Heights [from International Cloud Year (1896-97) data] and Lower Tropopause Mean Height [63].

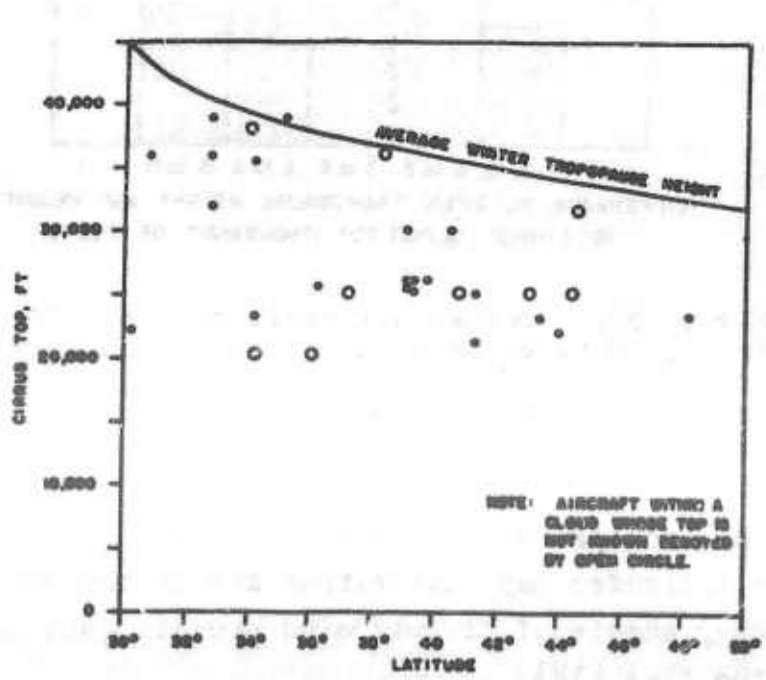

Figure 21. Heights of the Tops of Cirrus Cloud Layers (observed by flights of Project Wiback, winter-spring 1951) in Relation to the Average Winter Tropopause Height [22].

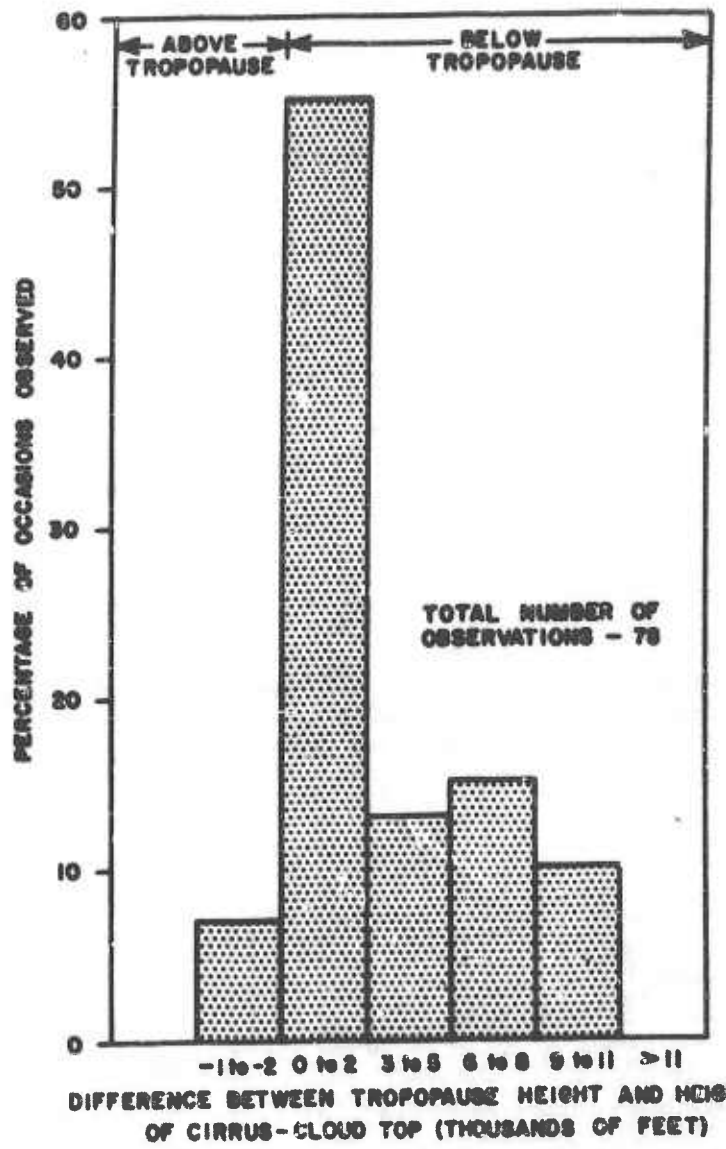

Figure 22. Frequency Distribution of Difference Between Tropopause Height and Height of Cirrus Cloud Top, British MR Flights, South Farnborough, 1949-52 [45]. Data grouped by 2000-ft intervals.

distance below the tropopause. Nevertheless, even the highest tropopauses in middle latitudes may have cirrus and in the equatorial convergence zone heavy sheets of cirrostratus prevail just under the tropopause most of the time [18].

James [36], analyzing the 1952-54 British MR Flights, found similar relations of cirrus to tropopause as Murgatroyd and Goldsmith, with a somewhat greater average distance of tops and bases below the

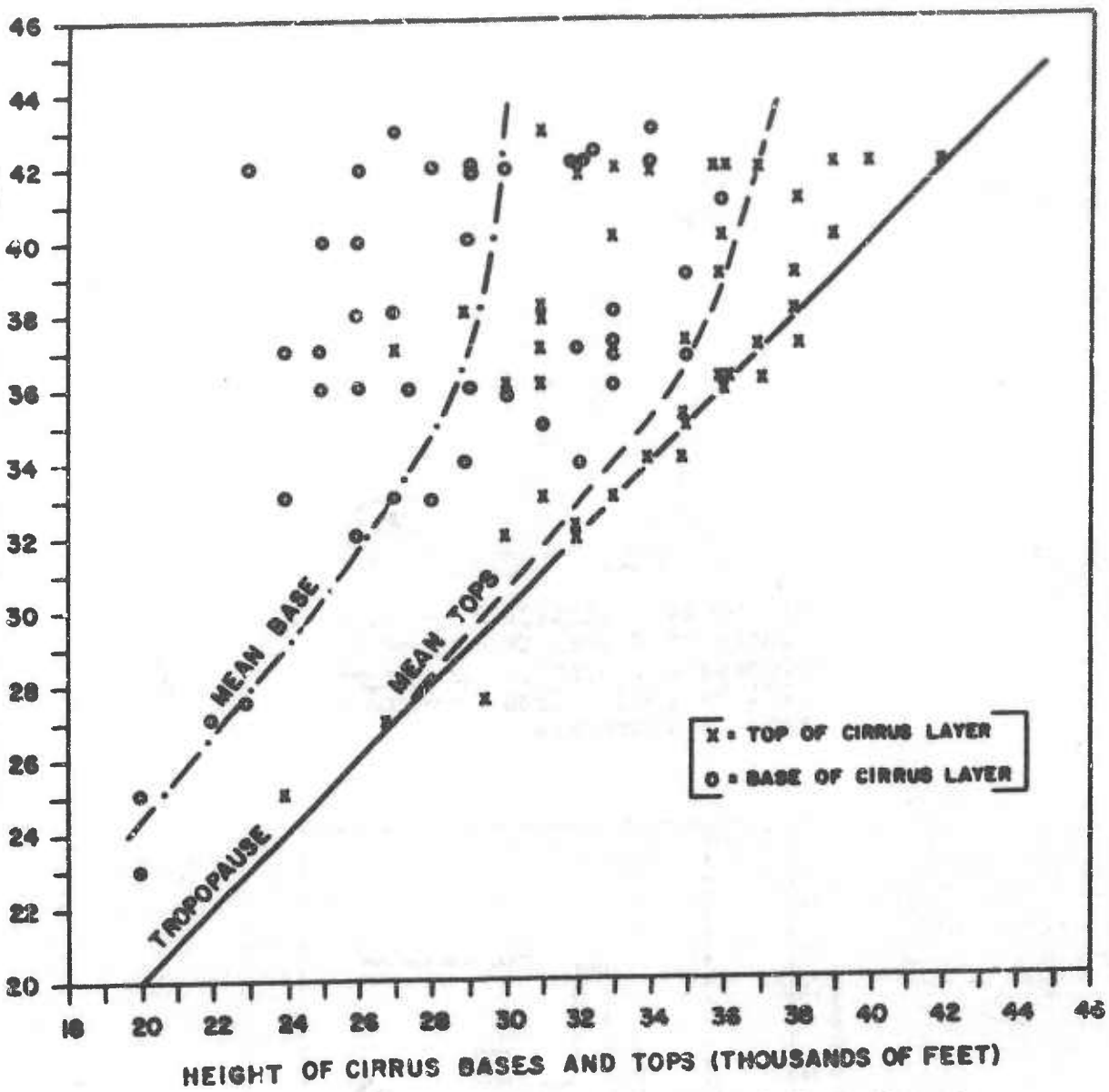

Figure 23. Heights of Cirrus Cloud Bases and Tops Versus Tropopause Height, British MR Flights, South Farnborough 1949-52 [45].

tropopause and with somewhat more (30) cases within the stratosphere (see Figures 24 and 25, and paragraph 3.1.3).

French and Johannessen [24], using cirrostratus observations from some B-47 flights over United States and adjacent Atlantic during January-February 1953 derived the following results on height of cloud top in relation to the tropopause (data included only broken and overcast cirrostratus decks extending for 100 miles or more):

433736 O - 57 - 5

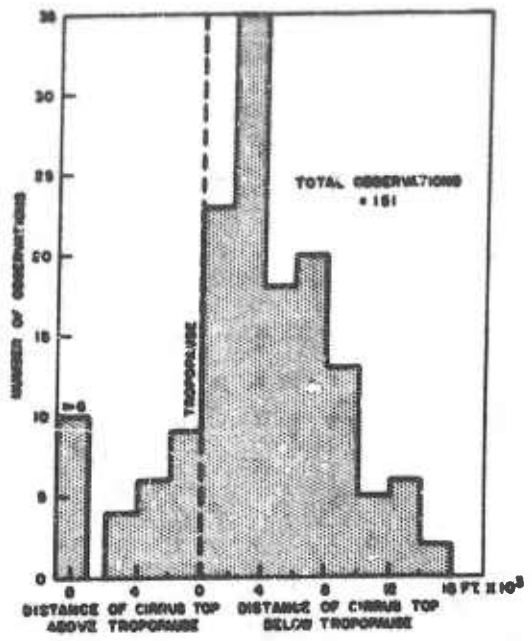

Figure 24. Distribution of Distances of Cirrus Tops from the Tropopause, British MR Flights, 1952-54 [36]. Data grouped by 2000-ft intervals.

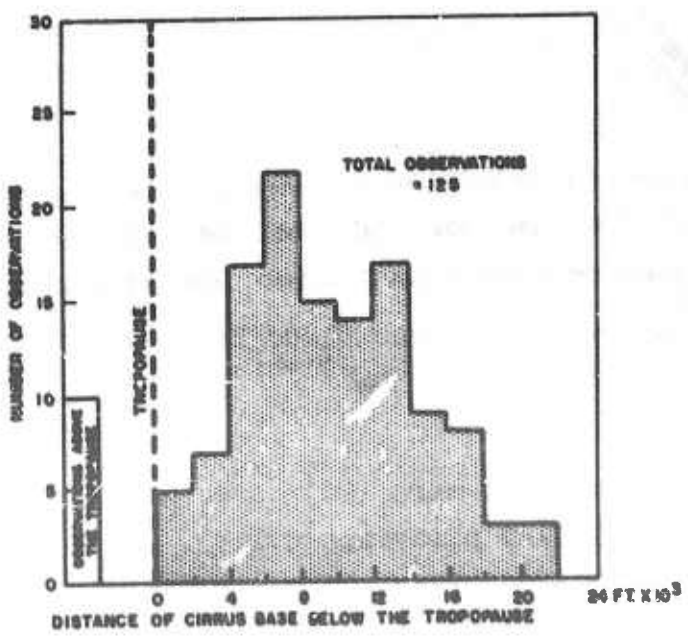

Figure 25. Distribution of Distances of Cirrus Bases from the Tropopause, British MR Flights, 1952-54 [36], Data grouped by 2000-ft intervals.

Height Difference: Cloud Top – Tropopause	No. of 100 Mi. of Cloud
Extratropical ("Polar") Tropopause (29,000-39,000 feet):	
More than 2000 ft above tropopause (3000 ft)	1
2000 ft above to 2000 ft below tropopause	44
2000 ft below to 3000 ft below	19
More than 5000 ft below	3
Tropical Tropopause (47,000-55,000 feet):	
From 15,000 ft below to 19,000 ft below	12
19,000 ft to 25,000 ft below	6
Total:	85

The important conclusion from this data is that most of the extensive cirrostratus has its top just under or at the "polar" or extratropical tropopause. This fact should be a valuable forecasting guide for middle latitudes, over North America at least. As a corollary, extensive cirrostratus tops should not be expected to reach to the tropical tropopause outside the tropics (see paragraph 3.5); and south of the "tropopause break" between polar and tropical tropopauses, the top of the extensive cirrostratus will reach only to about the height of the polar tropopause present to the north. However, patchy cirrus may be found closer to the tropical tropopause and even in the lower stratosphere.

Clodman [12] found verification of French and Johannessen's results in the RCAF flight data on cirrus over southern Canada: (see paragraph 3.1.6)

Season	Ht. of Max Occurrence	½ of Mean Thickness	Mean Ht. of Tops	Mean Tropopause Height	Difference: Tropopause Ht. Minus Cirrus-Top Ht.
Warm Months	30,800 ft	3,400 ft	34,200 ft	36,200 ft	2,000 ft
Intermediate Months	28,800	3,100	31,900	33,100	1,200
Cold Months	27,000	3,000	30,000	31,500	1,500
Average	28,900	3,200	32,000	33,600	1,600

A study by Endlich and McLean [80] [71], on data from Project Jet Stream, contains diagrams showing the distribution of all high-cloud reports around a model cross-section of the jet stream. The greatest frequency of high cloud was about 5000 feet below the polar tropopause, but at 15,000 feet below the tropical tropopause. Fine Ci usually occurred about 5000 feet closer to the polar tropopause level than Cs. Very little cloud was reported between the tropical tropopause and the level of maximum wind. Just above the polar tropopause a considerable percentage frequency (up to 16%) of cirrus (both extensive and patchy) is indicated. The data seem to suggest that very little or none of this cirrus extends above the level of the maximum wind (jet-core); however, very few flights were made in that region so no definite conclusion can be drawn.

4.1.11.1. Cirrus in the Stratosphere. The few cases of cirrus reported within the stratosphere are of special interest because they seem to contradict the general rule. Some of these cases are ones which have tops above the tropopause but bases below it, and others are entirely within the stratosphere. On theoretical grounds cirrus is quite possible anywhere in the stratosphere where there is enough moisture. Since the humidity generally decreases with height above the tropopause [7] [8] [17] [46], it is not surprising that little cirrus occurs there. Just above a tropopause which has recently formed at a relatively low level so that former troposphere air has been incorporated into the lower stratosphere, conditions should at least occasionally be favorable for cirrus. The region between the polar and tropical tropopauses over mid-latitudes but north of the jet-stream core is probably the locus of most of such cirrus. Several reports of very high "cirrus" in mid-latitudes were proven to be observations of dust clouds from volcanic eruptions [35]. The stratospheric cirrus is usually thin, but can be thick and rather extensive, as in some cases observed over England during the summer [4] [21] [29]. A widespread marked lifting of the tropopause region and high frost-points explain the case of August 9-10, 1951 [21]. Some of Project Jet Stream cases of cirrus above the tropopause were overcast or broken decks [71]. James [36], applying French and Johannessen's theory (see paragraph 4.2), suggests that the cirrus in the lower stratosphere occurs above the region with negative vorticity advection at 300 mb; this implies convergence, which gives downward motion at 300 mb in the troposphere

and upward motion in the stratosphere. No reports of cirrus in the stratosphere over the equator or the polar regions are yet at hand — the general stratospheric subsidence in high latitudes, the strong convective tropopause of the tropics, and the subsidence over the equatorial tropopause would seem to be unfavorable for injection of moisture into and hence cirrus formation in the stratosphere of these regions.

4.1.12. Wind Shear. The vertical windshear has been used as a cirrus forecasting parameter by several investigators. They chose the shear as a convenient measure of vertical motion or of thermal- and moisture-advection aloft. Schwerdtfeger [57], in a very primitive way, thought of the increase in wind speed with height as an indication of the existence of the "advection of cold air" aloft which he postulated as the cause of "convective cirrus" (see paragraphs 2.2.5 and 4.1.8). This assumption, of course, requires geostrophic departures and other conditions, which are generally admitted to occur often enough.

Fletcher and Sartor [22] [23] found a positive correlation between cirrus occurrence and simultaneous veering with height (warm-air advection) of the geostrophic wind from 700 to 300 mb. They suggested using this shear as a forecast aid. The cirrus-favorable regions would be found by placing the 300-mb over the 700-mb chart and shading the areas having crossings of 700-mb contours in the direction of increasing 700-mb heights. Areas with opposite kind of crossings are to be considered cirrus-unfavorable regions. This procedure could be applied to prognostic charts as well as current ones. The method was tested on 10 sets of daily charts (6-15 December 1948, 1500Z). The percentage of stations reporting clear skies at 1830Z was computed for different shear conditions, eliminating cases when lower or middle cloud was reported:

veering wind	8.2%
indefinite shear	16.8%
backing wind	35.8%

Cirrus was thus present (when not obscured) in 91.8% of the veering, 64.2% of the backing, and 83.2% of the indefinite conditions. However, in an unpublished test by Appleman on September data in which the presence of cirrus was correlated with sheears of actual winds, no significant relations were found. Perhaps this was because thunderstorm cirrus, which is presumably unrelated to shear, was common at this season.

In Gaylikian's cirrus forecasting method [27] (see paragraph 4.3)

there is a procedure for forecasting the cirrus heights based on the hypothesis that the top and base and thickness of "advective cirrus" have a close relation to the vertical wind shear. This was a subjective impression of the author and has not been tested statistically. He thinks the base is generally located where the wind profile starts marked increase in steepness and that the top is around the wind maximum. The type of profile having a pronounced wind maximum with strong shears is supposed to go with more and denser cirrus, a broad multi-maximum profile to have several layers of thin cirrus, and a flat profile probably no or very thin cirrus. It is difficult to apply these "rules" to the many profiles seen from GMD-1A soundings having numerous pronounced maxima and minima.

It would be of value to test these ideas objectively. However, any apparent association with the wind profile is probably incidental to the more direct correlations between cirrus and other parameters which are in turn related in some way to the wind profile.

James [36] attempted to test the idea of Fletcher and Sartor [22] on the relation of the shear to cirrus (see above). The number of occasions on the 1952-54 MR Flights on which warm or cold advection or neither were found with "cirrus" and with "no-cirrus" were tabulated separately for the 500-400, 400-300, 300-200, and 500-300-mb layers. (Cases with less than 5° or 5 knots change were classified as "neither.") Stratospheric cirrus was excluded. The results confirmed, for each of the layers, the greater probability of cirrus with warm advection than with cold advection, and of no-cirrus with cold advection than with warm advection. (In the "neither" cases cirrus occurred twice as often as no-cirrus.) The layer 500-300 mb gave the best correlation:

	Number of Cases		
	Warm	Cold	Neither
cirrus	70	37	35
no-cirrus	23	30	14

The use of wind shear as a parameter should give similar results as the use of the thermal wind or thickness advection (see paragraphs 4.1.10 and 4.1.11). In fact, Hendrick's method of cirrus forecasting

(see paragraph 4.4) adopts the wind shear as an indicator of the sign of the 400-300-mb thickness advection.

4.1.13. Lapse Rate. An AAF forecaster at Alamogordo, New Mexico [1] in 1943 devised an empirical cirrus forecasting rule, stated as follows: "Cirrus clouds will form over this station in the layer between 10,000 feet and 10 km when the difference in potential temperature ($\Delta\theta$) between these two levels is less than -14°C. Charts of the whole United States showed similar results but the extrapolation of the areas formed by isolines of $\Delta\theta$ values was far from successful. For periods of 6 to 12 hours, this rule can be used with a fair degree of confidence." No recent test of this is available.

Kimachi [38] suggested that steep lapse rates of temperature (0.2 - 0.4°C/100m) might be important in cirrus formation, but his limited data is not very convincing. Schwerdtfeger [57] had considered the theoretical amount of temperature change required to make the prevailing lapse rates at cirrus levels unstable through advection, mixing, lifting, etc. In his study of the conditions required for the mixing of air masses at an upglide front through release of latent instability, he notes a certain difference between ice-saturation and dry-adiabatic equilibrium lapse rates must be present. At high levels this difference is often insufficient, which is a difficulty with part of Schwerdtfeger's theory for cirrostratus formation. For the "pure" or "convective" cirrus, however, there is usually needed only a small differential cooling to make a shallow layer unstable at Ci levels. Following Schwerdtfeger's reasoning, certain lapse rates should be more favorable for cirrus formation, though it is not clear how these can be determined except from much more accurate soundings than yet available. James [36] could not find any significant difference of lapse rate between cirrus and no-cirrus situations in the 1952-54 MR Flights.

Appleman tried the temperature difference between 500 and 300 mb (T_3-T_5) as a predictor in his objective cirrostratus forecasting study (see paragraph 4.5). For most stations and seasons some predictive value was found when this parameter was combined with others. However, there did not seem to be any given range of T_3-T_5 which either locally or universally distinguished cirrus from no-cirrus; the frequency spectra of T_3-T_5 values for cirrus and no-cirrus varied considerably in shape and modal value from station to station and season to season.

Krebs and Doege [39] attempted to forecast cirrus occurrence and

heights over Germany on the basis of an idea suggested by Schwerdtfeger's work [57], viz., that "pure cirrus" layers should be associated with layers having relatively-steeper lapse-rate than above or below the cloud. Noting that pilots seemed to find cirrus clouds where predicted by this hypothesis, they collected pilot reports to analyze the relation further. From 183 pilot reports by USAFE jet flights penetrating clouds above 18,000 feet over Germany and adjacent regions, they selected 84 reports which gave data on the heights. These cases covered 37 out of the 59 days in the December 1954 – February 1955 period when pilots reported cirrus. It was not reported by the pilots what the types and amounts of cirrus were. The authors compared these cases with nearest radiosondes (mostly within 6 hours), tabulating the lapse rates associated with the reported cirrus layers. The results were grouped as follows:

I. (64 reports, 39 soundings) the lapse-rate changes near or at bottom and top of the cirrus were all within the troposphere and bounded by lapse-rate changes as predicted by the working hypothesis. In 33 cases the top was not identical with the tropopause.

II. (9 reports, 5 soundings) there was a relatively-steep lapse beginning somewhere in the middle-cloud levels, and a weakening of the lapse somewhere in the upper troposphere.

III. (11 reports, 7 soundings) no noticeable lapse-rate changes in cirrus levels.

The frequency of differences between the height of cirrus bases and the height of the lower change of lapse-rate, and between the height of cirrus tops and the height of the upper change of lapse-rate, was as follows:

Tops	
Height Difference	No. of Cases
-4,000	1
-3,000	1
-2,000	9
-1,000	6
0 (±900 ft)	15
+1,000	8
+2,000	4
+3,000	1

Tops	
Height Difference	No. of Cases
+4,000	6
+5,000	2
+6,000	2
+7,000	0
+8,000	0
+9,000	2
+10,000	1
+11,000	1

Bases		Bases	
Height Difference	No. of Cases	Height Difference	No. of Cases
-9,000	1	0 (±900 ft)	9
-8,000	0	+1,000	2
-7,000	0	+2,000	3
-6,000	0	+3,000	3
-5,000	1	+4,000	1
-4,000	0	+5,000	2
-3,000	5	+6,000	0
-2,000	3	+7,000	0
-1,000	8	+8,000	0

The authors' conclusion that the above results make their hypothesis seem probably true is not fully justified because they have not shown how frequently the various lapse-rate changes occur without cirrus being associated.

The authors also tabulated the values of the lapse rates found in cirrus (55 cases; if several different lapses in the cloud, each was counted):

Lapse	Frequency (No. cases)
>0.95°C/100m	3
>0.85 – 0.95	24
>0.75 – 0.85	20
>0.65 – 0.75	4
>0.55 – 0.65	3
>0.45 – 0.55	0
>0.35 – 0.45	0
>0.25 – 0.35	1
TOTAL	55

The same data were recomputed in terms of departure of the lapse from wet-adiabatic, and grouped according to change from the preceding sounding:

Departure From Wet Adiabatic °C/100m	Number of Cases: Total	Steepening Compared to Previous Sounding	Weakening Compared to Previous Sounding	No Change Compared to Previous Sounding
0 or Negative	9	6	0	3
>0.00 – <0.10	28	22	4	2
0.10 – <0.20	12	9	2	1
0.20 – <0.30	3	2	1	0
0.30 – <0.40	2	1	1	0
0.60 – <0.70	1	1	0	0
TOTAL	55	41	8	6

Of the nine lapse rates with conditional instability, only two could be defined as dry adiabatic lapse rates, a fact which the authors claim disproves Schwerdtfeger's hypothesis. They argue that if lifting causes cirrus, then it is only to be expected that the lapse rates in the lifted layer be steeper than in the layers just above and below, but not necessarily unstable, which is what the Table shows. Nor does the Table support the idea that any particular initial lapse rate favors cirrus formation.

Unfortunately, no particular forecasting conclusions can be drawn from the above statistics since we do not know the overall frequencies of these lapse rates and their time changes regardless of cloud – it could well be that their distribution is similar with and without cirrus, in which case they would not support either the Schwerdtfeger or Krebs-Doege hypotheses, and no cirrus-forecasting value in the lapse rate would be indicated. On the other hand, the figures do not rule out the hypotheses, except to the extent that lumping together of the "pure" cirrus and cirrostratus cases is inconsistent with Schwerdtfeger's original hypothesis on cirrus formation. Krebs and Doege's discussion of these data is somewhat confused and illogical, but it would be worthwhile to investigate the lapse-rate hypothesis further. H. Appleman, at Headquarters, 2d Air Weather Wing, suggests that use of the Krebs-Doege procedure as a means for estimating the height of bases of observed cirrus would give results as good as the use of the contrail curve (see paragraph 3.1.7).

4.1.14. Vertical Motion. This parameter, which would seem to be, along with humidity, the most directly related to cirrus of all, is unfortunately not yet accessible to satisfactory evaluation in practice. The analyses of large-scale vertical-motion charts by the procedures developed at New York University in 1945-46 and recently by NWP methods indicate only a rough correspondence of areas of rising air with precipitation [20]. The approximations and smoothing inevitable in such procedures may mask some of the expected correlation, but it seems more likely that the instantaneous field of mean vertical motion would not prove to be as good an indicator of upper clouds as the amount of vertical displacement over a period of time. Indirect methods of evaluating the effects of vertical motion for cirrus forecasting are discussed in paragraphs 4.1.5, 4.1.7, 4.1.10, 4.1.12, and 4.1.16.

4.1.15. Humidity. Lack of suitable equipment has prevented accurate routine measurements of humidity in high-level soundings. Several equipments of experimental or research nature have been used in recent years to obtain a few useful humidity soundings in the cirrus region. Aufm. Kampe [37] and Weickmann [65] were the first to develop explicitly the hypothesis that the cirrus ice-crystals form only through saturation with respect to water in atmospheres with ice-supersaturation and that the cirrus clouds and contrails persist only in regions near ice-saturation. From their flights from Ainring (1939-42) they computed some humidities under contrail conditions, which indicated qualitatively that the above hypothesis is correct. They concluded that in old cirrus clouds ice-saturation prevails, whereas in newly-forming cirrus ice-supersaturation prevails. Aufm. Kampe mentioned that usually a rapid decrease in humidity seems to occur above the tropopause, which would explain the rarity of cirrus in the stratosphere.

Gluckauf found ice-supersaturated humidities (up to 162%) in 10 out of the 36 daily balloon soundings in England [28] which he evaluated by a special technique.

On the British MR Flights a Dobson-Brewer frost-point hygrometer has been regularly operated [36] [7] [8] [58] [59] [46]. The readings were taken visually and the rapid micro-fluctuations of frost point (often 5°-10°F in less than a mile) thus smoothed out. In or near cirrus the readings were more often than not unsaturated with respect to ice, averaging about 80% relative humidity (3° frost-point depression below ice saturation) [45]; only 38 out of 86 cases were ice

saturated or supersaturated. This is not inconsistent with aufm. Kampe and Weickmann's prediction [37] [65] that the cirrus could persist a while after falling into relatively moist but unsaturated air. Sometimes, however, cirrus seemed to persist even at readings of 60% — perhaps because there were locally-saturated areas missed by the instrument. Nevertheless, such large frost-point depressions suggest that a systematic error of several degrees in the instrument is also likely [45]. Even when cirrus was reported "in the distance" there was usually a relatively moist layer (frost-point depressions up to 15° or 20°F) passed through by the aircraft at the same height. Murgatroyd and Goldsmith [45] suggest that a network of humidity soundings would give valuable information for predicting high cloud. They tabulated the height of tops and bases of these moist layers relative to the tropopause (Figure 26). The distribution is remarkably similar to that of

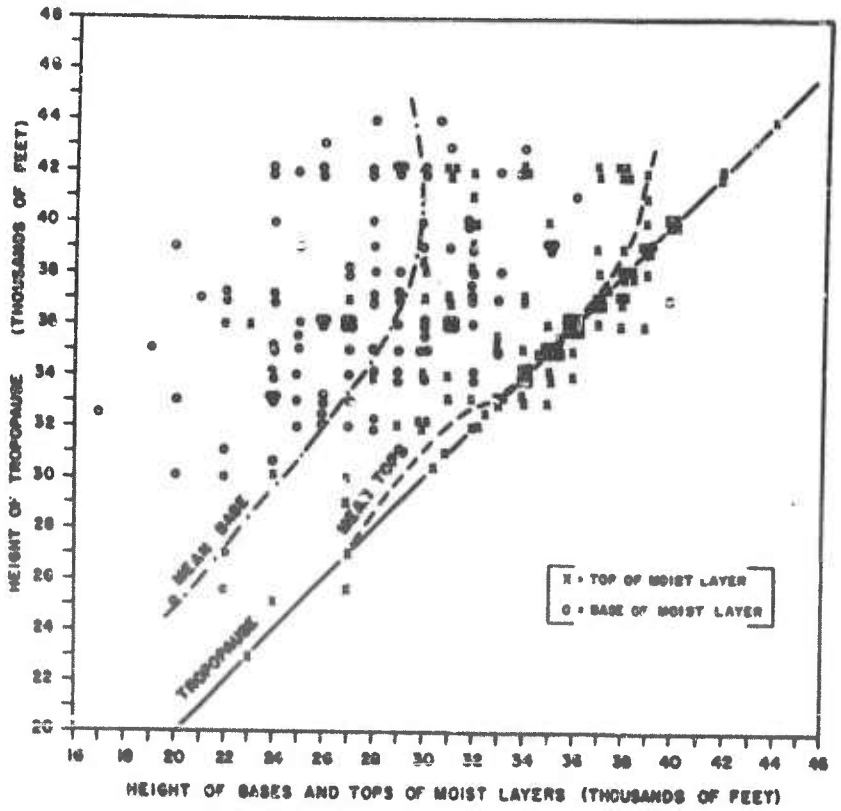

Figure 26. Heights of Bases and Tops of the "Moist Layer" Versus Tropopause Height, British MR Flights, South Farnborough, 1949-52 [45].

the cirrus bases and tops (cf. Figure 23). It is interesting to note that in both distributions it was the region around 32,000-40,000 feet where most cases of tops in the stratosphere occurred (see paragraph 4.1.12).

A summary of the frost-point (F.P.) soundings from MR Flights by Bannon et al [14] [45] [54] [7] [8] shows a general slow decrease in temperature-frost-point depression with height, with a minimum depression (maximum of relative humidity with respect to ice) near the tropopause and a more rapid increase in depression above the tropopause. A sharp change in lapse rate of frost point sometimes occurs at the tropopause but is always confined to a shallow layer; this probably occurs in the area of subsidence above a tropospheric low. Air at the level of the jet-stream core and within several hundred miles is usually nearer saturation than at lower and higher levels. The moisture (i.e., relative-humidity) maximum is generally reached around the tropopause on the cold side of the jet, but somewhat below the tropopause on the warm side. Some cases of steadily-decreasing relative humidity through the troposphere are also found. There are often large changes in frost-point depression through frontal surfaces. Murray [47] found the frost point averaged lower and the frost-point depression higher on the low-pressure side than on the high-pressure side of the jet-stream axis; this is consistent with the cloud distributions (see paragraph 4.1.16).

Some soundings made with a sensitive electronic dew-point hygrometer developed by Barrett et al [5] [6] give a good idea of the probable fine-structure in humidity distribution with height. There are many shallow layers of high humidity between dry layers [17]. This would account for the multi-layered cirrus.

In the absence of humidity measurements at cirrus levels, some indirect relations may be useful [22]. James [36] found the depression of dew point at 500, 450, and 400 mb was about 8°F (4.4°C) greater with no-cirrus than with cirrus. If the cases when dew-point depressions were simultaneously lower at all three levels than the mean depressions for "cirrus," and the cases where the depressions were all greater than the mean for "no-cirrus," had been forecast by these criteria, the accuracy would have been 84% and 80% respectively. In this connection it is of interest that Bannon [7] [8] found a correlation of .80 between temperature at 500 mb and frost point at 300 mb, and of .82 between T_{500} and FP_{250}. Hendrick [31] uses an index of "moisture above 400 mb"

as a parameter in his cirrus-forecasting method (see paragraph 4.4). Any reported humidity in the radiosonde ascent above 400 mb is taken as the indicator of "moisture present" and no reported humidity as "no moisture present." This is admittedly a very crude procedure, but nevertheless contributes some predictive value to Hendrick's method.

There are possibilities of improved forecasting through greater use of the humidity indications of some present radiosonde models (such as the AN/AMT-4 and those equipped with goldbeaters skin or Falckenburg hair elements) which respond to large changes in humidity at temperatures even to well below -60°C, though the magnitude of the humidity cannot be evaluated. When the lapse rates of measured dew points at high levels are examined carefully, sudden changes in slope often coincide with observed cloud layers (cf. paragraph 4.1.13). Use of such indications cannot be made in the field unless or until the transmitted dew points or some index of them include the maximum heights to which any humidity is observed.

A preliminary examination of the humidity traces on the radiosonde records for some of the ascents made during Project Cloud Trail gives strong indication that wherever the humidity trace at high levels up to the tropopause increases above the minimum ordinate value, a cirrus layer is usually reported; and vice verra, that most aircraft-observed cirrus layers over 1000 feet thick are associated with such an indication of increased humidity. If the heights of such "moist layers" revealed by the soundings above 25,000 feet were transmitted, forecasters might be able to delimit the spatial extent of the moist regions and relate them to the vertical-motion or wind field in such a way that: a) presence of cirrus layers obscured by lower clouds could be inferred, b) the future location of moist regions could be predicted and used to refine cirrus forecasts from the vertical-motion (vorticity) field.

4.1.16. Jet Stream. Sawyer and Ilett [54] undertook an investigation to determine whether the middle- and high-cloud distribution has a recognizable pattern with respect to the jet stream. It was thought that such a pattern would be an aid in analysis and forecasting of both the clouds and the jet stream when upper-air observations are few, and might permit an aircraft navigator to determine his location with respect to the jet stream merely by watching the clouds. From upper-air charts of 1949 over the British Isles the cloud observations from the

ground were tabulated according to their position in relation to the jet stream. Cases with 4 octas or more of low cloud were omitted; if the low clouds were less than 4 octas and no cirrus reported, none was assumed to be present. The area around the jet was divided into eight sectors (Figure 27) for which tabulations were separately made. The results showed cirrus of 4 octas or more was considerably more frequent to the right of the axis of the jet stream (sectors CDGH) than to the left (sectors ABEF). "Frontal" and "layer" types of cirrus and medium cloud were more common to the right, and the "anvil" cirrus and cirrocumulus to the left. The observations were mainly typical of the middle region of the jet, and there was little difference longitudinally (though few observations were made near entrance and exit to the jets). Sometimes the boundary of the cirrus was well defined near the jet axis (usually when associated with an active front), but in some cases there was little or no cirrus at all (mostly jets passing over surface highs). The patterns were similar for strong and weak jets.

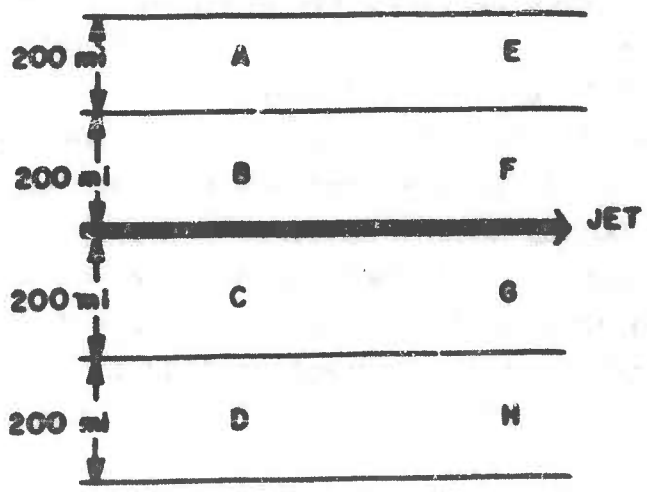

Figure 27. Sectors Used for Sawyer and Ilett's Study of Cloud Distribution in Relation to the Jet Stream [54].

Murray [47] analyzed the 1951-52 MR flight observations of cirrus in relation to the jet stream. When flying on horizontal legs, the following percentages of flight time were in cloud on various legs relative to the jet (20 flights, 39 legs, 26½ hours total):

	Above Jet Axis	Below Jet Axis	Above and Below
Ci, Cs, and Anvil Ci	0	2.9%	1.8%
Ns, As, and Ac	0	3.6%	2.2%
All	0	6.5%	4.0%

Thus, cirrus was met with only a small percent of the time.

On the 16 legs located above the jet axis, no clouds were encountered, and only on three of them were patches seen above the aircraft. The cirrus was, in these flights, observed from 30 to 400 n.m. to the high-pressure side of the axis; no cirrus on the low-pressure side was seen.

On the seven legs which traversed some cloud (including anvils, Ns, As, Ac, and Cs) the clouds were 70 to 400 n.m. on the high-pressure side.

On the 7 flights when no cloud was observed at or above the bottom leg, there was only some low Cu or Sc seen; these jets were mostly ones not associated with a surface front.

Thirteen flights had some cloud at or above the bottom leg, scattered from 70 n.m. on the low-pressure side to 400 n.m. on the high-pressure side, mostly on the latter.

The general conclusion was that cloud above 400 mb is predominantly on the high-pressure side of the jet axis, especially from 150 to 450 n.m. out; and that no cloud (except anvils) is found on the low-pressure side between 100-250 n.m. out. From 100 n.m. on the low-pressure side to about 150 n.m. on the high-pressure side there may be none or any amount of high cloud, depending on the case. Murray found the frost-point depressions were generally greater on the low-pressure than on the high-pressure side, which is consistent with the cloud distribution found.

Murgatroyd and Goldsmith [46] noted on the 1949-52 MR Flights that the boundary between cloud and no-cloud areas at the jet axis was most well-marked with jet streams having a considerable northerly component, cirrus then often being present over western, but not over eastern, districts of the British Isles.

James [36] analyzed the 1952-54 MR Flight cirrus data in relation to the jet stream, obtaining a general confirmation of the previous

studies. At 300 mb the majority of the cirrus reported lay on the high-pressure side of the jet axis (see Figure 28). The cases of no-cirrus were much less numerous in total than cases of cirrus, and showed some tendency to occur more often on the low-pressure side. Cirrus on the low-pressure side of the jet was mostly within 200 n.m. while on the high-side cases were numerous out to 700 n.m. However, many cirrus and no-cirrus reports had no obvious association with the jet stream at 300 mb.

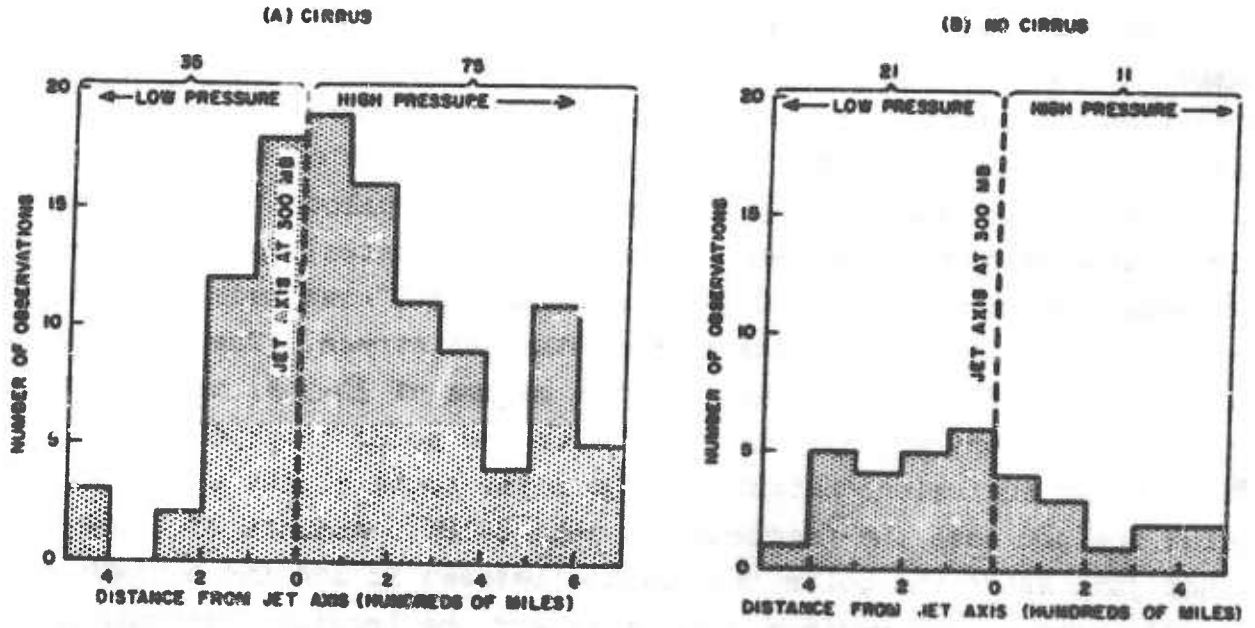

Figure 28. Frequency of Reports of Cirrus (A) and No-Cirrus (B) at Various Distances from the Jet-Stream Axis at 300 mb. From British MR Flights 1952-54 [36].

The average pattern of cirrus and no-cirrus distribution around the jet stream revealed by the various studies mentioned above seems to call for a circulation model which has ascending motion on the high-pressure side and descending motion on the low-pressure side. An effect of this sort has been postulated in theoretical models of the jet stream.

However, comparison with the models of Murray and Daniels [48] and of French and Johannessen [24] (see paragraph 4.2) indicates there should also be a more definite longitudinal variation, which perhaps is partly obscured by the crudity of the observations available and the persistence of cirrus after formation.

Schaefer [56] claims that certain forms of high cloud moving at

high speed are characteristic of the state of sky when a jet stream is overhead, in particular, States of Sky Codes C_H4, C_H5, and C_H9 (also C_M3, 4, 5, and 7). He suggests that the presence of these clouds may be used as a "rule of thumb" for identifying a jet stream. It is certain that the types of clouds cited also occur independent of a jet stream; only a detailed study could verify the utility of Schaefer's hypothesis. Similar clouds are reported with jet streams over Tasmania [19], but not over Australia [19].

A BOAC pilot, Captain B. C. Frost, has, from his flying experience, independently derived [26] a notion rather similar to Schaefer's. He emphasizes the parallelism of the long narrow cirrus bands to the wind direction (cf. also Saito and Narikawa [53]). However, he has admitted that these clouds accompany only a small percentage of the jet streams.

Endlich and McLean [71][80] summarized the pilots' cloud observations from Project Jet Stream (eastern United States), plotting their frequency distribution by 5000-ft vertical and 1°-latitude horizontal intervals with respect to the core of the jet stream. The frequency of all "high clouds" (Figure 29a) had two maxima of 30-35%, one 275 miles north of the core around 5000 feet below the polar tropopause, the other at an equivalent height but 350 miles south of the core. At and below the jet core the frequency is only 8-18%. Amounts of 8-16% were found just above the polar tropopause (between it and the maximum wind level); between the maximum wind level and the tropical tropopause, the frequency falls to 0-10%. The general picture is thus similar to the British results. Figures 29b, c, and d, show the frequencies separately for Ci, Cs, and Cc. There is proportionately more Ci north of the jet, and more Cs south of the jet. Cc are rare but clustered just above the "jet-front" well south of the core and lower than Cs and Ci. The maximum of frequency south of the jet core may be related to the frequent occurrence of secondary (subtropical) jets over southeastern United States. Since 80% of the Project flights crossed the jet in the region from ridge to trough where clouds are less frequent than ahead of the trough, the above Figures may tend to be somewhat lower than those which would be representative of jet streams as a whole.

Major Gayikian [77] has extended his cirrus study reported in paragraph 4.3, to include a highly-generalized model of cirrus distribution around a jet stream and associated long-wave trough over the United States (see Figure 30). This model gives dense-cirrus areas to

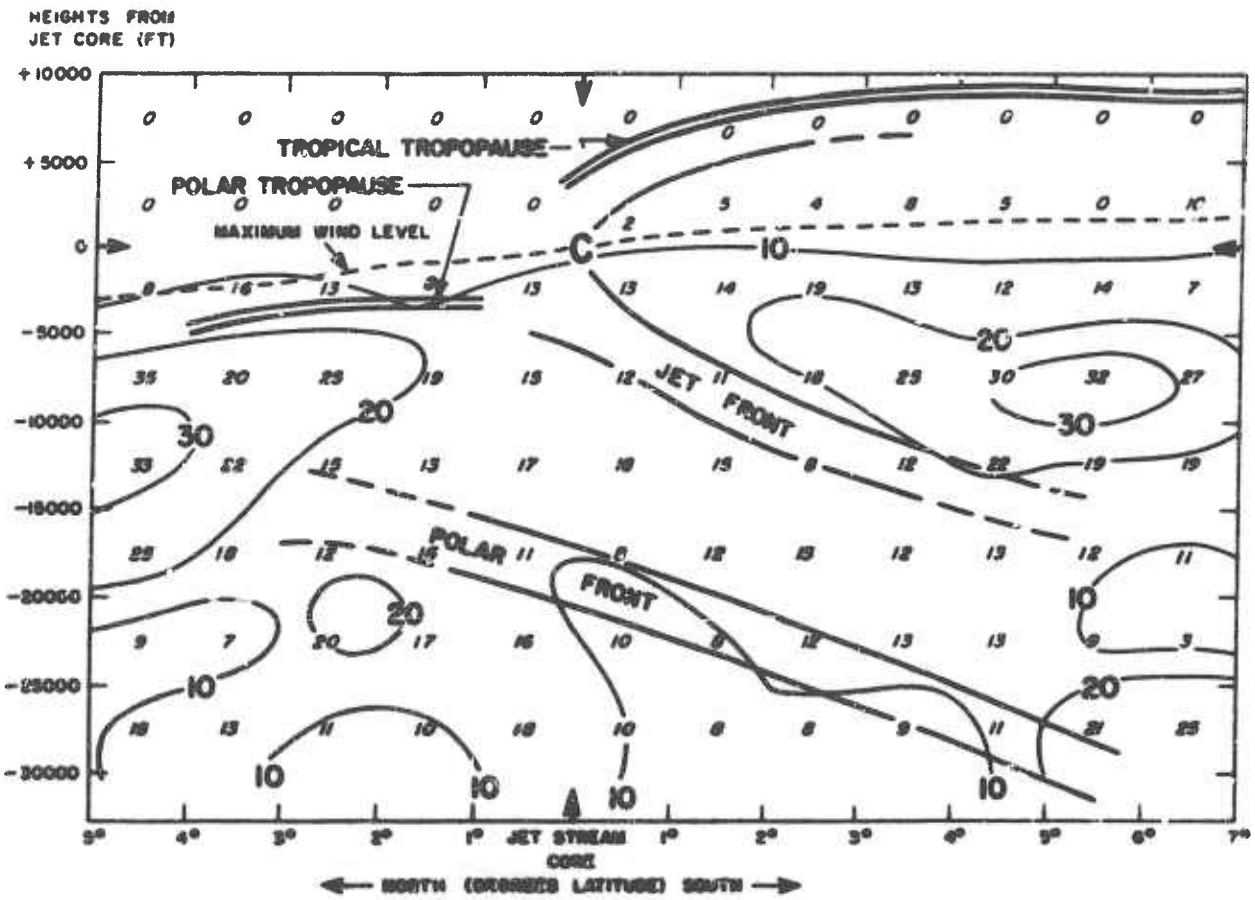

Figure 29a. Cross-Section of Model of the Jet Stream Based on Project Jet-Stream Flights Over Eastern United States, with Percentage Frequency of All High Cloud Plotted with Reference to the Jet-Stream Core (after Endlich and McLean [71] [80]). There is a certain amount of sampling bias in this data, because the aircraft observers could not observe from flight level the complete vertical distribution of clouds. The clouds reported below 18,000 feet below the jet-core level were probably nearly all middle clouds; their actual frequency must be much greater than shown. Other diagrams [80], not reproduced here, show the distribution of cloud cases reported broken or overcast and scattered. The patterns are similar, and the frequencies of the overcast or broken are generally 1/2 to 3/4 of the total frequencies.

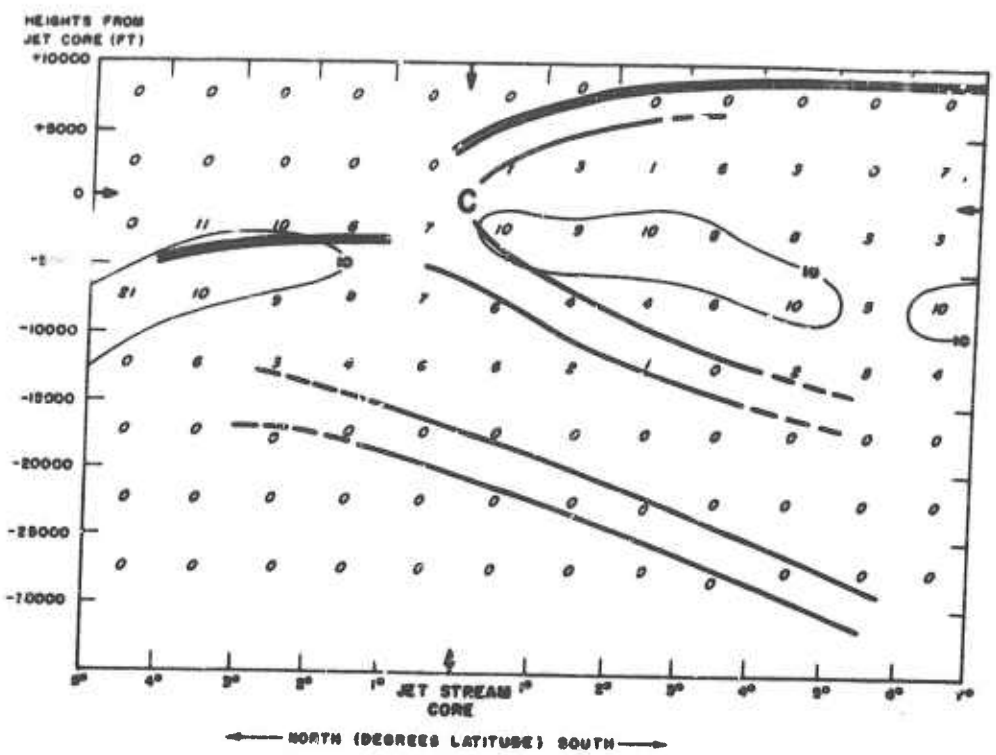

Figure 29b. Same Model as in Figure 29a but Showing Frequency of Cs Clouds [80].

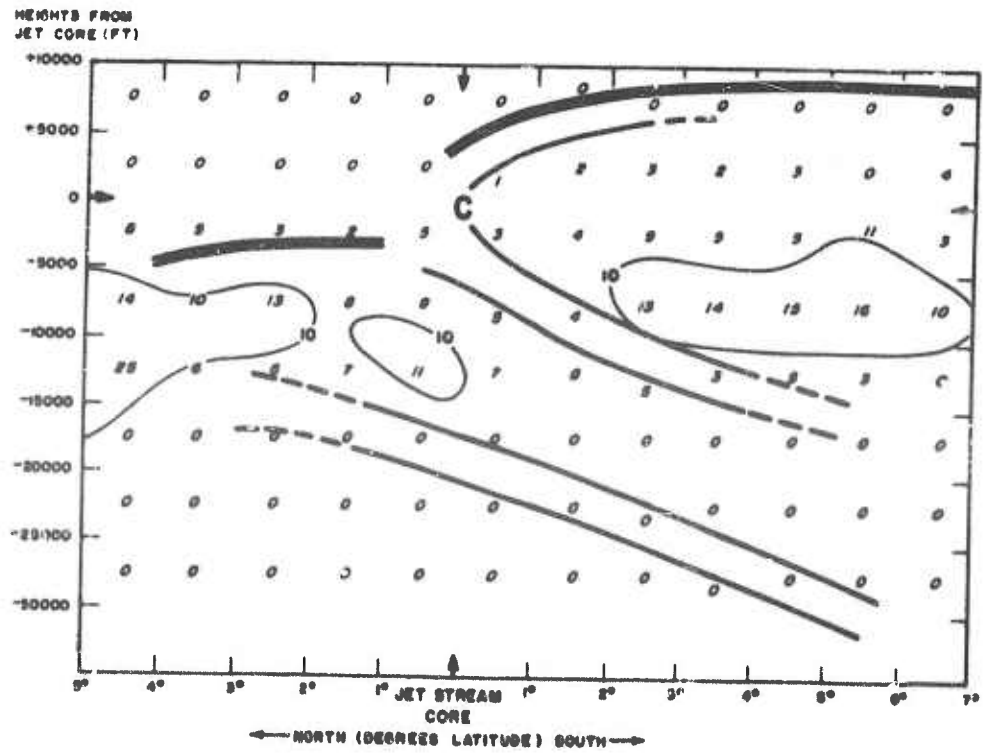

Figure 29c. Same Model as in Figure 29a but Showing Frequency of Ci Clouds [80].

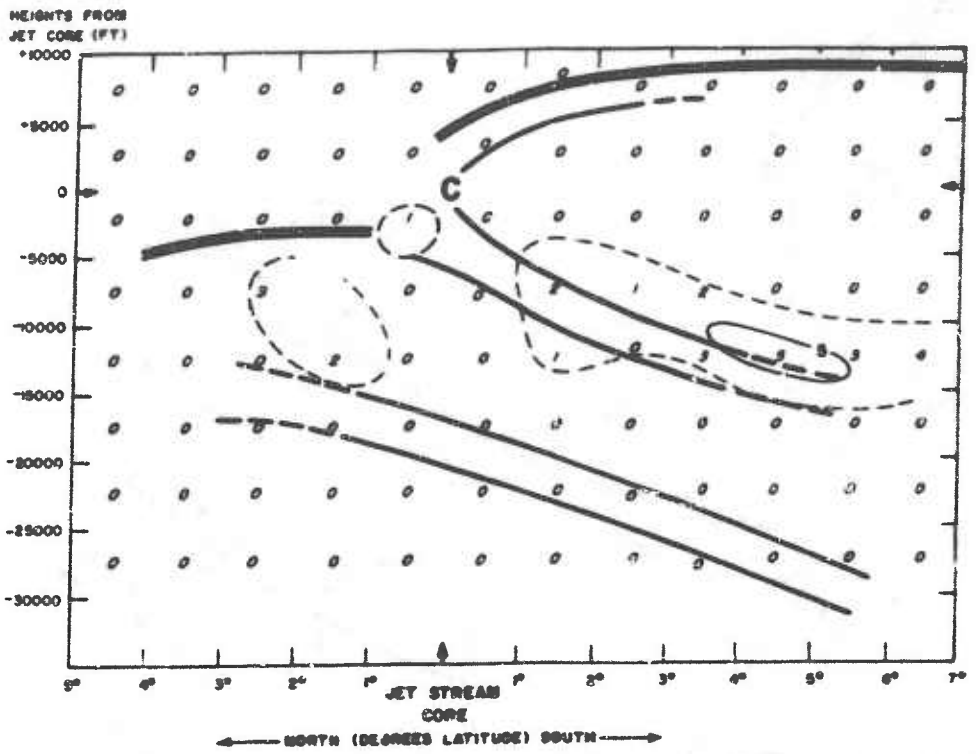

Figure 29d. Same Model as in Figure 29a but Showing Frequency of Cc Clouds [80].

the right side of the jet axis on both limbs of the trough as other studies show, and a clear area in the bottom of the trough. Over southeastern United States the model includes a subtropical jet and a combined cirrus pattern that agrees well with Endlich's data (Figure 29). Gayikian, however, does not show any cirrus north of the jet, where both the British and Endlich's data indicate much "high cloud" occurs. This discrepancy is minimized if Gayikian's model is applied mainly to the level of the wind maximum rather than to 300 mb or other levels below the wind maximum. However, all studies reported here agree that most of the more extensive and dense cirrus is on the high-pressure (right, or south) side of the jet axis. Furthermore, Major

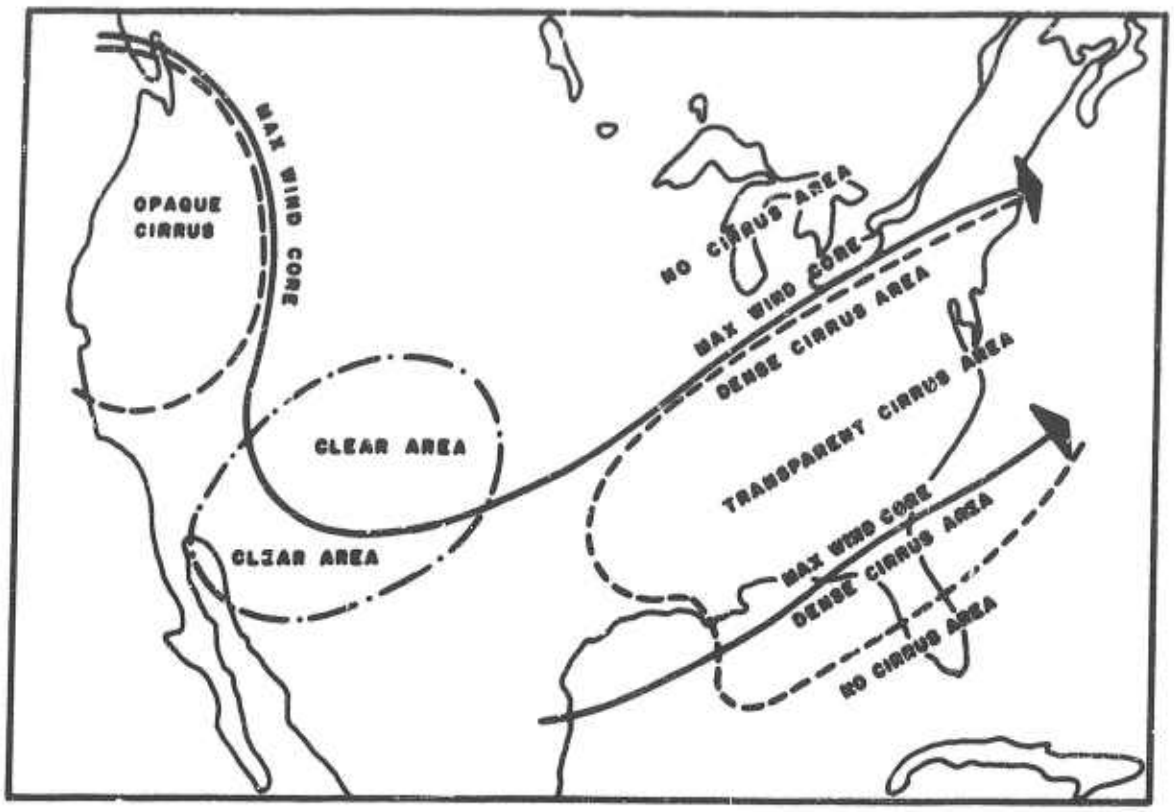

Figure 30. Model Distribution of Extensive Dense Cirrus at Maximum-Wind Level with Reference to a Long-Wave Trough Over the United States and Associated Jet-Stream Axes (after Gayikian [77]).

Gayikian's model is intended only to show the dense and extensive cirrus areas, and does not deny the occurrence of much scattered, fine, and thin cirrus elsewhere.

Much of the large observed frequency of high cloud well north of the jet axis can probably be accounted for as the upper reaches of cold frontal systems or cold lows not directly connected with the jet stream; in some parts of a trough this high cloud may tend to be dense and in other parts thin or scattered.

There is some difference of opinion as to how (if at all) the cloud distribution in the cross-sectional normal to the jet axis may vary longitudinally along the jet, between "entrance" and "exit" areas, in and out of maximum isotach centers, etc. Only further observations can answer this.

4.2.0. Forecasting High Clouds From High-Level Constant-Pressure Charts, by J. E. French and K. R. Johannessen [24]. These investigators show there is a very definite association between occurrence or non-occurrence of extensive cirrostratus and the 300-mb patterns. They show how the sign and magnitude of the vorticity-advection term serves quickly and with high accuracy to mark off the large areas on the chart where extensive Cs is not likely to occur. Within the region having large positive-vorticity advection, which by hypothesis should contain most of the extensive cirrus, the high clouds usually cover less than half the area because in part of the area the air is too dry or the lifting has not continued long enough. Statistically, however, 86% of the extensive high cloud reported were found somewhere within the positive area. There are also several situations where some of the cirrostratus shield is apt to occur outside but adjacent to the positive-vorticity-advection-term area: one is in sharp troughs surrounded by strong winds and in cold lows that show movement, and the other is in the lee of the 300-mb ridge line where descending motion prevents new formation of cirrus but where old cirrus which drifts in from upstream may persist for 300-400 n.m. past the ridge, because the air is still ice-saturated. Nevertheless, the extensive Cs is mostly formed in the region from the trough line to the ridge line. The vorticity-advection criterion for cirrus vs. no-cirrus can be applied in practice simply by qualitative inspection of the 300-mb pressure-contours and winds (for principles see Appendix B, AWSM 105-50/1A). The addition of some direct or indirect moisture indication would undoubtedly improve the results (see paragraph 4.4). The authors do not believe that the occurrence of scattered patchy cirrus can be forecast by any general synoptic approach with the type and density of upper-air observations available today. The essential part of their paper follows:

4.2.1. Trial of Nephanalysis. It might be mentioned here that initially attempts were made to analyze a series of maps for high-cloud occurrence by means of synoptic observations of high clouds. It was found, however, that the confidence in the nephanalysis arrived at in this manner was low. A large amount of guessing based on preconceived ideas about the distribution of high clouds was necessary to complete the maps, a thing that naturally should be avoided. It was estimated that about half the time the high clouds were hidden from surface observation by low or medium clouds. Observations taken during the hours

of darkness were found unreliable, and continuity from the nighttime maps to the daytime maps was poor. Further, it was found difficult to analyze obectively the amounts of high clouds, e.g., to establish where the edge of a cirrostratus deck should be. The surface observations of the height of the base of high clouds were found completely unreliable by H. Appleman [AWS TR 105-110] who found they contained an average error of almost 10,000 feet. Considering all this, it is not surprising that so little factual knowledge has been collected about the distribution of high clouds in relation to synoptic patterns.

For these reasons, it was decided to abandon the nephanalysis based on surface observations and to base the study entirely on aircraft observations. Thereby, it was hoped to achieve a higher degree of objectivity. Surface observations were consulted only as a check when the aircraft observations appeared to be inconsistent or incomplete.

4.2.2. Observations Used. The cloud observations were made from B-47 aircraft flying mostly above the top of the highest cloud layers. The observers had been instructed to report the tops of cloud and amounts above 25,000 feet and record particularly locations where large changes in the height of cloud tops and amounts occurred. The amounts were reported as overcast (10/10), broken (6/10 - 9/10), scattered (5/10 or less) and clear.

The height 25,000 feet was chosen somewhat arbitrarily. The average temperature at this level over the United States in wintertime is about -35° to -40°C. This temperature range corresponds to that in which various investigators have found that abundant freezing nuclei become active. In other words, 25,000 feet is roughly a level above which the clouds are predominately ice-crystal clouds [see paragraph 2.2.2].

The tracks flown extended all over the United States and adjacent areas of the Atlantic. The total distance flown was about 45,000 miles. The flights took place in January and February 1953. They were mostly spaced several days apart, and the tracks changed each time so that it was not possible to follow in space and time the development of the high-cloud systems. The conclusions of this study are therefore mostly of a statistical nature.

The height of the aircraft above the cloud was estimated visually. Since the aircraft could be flying as much as 10,000-12,000 feet above a reported cloud layer, it was thought that errors in cloud-top

reports of as much as 3000 feet could occur. Most of the time, though, the flights would be conducted only a few thousand feet above the high cloud, and it is estimated that the average error is between 1000 and 2000 feet.

The types of vertical motion leading to high-level clouds may for this study conveniently be classified as:

a. Slow, large-scale ascent, eventually producing extensive sheets of cirrostratus.

b. Penetrative Cb convection from low levels, producing anvil cirrus as the typical high-cloud form; in due course the degeneration products of the anvils may take on various aspects such as cirrus spissatus and even cirrostratus and cirrus fibratus when vertical shear detaches the ice clouds from their parent cloud and conceals their origin.

c. Convective currents in shallow unstable layers at high levels. [Cf. Schwerdtfeger's "pure" or "convective" cirrus.]

Only the first type is treated here. To isolate the high-cloud occurrences that were thought due to slow vertical ascent, the high-cloud layers of 6/10 or more and extending for at least 100 miles along the track were selected. It was thought that there would be little hope of detecting areas of vertical motion of a scale less than this from the usual smoothed flow charts at upper levels. On the other hand, it was hoped to eliminate types (b) and (c) by requiring the cloud layers to be extensive. The occurrences for each 100-mile stretch were divided as to amounts of either 6/10 - 9/10 or 10/10 cloud. This was done because it was of some operational importance to be able to distinguish between a completely-overcast cloud deck and cloud layers with breaks; this also afforded some clue as to the thickness of the clouds.

4.2.3. Divergence and Vertical Motion Near the Tropopause. The studies that have been made of the distributions of high clouds have almost exclusively associated them with features of the surface maps such as fronts and frontal systems, lows, highs, troughs, and ridges. [See paragraph 4.1.] On the other hand, we know that extensive sheets of high cloud at times occur without any recognizable counterpart on the surface map, though they may be associated with well-defined characteristics on high-level maps, e.g., the 300-mb map. Among such features of the 300-mb map can be mentioned jet-stream-isotach-maxima, troughs,

and cold lows. At times, these features are so exclusively high-level phenomena that they are not clearly reflected even on the 500-mb map.

An attempt to associate high-level clouds with the 300-mb map, therefore, seems logical. The first step was to try to infer the vertical motion in the high-cloud region for the 300-mb map.

The vertical motion at a level relative to some boundary level can be obtained from the vorticity equation (1) and the equation of continuity (2):

$$(1) \qquad \frac{d \ln (\zeta + f)}{dt} + \nabla_p \cdot \vec{v} = 0$$

$$(2) \qquad \nabla_p \cdot \vec{v} + \frac{\partial}{\partial p} \frac{dp}{dt} = 0$$

Here ζ is the vertical component of relative vorticity (isobaric), f the Coriolis parameter, $\vec{v}$ velocity, and ∇_p the horizontal del-operator applied to a quantity on an isobaric surface.

The term involving the tilting of the horizontal component of vorticity by differential vertical motion through the pressure surface has been left out, though this may be appreciable near jet streams where the vertical wind shear and the horizontal gradient of vertical motion normal to the wind shear may both be large.

By combining (1) and (2) and integrating between two pressure levels p and p_T, we obtain the well known relationship:

$$(3) \qquad \frac{dp}{dt} - \left(\frac{dp}{dt}\right)_T = \overline{\frac{d}{dt} \ln (\zeta + f)}(p - p_T)$$

where the bar indicates the average value between p and p_T.

As boundary conditions, we will assume that the individual pressure change at the tropopause or some level near the tropopause is small in magnitude compared to the individual pressure change further down.

Several authors have investigated the distribution of vertical velocity with height. M. Doporto, (Ber. d. Wetterd., No. 35: 103), found that on the average the height of zero vertical motion was found at 9-10 km over northwestern Europe (Valentia). H. Faust, (Met. Rund., 6: 6), found it at 10 km over central Europe and named this the zero-level. A. Eliassen and W. E. Hubert, (Tellus, 5: 196), studying individual cases found locations of large vertical motions at 300 mb. Others using the wind field directly have also found vertical motions at the tropopause level. P. A. Sheppard, (Quart. Jn., 75: 188), found that in statistical averages |dp/dt| has a maximum below 300 mb both

for ascending and descending motion.

The subject seems controversial; nevertheless, it was thought worth while to try a model where

$$\left(\frac{dp}{dt}\right)_T \approx 0 \tag{4}$$

T is some level near the tropopause, that possibly more synoptic research will allow us to identify better.

For $\overline{d \ln (\gamma + f)/dt}$ we substitute the value at 300 mb, assuming it to be representative for the layer between the boundaries. For the wind and the vorticity their geostrophic values were adopted.

The geostrophic vorticity was computed by the finite-difference approximation:

$$\gamma_g = \frac{2g}{fd^2}(\bar{z} - z) \tag{5}$$

where z is the height of pressure surface and $\bar{z}$ the mean height on a circle with radius d. The quantity d was chosen = 6° latitude at 60°N on the map. Maps of $(\bar{z} - z)$ for the 300-mb surface were constructed by a graphical method devised by R. Fjörtoft [see AWS TR 105-131 and AWSM 105-50/1]. This method is particularly well-suited for operation in a weather central. Thirty to forty minutes are required to construct the $(\bar{z} - z)$ map at 300 mb for an area covering the United States and Canada and adjacent ocean areas (1:12,500,000).

Since the factor $4g/fd^2$ varies only slowly in the north-south direction on the map, the isopleths of $(\bar{z} - z)$ were taken to be isopleths of vorticity. The change in f along the contours of the 300-mb maps is mostly only 0-20% of the change in γ_g and was hence neglected. By also neglecting the vertical transport of vorticity, we arrive at the final form of the individual change of logarithmic vorticity,

$$\frac{d \ln (\gamma + f)}{dt} = (\gamma_g + f)^{-1} (V_g - c) \frac{\partial \gamma_g}{\partial s} \tag{6}$$

where c is the speed of the vorticity line along the contour s. Writing $1 - c/V_g = k$, where k measures the relative speed with which the air flows through the vorticity pattern, we finally obtain the relationship between the vertical motion and the vorticity advection in our model:

$$\frac{dp}{dt} = \left\{(\gamma_g + f)^{-1} k V_g \frac{\partial \gamma_g}{\partial s}\right\}_{300\ mb} (p - p_T) \tag{7}$$

When $k > 0$, as is usually the case, this model leads to the simple scheme of vertical motion in the neighborhood of the tropopause illustrated in Figure 31.

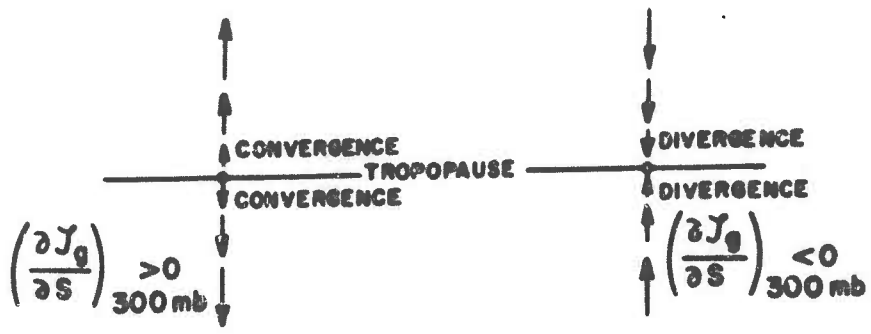

Figure 31. Scheme of Vertical Motion Near the Tropopause.

In the regions where $\partial \gamma_g / \partial s > 0$ at 300 mb, there is descending motion increasing downwards below the tropopause. In regions where $\partial \gamma_g / \partial s < 0$ at 300 mb, there is ascending motion increasing downwards below the tropopause.

If it is felt that the assumption of no vertical motion at the tropopause is too unrealistic, it may be pointed out that the model can be formulated less rigidly by only requiring that $|dp/dt|$ has a maximum well below 300 mb. Also, in this less restricted model, $\{(\gamma_g + f)^{-1} k V_g (\partial \gamma_g / \partial s)\}_{300\ mb}$ should be expected to give the correct sign of the vertical motion and, provided the values of k are comparable in different situations, also to indicate the magnitude of the vertical motion.

The favorable region for formation of high clouds would be in the upper troposphere in the regions with positive vorticity advection at 300 mb. The tops of the high cloud would tend to approach the tropopause to a closeness dependent on the initial humidity distribution, the strength of the divergence field, and the time the air is exposed to this divergence field.

Another region where this model would favor high clouds is in the stratosphere above the region of negative 300-mb vorticity advection. The rarity of cases of high cloud observed in the stratosphere is probably due to the dryness of the stratosphere and to the small vertical motions.

Cressman (Jn. Met., February 1953, p. 17ff) measured the ratio $c/V_g = 1 - k$ over North America on two series of five 300-mb maps each, one in January 1952 and the other in June 1952. The ratio was found positive and less than unity at all points measured. The average was about 0.5 in both seasons, with a variability somewhat greater in summer (18% standard deviation) than in winter (12% standard deviation). No dependence on wind speed was apparent.

According to this we should expect the vorticity advection term to give a fair measure of the divergence at 300 mb, and we can expect to make few mistakes as to sign but some mistake as to magnitude in individual cases by regarding k as a constant (0.5).

4.2.4. Occurrence of Extensive High-Cloud Layers in Relation to the Vorticity-Advection Term at 300 mb. It should be pointed out that, other things being equal, the vorticity-advection term does not only depend on the vorticity advection $-V_g (\partial \zeta_g / \partial s)$, but also on the absolute vorticity $(\zeta_g + f)$.

Since the latter is mostly positive, the denominator in the advection term is positive when the relative vorticity $(\bar{z} - z)$ decreases downstream (e.g., from trough to ridge). When the shear and the Coriolis parameter become equal, the absolute vorticity becomes zero and the vorticity advection becomes very large leading to dynamic instability. Cirrus was generally found with such conditions [see below].

Figure 32 shows the 300-mb map 1500Z, 22 January 1953, with contours and isopleths of $(\bar{z} - z)$ which can be regarded as isopleths of relative vorticity. The track of the observing aircraft has been entered. The figures along the track give the distance flown in 100's of miles. Thick parts of the track indicate 10/10 high cloud, thin < 6/10, hatched 9/10 - 6/10.

This map is typical of the distribution of high clouds found in open waves in the high-level flow. The air moves fast through the vorticity pattern, leaving no doubt that the vorticity advection gives the correct sign of the divergence: The high cloud is found in the regions of positive vorticity advection. The upstream edge of the cloud layer is found some distance downstream from the line of zero advection, which is to be expected since saturation will be reached only after some ascending motion.

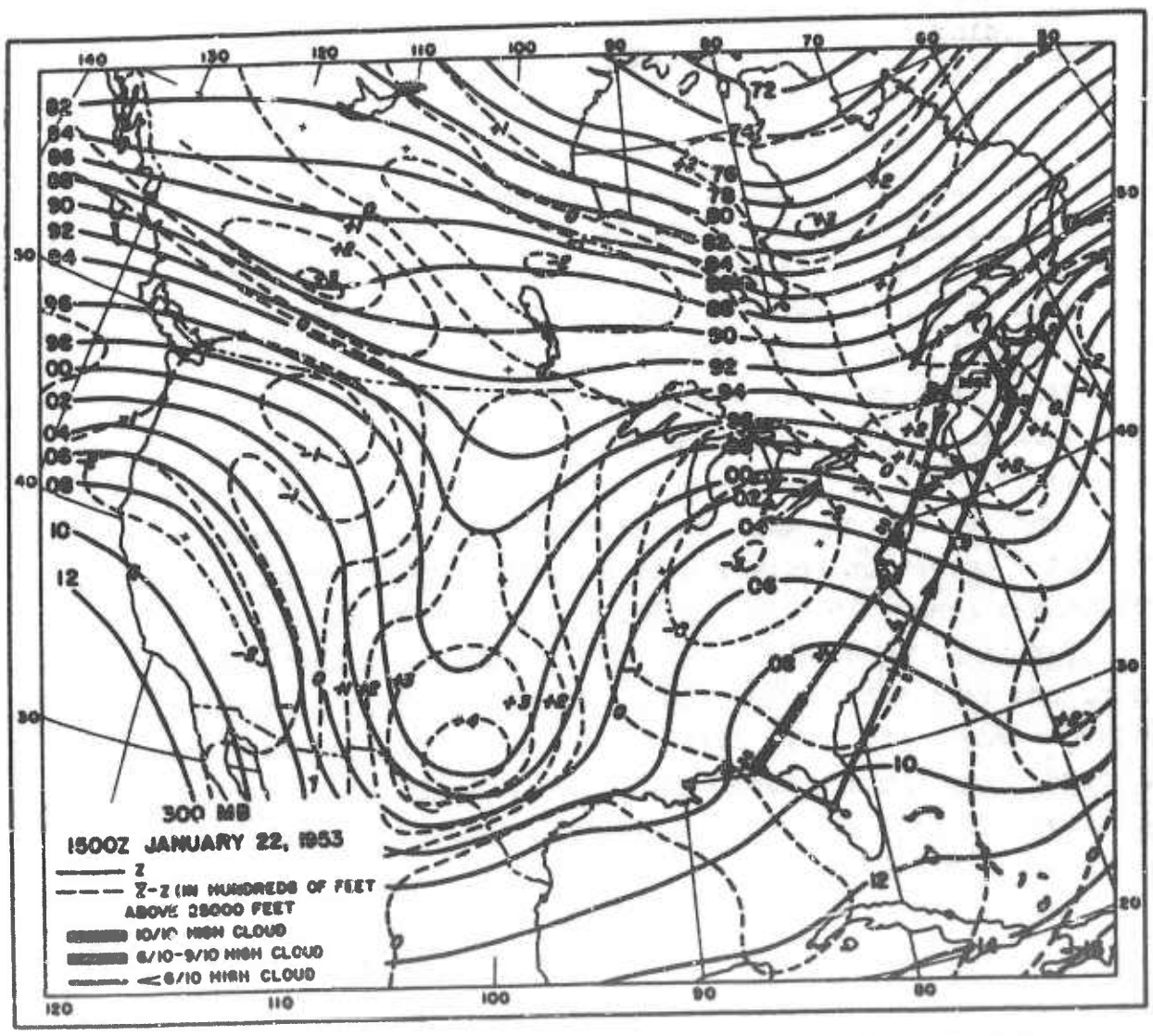

Figure 32. 300-mb Chart at 1500Z, 22 January 1953. Full lines are contours at 200-ft intervals, dashed lines isopleths of $(\bar{z} - z)$ at 100-ft intervals. The track of the observing aircraft is entered and position at map time indicated by arrow. Thick portions of track mark where 10/10 of cloud above 25,000 feet extending for at least 100 miles along track was encountered, hatched portions where correspondingly 6/10 - 9/10 was observed, and thin portions where less than 6/10 was observed.

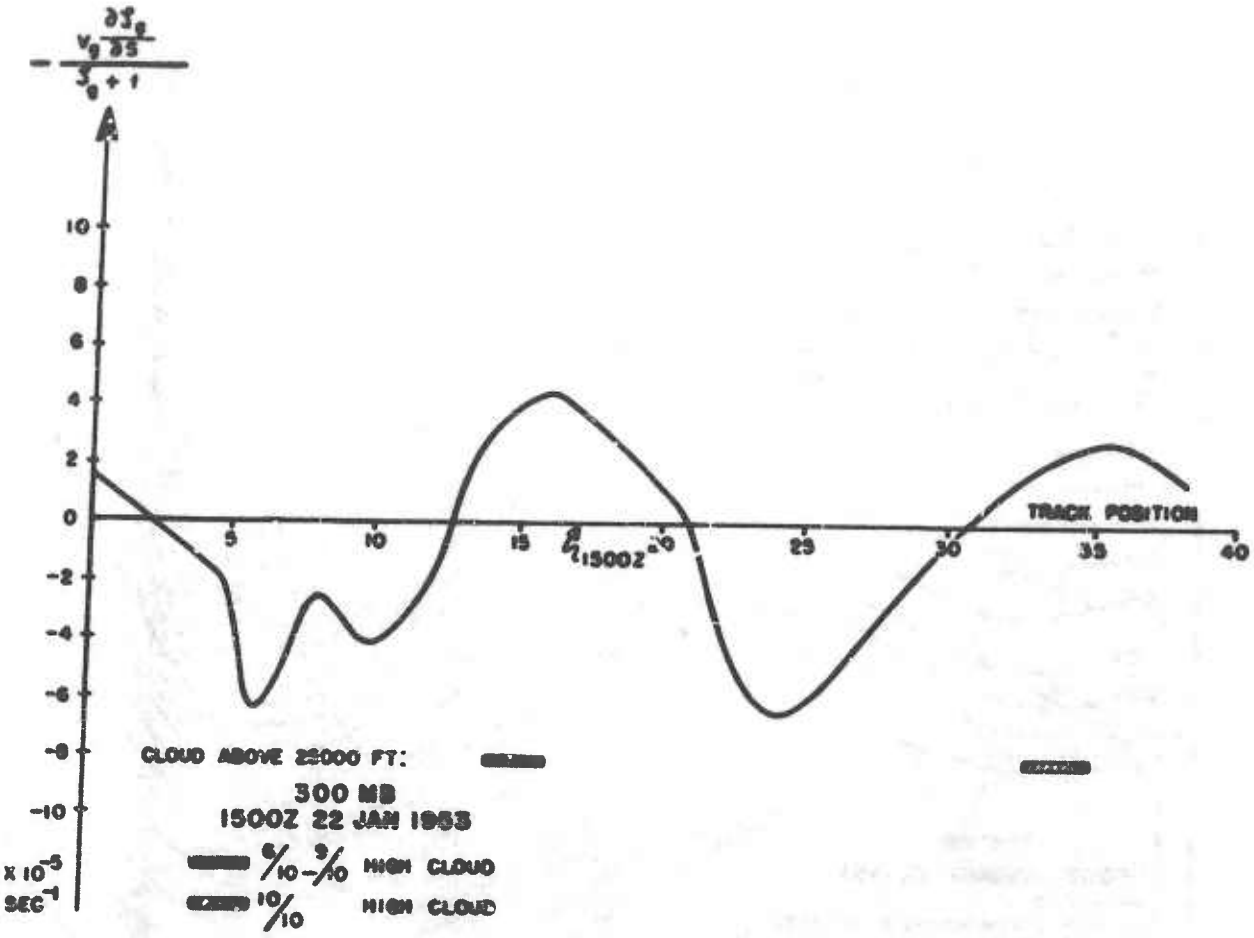

Figure 33. Vorticity-Advection Term at 300-mb, 1500Z, 22 January 1953, along Track of Aircraft. Units 10^{-5} sec^{-1}.

Figure 33 shows the advection term, computed for various points along the route from the chart in Figure 32. As here the cloud deck was usually, but not always, centered near the location where the advection term was largest.

Figure 34 shows a case where the absolute vorticity formally comes out as negative. When f is added to the relative vorticity in the minimum off New England, a narrow zone shows dynamic instability. In this zone and neighboring areas, 10/10 high cloud extending up to the tropopause was observed. Without discussing the reality of these regions of dynamic instability, it is interesting to notice that they were met in six different sections of the total distance flown and in all sections extensive overcasts of high cloud did occur.

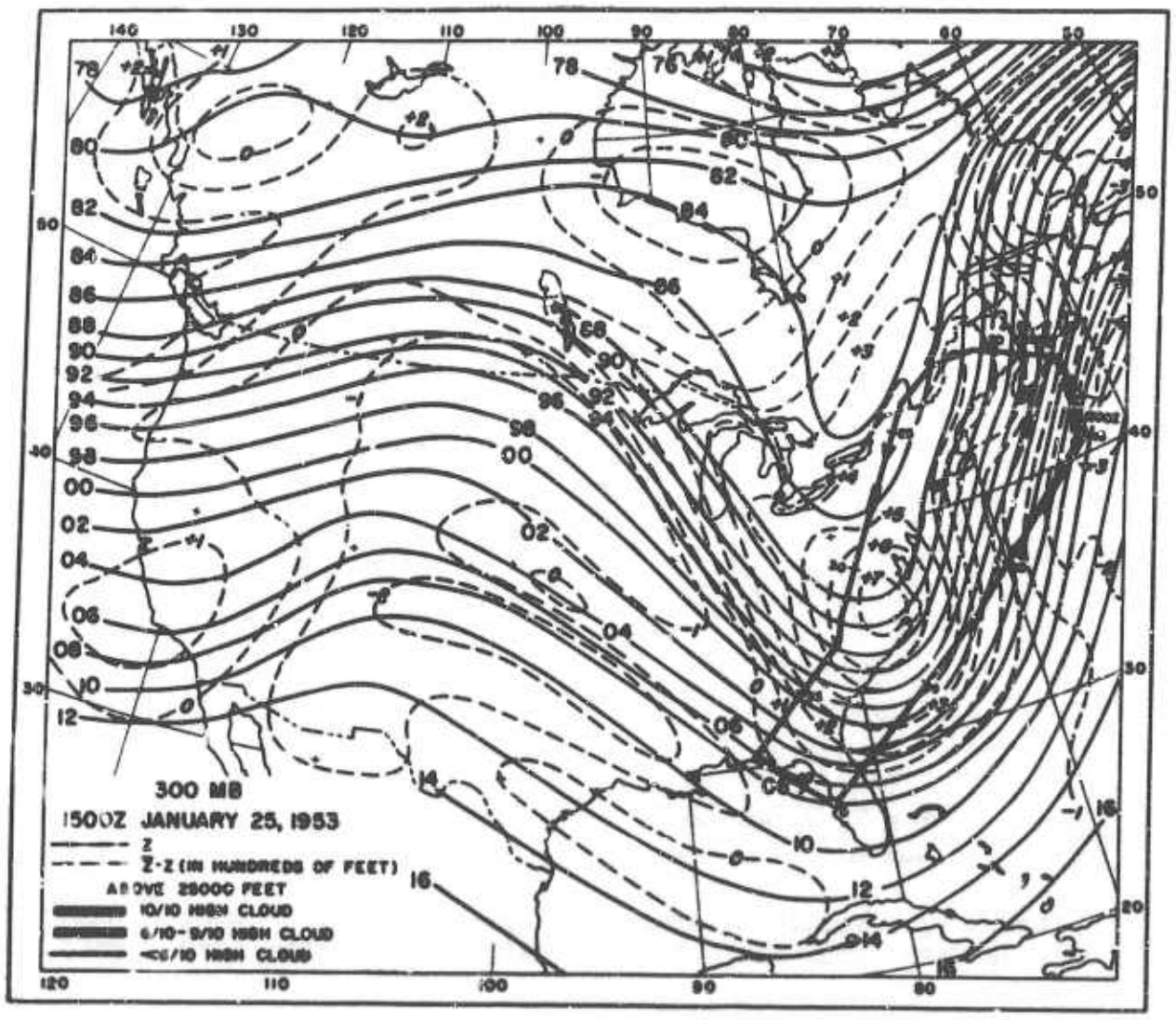

Figure 34. 300-mb Chart at 1500Z, 25 January 1953. For legend see Figure 32.

Figure 35 shows that the advection term was large also in positions 7 to 10, but no high clouds were encountered. This indicates that humidity observations at high levels probably will be needed before we can predict with more certainty where the high clouds will form.

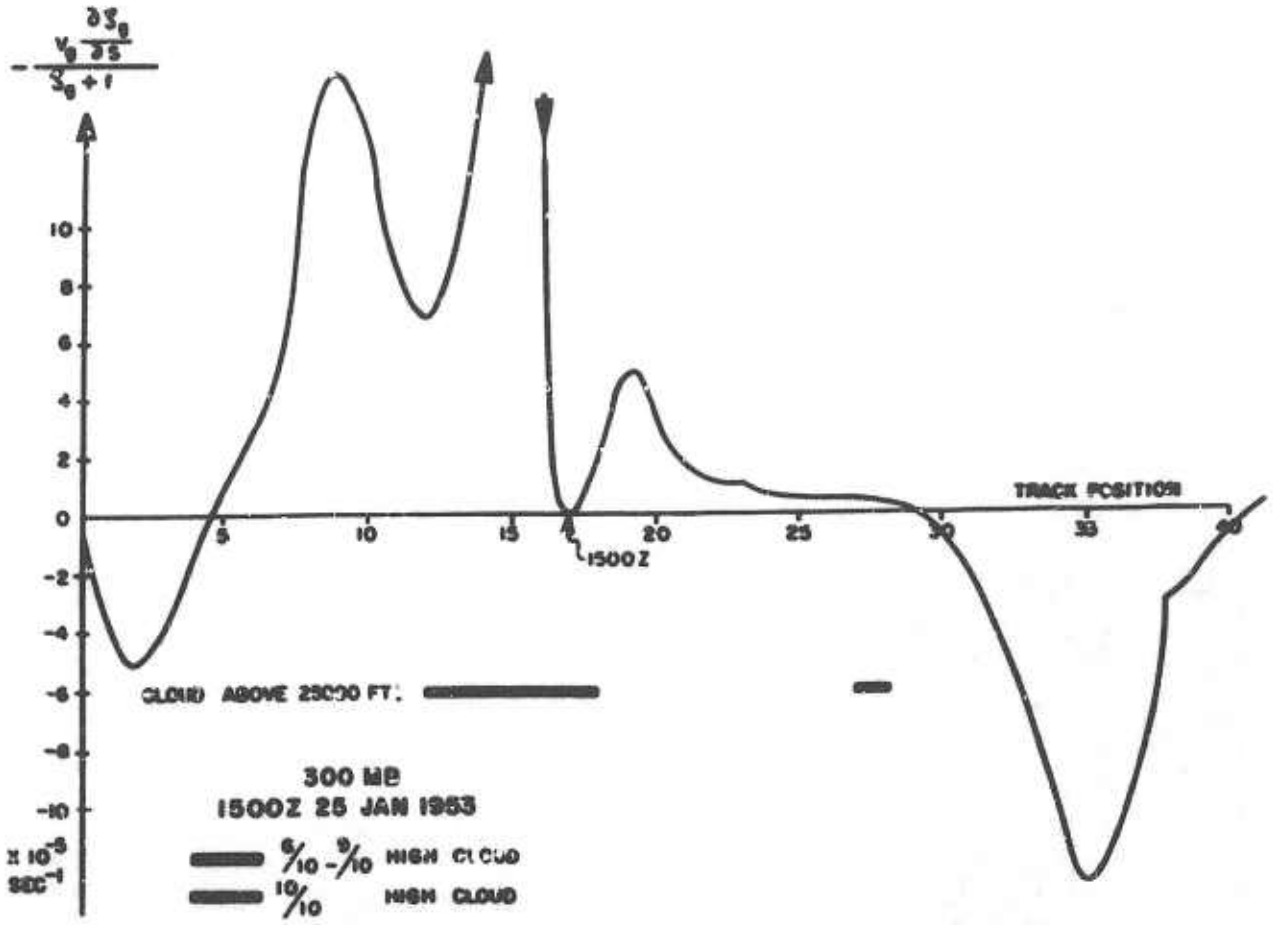

Figure 35. Vorticity-Advection Term at 300 mb, 1500Z, 25 January 1953, Along Track of Aircraft.

Figure 36 shows another example: The layers of high cloud are found associated with positive vorticity advection.

Figure 37 illustrates how the values of the vorticity-advection term for each point of the track were adjusted to the time when the aircraft was in that position. Vorticity maps were drawn for the two consecutive 300-mb maps that best covered the period of the flight, and the vorticity-advection term was computed for points along the track and curves drawn. A composite curve was then constructed by interpolating on a linear time-and-space scale between the phase and the amplitude of the two curves, thus obtaining the vorticity-advection term as a function of the track position at the time when the aircraft

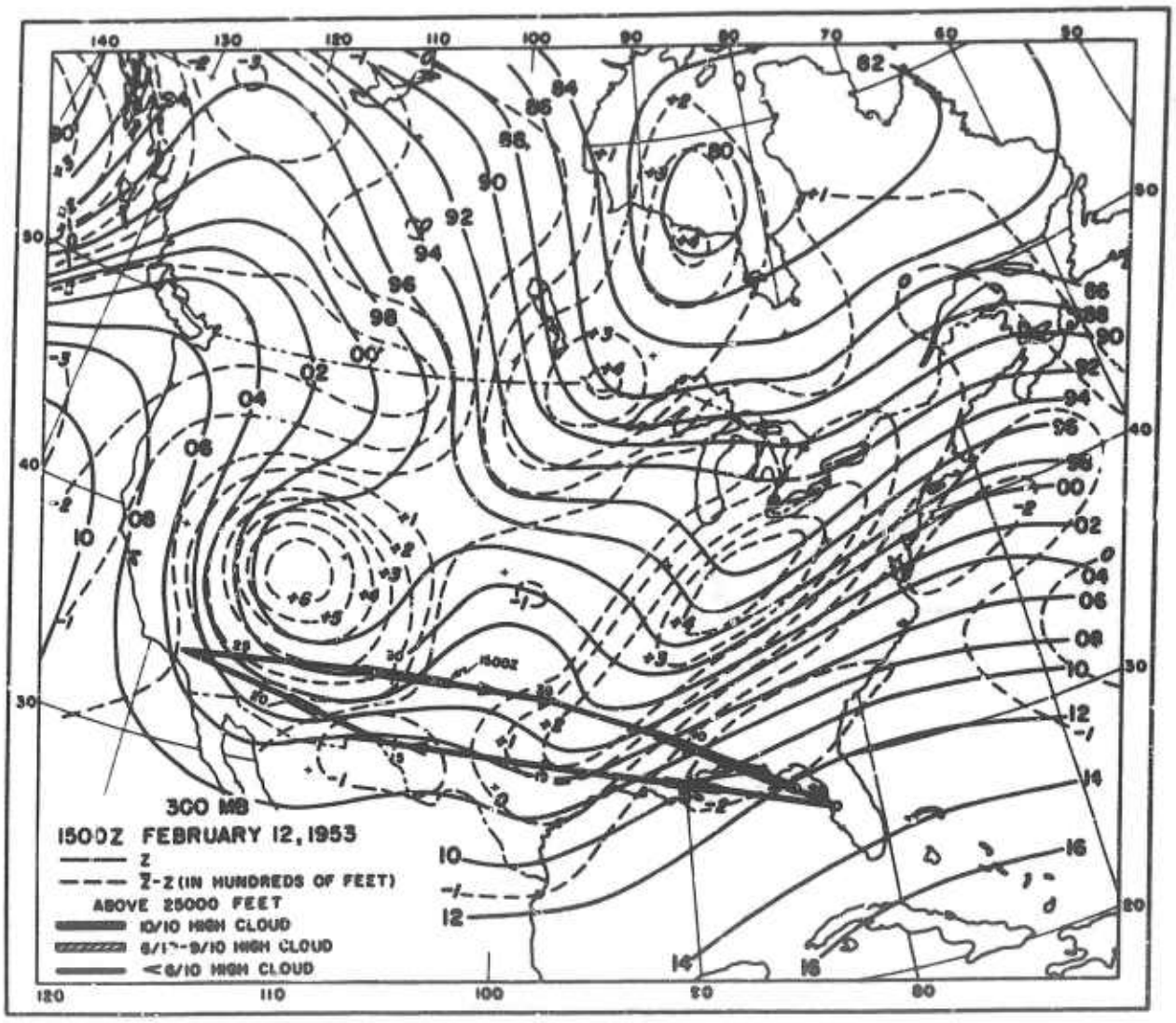

Figure 36. 300-mb Chart, 1500Z, 12 February 1953. For legend see Figure 32.

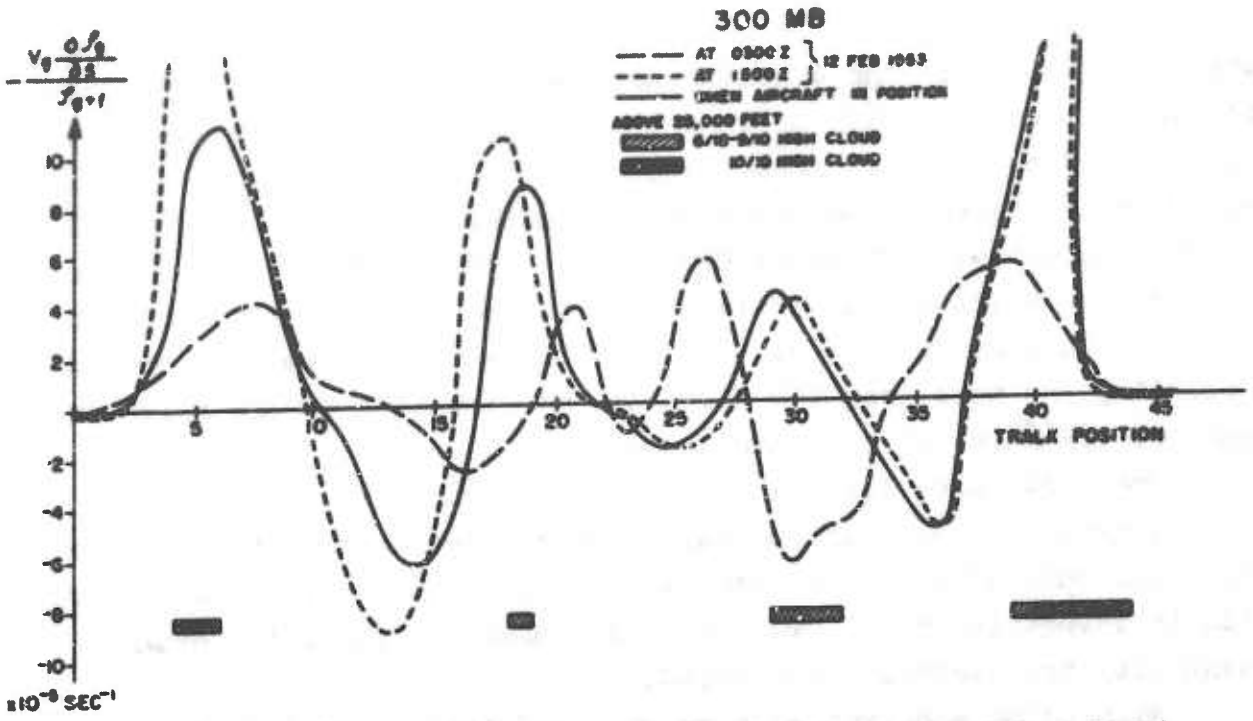

Figure 37. Vorticity-Advection Term at 300 mb Along the Track of Aircraft. Dashed curve at 0300Z, dotted curve at 1500Z, 12 February 1953. Full curve applies to the time when aircraft was in the position marked on the abcissa.

actually was in that position. This was done for all flights, and the values of the vorticity-advection term were grouped and compared with the occurrence of high-cloud layers. Table V shows the results:

TABLE V

Frequencies (Number of 100 miles) and Relative Frequencies (%) of Cloud Covers Above 25,000 Feet in Relation to the Vorticity-Advection Term at 300 mb.

$-\frac{V_g \partial f_g/\partial s}{f_{g+0}} 10^{-5}$ sec^{-1}	+ 0	>10	6 TO 10	4 TO 6	2 TO 4	0 TO 2	-2 TO 0	-4 TO -2	-6 TO -4	-10 TO -6	<-10	− 0	TOTAL
FREQUENCY OF ADVECTION TERM	7	8	13	30	62	120	126	57	18	7	3	0	435
FREQUENCY OF CLOUD COVER > 6/10	6	2	4	12	24	25	6	5	1	0	0	0	85
FREQUENCY OF CLOUD COVER 6/10-9/10	0	0	2	0	6	6	2	0	0	0	0	0	16
FREQUENCY OF CLOUD COVER 10/10	6	2	2	12	18	19	4	5	1	0	0	0	69
RELATIVE FREQUENCY (%) > 6/10	86	40	31	31	39	21	5	13	6	6	0	0	20
RELATIVE FREQUENCY (%) 6/10-9/10	0	0	15	0	10	5	2	0	0	0	0	0	4
RELATIVE FREQUENCY (%) 10/10	86	40	16	31	29	16	3	13	6	0	0	0	15

The first line of Table V shows the grouping of the vorticity-advection terms. ∞ denotes sections along the track where the absolute vorticity is computed to be negative, $+\infty$ where $\partial \gamma_g / \partial s < 0$ and $-\infty$ where $\partial \gamma_g / \partial s > 0$. The second line gives the distribution of flown distance in units of 100 miles within these groups. The third line gives the frequency of broken or overcast high cloud. Of the total of 43,500 miles flown, 8500 miles or 20% had broken or overcast cloud above 25,000 feet. Of these 8500 miles, 7300 or 86% occurred in areas of positive vorticity advection. The fourth line gives the frequency of broken cloud; only 4% of the total distance had broken high cloud extending for more than 100 miles in the direction of the flight as against 16% with overcast high cloud.

The last three lines show relative frequencies of the three amount groups, broken or overcast, broken, overcast. The probability of occurrence of extensive overcasts clearly increases with the vorticity advection term: 600 out of 700 miles of indicated dynamic instability had overcast high cloud.

High cloud occurred with negative advection for 1200 miles or 14% of the total cloud. Two single cloud layers accounted 1000 miles, as shown in Figures 38 and 39.

Figure 38 shows a detail of the map at 0300Z on 1 February 1953. The aircraft was in the position marked 0300Z at the time of the map. The dotted line separates the areas of positive and negative advection. The high-cloud overcast to the left of this line clearly existed in an area of negative advection even if this was not particularly large in magnitude. On closer examination, this was found to be a case where the local change of vorticity to the rear of the trough exceeded the advective change. The trough and the associated tightly-packed vorticity lines to the rear of it moved eastward rapidly, following a surface low that moved northeast at 30-35 knots. This shows that it is necessary to check the local change of vorticity in areas of the map where highly-packed vorticity lines are nearly parallel to the contours and show motion normal to themselves. This will be the case in sharp troughs surrounded by strong winds and also in cold lows that show movement. It is well-known from synoptic practice that also medium and low cloud and precipitation at times extended to the rear of such high-level circulation patterns.

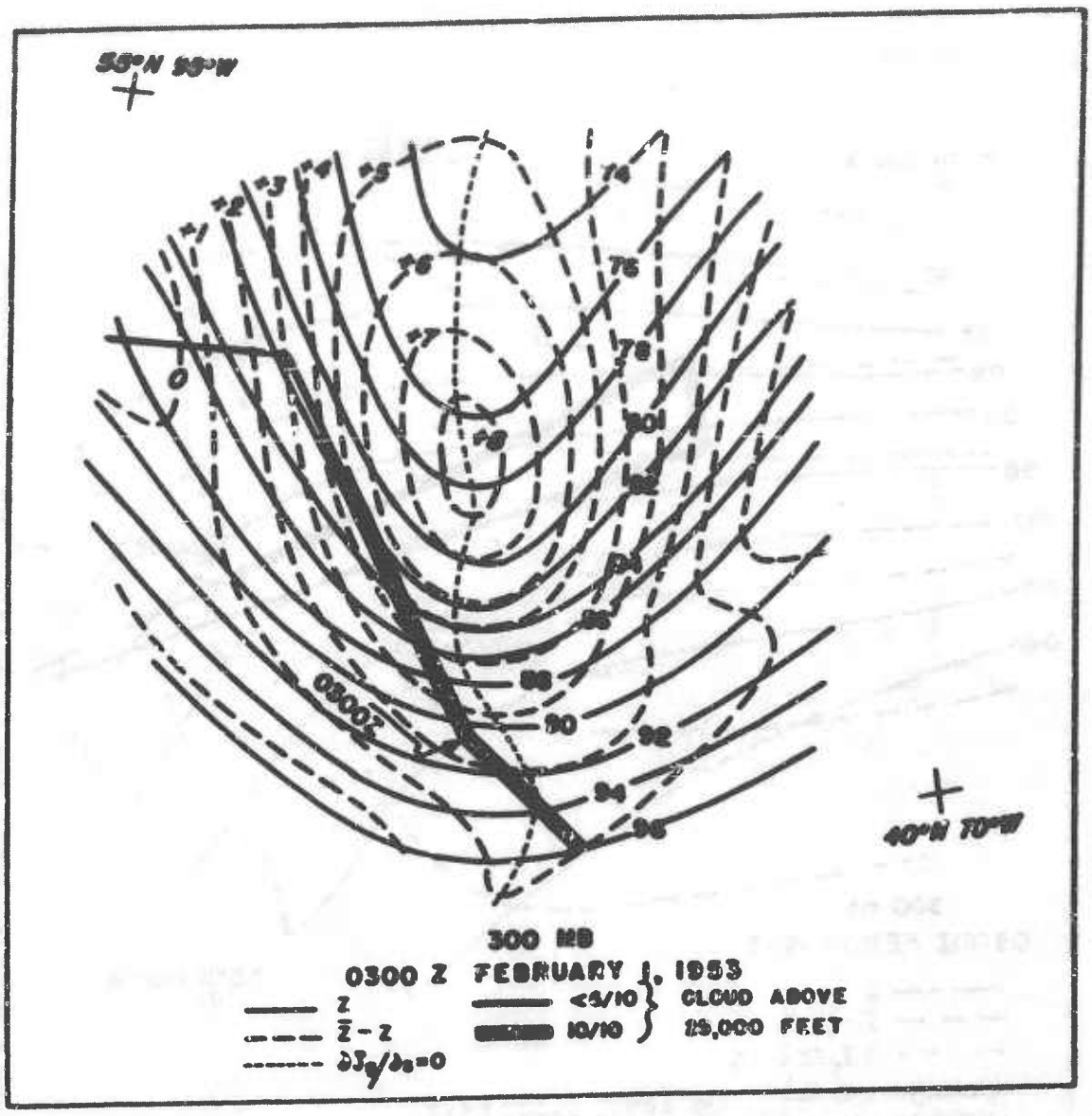

Figure 38. Detail of 300-mb Chart, 0300Z, 1 February 1953. Position of observing aircraft at map time indicated by arrow.

Figure 39 illustrates that high clouds that probably had formed in ascending motion west of the ridge at 300 mb extended for a considerable distance into the area where descending motion should be expected. The high clouds were observed during the period 1900-2100Z on the 16th. The position of the zero advection line at 2100Z on the 16th was therefore interpolated between its positions at 1500Z on the 16th and 0300Z on the 17th. That is the line marked 2100Z on the map. The position of the aircraft at 2100Z is also indicated. The high-cloud deck extended for about 350 miles into the negative-advection area at this time. The

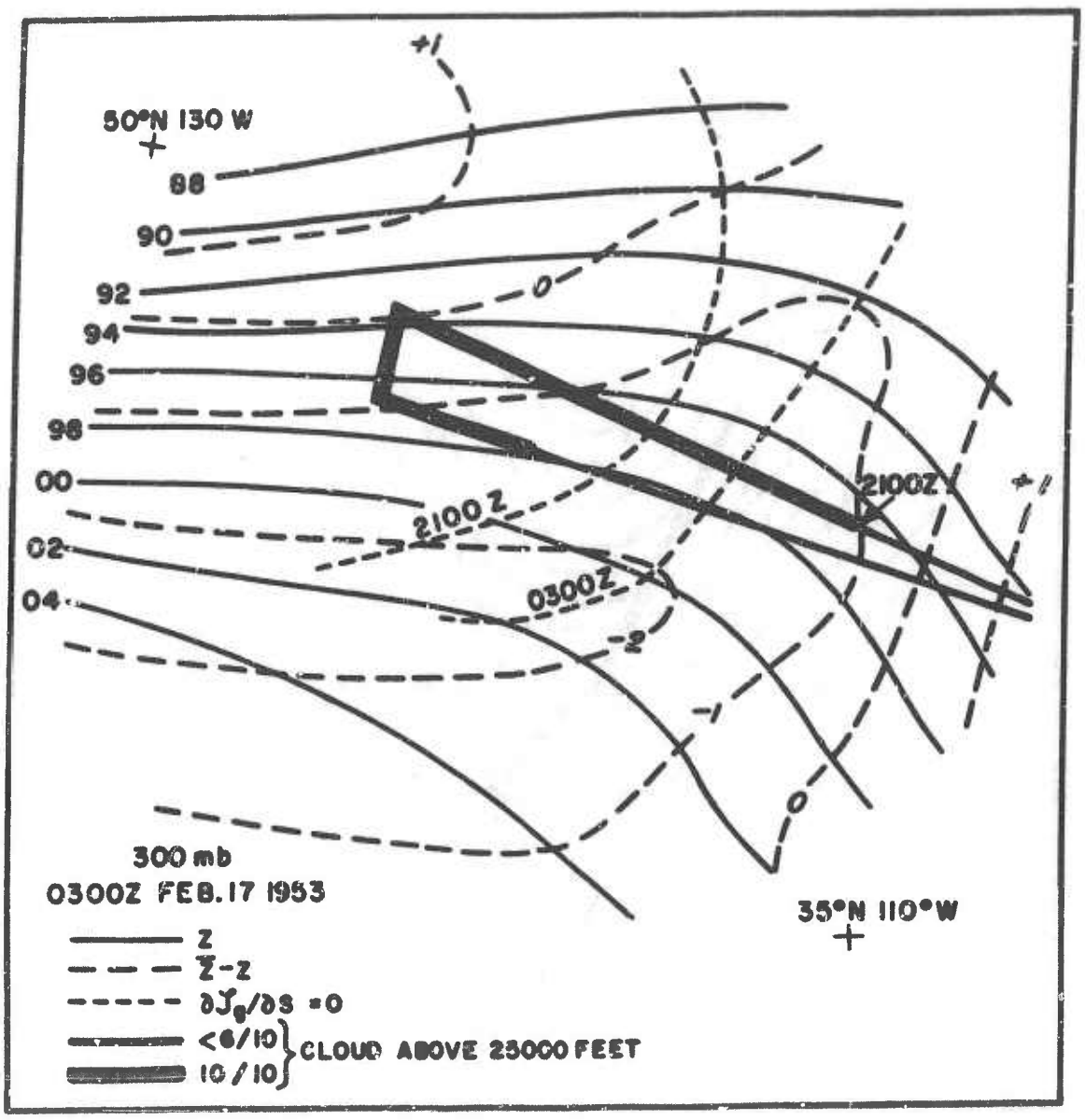

Figure 39. Detail of 300-mb Chart, 0300Z, 17 February 1953. Dotted lines are zero-advection lines at map time and at 2100Z, 16 February. Position of observing aircraft at 2100Z marked on track.

top of the cloud deck fell from 34,000 feet at the ridge line at 2100Z to 30,000 feet where the cloud deck broke up. This also points towards descending motion east of the ridge line.

This continued existence of ice clouds for hundreds of miles into areas of descending motion is most likely due to the different saturation pressures over ice and water. It is generally accepted that the

ice-phase of the cloud particles is reached through the water phase [see paragraph 2.2] [51]. Condensation in any quantity does not occur till water saturation is reached. Once water saturation is reached, water droplets form, which in turn freeze on freezing nuclei (become active below -35° to -40°C), and the crystals continue to grow so long as the air is ice supersaturated.

In a cloud in an ascending air mass, the adiabatic cooling tends to maintain water saturation, whereas the growth of the crystals tends to establish ice saturation. The humidity in the cloud will be somewhere between the two limits, probably nearer water saturation, at least in the top of the cloud. From levels in the temperature range from -35°C to -55°C, adiabatic descent of about 1300 feet will bring air originally water-saturated to ice saturation. Assuming a mean downward velocity of 3 cm/sec and a wind of 80 knots, the air will be displaced about 300 miles during the descent before the ice crystals cease growing. Subsequent evaporation, at a rate which is unknown, may be so slow at high levels that the cloud may be removed still further from where it was formed before it dissolves. When forecasting high clouds, we must, therefore, consider not only the areas where it can form (i.e., where cooling to water saturation can be reached), but also the subsequent life history of the cloud as it moves into regions of descending motion.

The fall-out speed of the ice crystals complicates this problem. If the fall-out speed is large, the cloud could not drift very far from the active-formation area. The example shown suggests that the ice crystals in extensive clouds have sufficiently small fall-out rates for a considerable displacement to take place into areas of moderate downward motion.

4.2.5. Conclusions. The main results of this study may be summarized as follows:

(a) 86% of the extensive cloud layers above 25,000 feet were found in areas of positive vorticity advection at the 300-mb level.

(b) The cloud layers were often found centered on the areas of maximum values of the vorticity-advection term, although there were exceptions to this rule.

(c) The areas where the outlined method of computing the vorticity gave negative values for the absolute vorticity contained on all occasions an overcast high-cloud deck.

(d) The probability of occurrence of extensive high clouds

increases markedly with the vorticity-advection term. However, since 50% (on the average) of the area of the 300-mb map will indicate positive vorticity advection and only 20% will have extensive high clouds, some parameter or parameters other than the vorticity advection will be needed for a closer determination. It is obvious that the humidity distribution at high levels is important. Since synoptic humidity reports above 500 mb are unreliable or nonexistent, a quantitative analysis of the humidity distribution at high levels cannot be undertaken at the present time. It is possible, however, that a humidity analysis at some lower levels (e.g., 500 or 700 mb), in conjunction with vorticity-advection charts at 300 mb, may prove useful [see paragraphs 4.1.15 and 4.5]. This has not been attempted in this study.

(e) 14% of the high cloud fell in areas of negative vorticity advection. These exceptions from the main rule were found to occur either as an upstream extension of the normal cloud sheet east of a sharp trough, or as a drift to the east of a ridge line of clouds presumably formed originally west of the ridge line.

[Note: The discussion on cirrus and the tropopause included in the original paper will be found in paragraph 4.1.11.]

4.3.0. A Method of Forecasting Cirrus Clouds, by Captain Hyko Gayikian [27]. From March 1953, the AWS detachment at MacDill AFB used this empirical method for forecasting the extent and height of cirrus clouds. The results there were successful enough to make it a recommended procedure in the 1st Weather Group (now the 3d Weather Wing)[27].

Gayikian's method has two phases, one for forecasting the extent of cirrus, the other for its height. The association of cirrus with the contour patterns, which forms the basis of the cirrus-extent forecasting, was derived from the author's observations, but finds a physical explanation in the work of French and Johannessen [24] (see paragraph 4.2). It has not been given a formal test and no verification statistics are available. Gayikian's description is given here without change. At points his presentation is not clear, as certain terms are not sufficiently defined: "convective cirrus," "advective cirrus," "difluent," "confluent," etc. The wind profiles illustrated for the cirrus-height forecasting method are so generalized that one may have difficulty comparing them to many actual profiles. Consequently, the methods can only be applied with a large amount of subjectivity. This does not necessarily detract from their usefulness, but it does mean

that some experience or experimentation with them may be required in order to obtain as good results as the originator does. Also, the empirical type of approach leads to a considerable number of rules which must be learned. The results of French and Johannessen's study (paragraph 4.2) permit one principle, which can be applied qualitatively, to take the place of many rules. Gayikian's article follows:

4.3.1. Introduction. Cirrus clouds are of two primary types, advective and convective. The advective cirrus appear to have a relationship to the orientation, wave length and amplitude of the maximum wind isotachs and wind flow at a level just below the tropopause. These clouds are relatively easy to forecast by this technique, while convective cirrus, both thunderstorm and frontal, are more difficult to forecast, but not impossible. A model is shown in Figure 40 for the idealized advective-cirrus pattern. Variations exist, but they are usually indicative of cirro-genetical and "cirro-lytical" conditions.

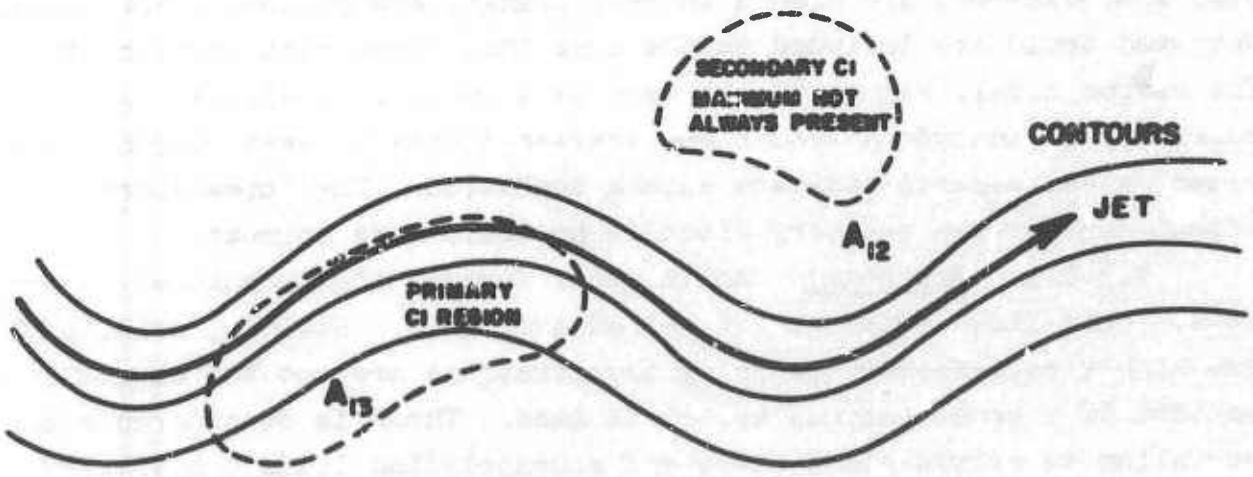

Figure 40. Model of 200-mb Flow and Jet Axis and Associated Cirrus Distribution.

4.3.2. Procedure for Determining Cirrus Extent.

4.3.2.1. Plotting. A fairly large-scale chart is best, the WRC 4-4E was used at MacDill AFB weather detachment and has been found to be very satisfactory. Data is plotted from the 1830Z hourly sequences in the following manner:

Clear
Scattered
Broken
Overcast
Obscured

The hourly sequences were chosen rather than synoptic or 3-hourly weather because they are believed to present a better picture. The obscured symbol is used when the upper sky is hidden by lower clouds or obstructions to visibility. When this condition exists, the sequences are checked three hours prior and subsequent to chart time along with pilot reports to determine if cirrus was possibly present at the time of obscuration. In addition, all sequences are scanned for reports of shower and thunderstorm activity. When present, the standard symbol is plotted adjacent to the station.

4.3.2.2. Analysis. Prior to actual analysis, the 200-mb jets and low centers are entered on the chart. The areas of overcast, broken, and scattered are shaded in red, orange, and yellow, respectively. Obscured areas are included in the area that seems most appropriate. The cirrus model, Figure 40, is used as a guide to analysis. It is not necessary to include a broken and scattered area between overcast and clear unless reports indicate such a condition. The "break-line" method can be used and very often is probably more correct.

4.3.2.3. Prognosis. As in other forecasting techniques, there is no "sure-fire" or short-cut method available. However, results that are highly satisfactory to using organizations are not too difficult to achieve if a conscientious effort is made. There is considerable conservatism to cirrus-cloud cover and extrapolation lends itself very well.

Before all else, a careful study of upper-air troughs, ridges, and jet streams should be made. Careful consideration to wave length, amplitude, confluent and difluent regions are important. From this, make a 200-mb jet prognosis and enter on the chart. The resent areas of cirrus are then progged downstream using the following rules (applicable to advective cirrus only): (see Figure 41)

RULES A1 THRU A9
(See Figures 41a thru 41c.)

AMPLITUDE OF JET

WAVE LENGTH OF JET	No Change	Increase	Decrease
No Change	RULE A1 Cirrus forecast to exist in same area relative to the jet that it is now existant. Cirrus generally spreading eastward.	RULE A2 Cirrus spreading northward and diminishing in south slightly. Cirrus denser.	RULE A3 Entire cirrus area decreasing. Cirrus less dense.
Increasing	RULE A4 Cirrus extending more east-west and less north-south. Cirrus less dense.	RULE A5 Cirrus spreading northeastward. Little change in density.	RULE A6 Cirrus will tend to dissipate or area of cirrus cover decrease. Cirrus less dense.
Decreasing	RULE A7 Cirrus area will decrease in eastern portion. No change in density.	RULE A8 Cirrus area will decrease, but spread to north. Slight density decrease.	RULE A9 Cirrus area will decrease.

RULE A10. If a confluent area is developing, cirrus will form downstream near the point of inflection (see Figure 41d) and build or form both up and down the stream (see Figure 41e). Upstream from the point of maximum wind, the cirrus will be stable and generally cirrostratus; downstream from the maximum wind it will be unstable and generally cirrocumulus. Greatest density will be at point of maximum wind.

RULE A11. If a difluent area is developing, cirrus will dissipate in the difluent area (see Figure 41d) and the area of dissipation will spread upstream (see Figure 41e).

RULE A12. Cirrus rarely exists in the area south of a jet trough, but a secondary area of cirrus may be present in the low center to the north. There will be a clear area or band between this area and that to the east of the trough. (See Figure 40.)

RULE A13. Cirrus usually exists in the center and back part of a ridge area to the south of the jet. (See Figure 40.)

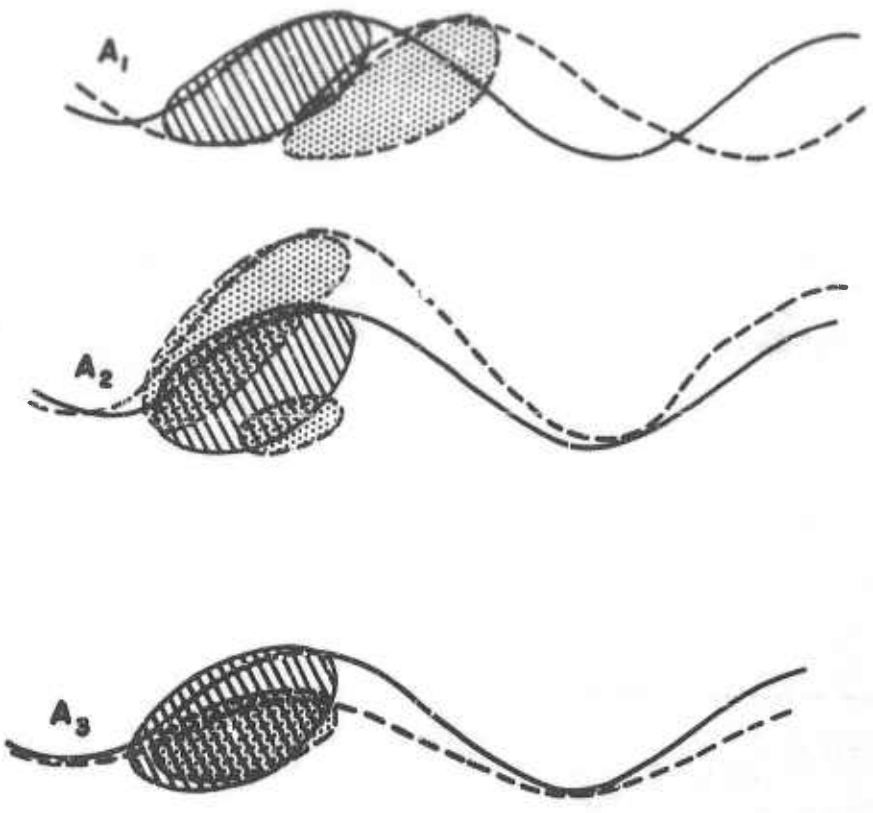

Figure 41a. Rules A1, A2, A3.

Figure 41a. Models of Cirrus-Level Flow and Cirrus Distribution Illustrating Various Prognostic Rules (see Text). Where two sets of contours and cirrus areas are shown, those in solid lines are the initial condition and those dashed are the condition towards which the situation is trending. Cross-hatched areas are cirrus associated with solid-line contours, dotted areas, those associated with dashed contours.

RULE A14. If the wind maximum (jet) crosses contours towards higher height downstream, cirrus is more likely to exist than if the jet crosses contours toward lower heights. (See Figure 41f.)

RULE A15. The presence of frontal or thunderstorm activity within the maximum cirrus area must be considered. The usual effect is to thicken the cirrus, lower the base, increase the height of the top, and extend the cirrus area more easterly.

For purely convective cirrus, both thunderstorm and frontal, the following rules can be applied:

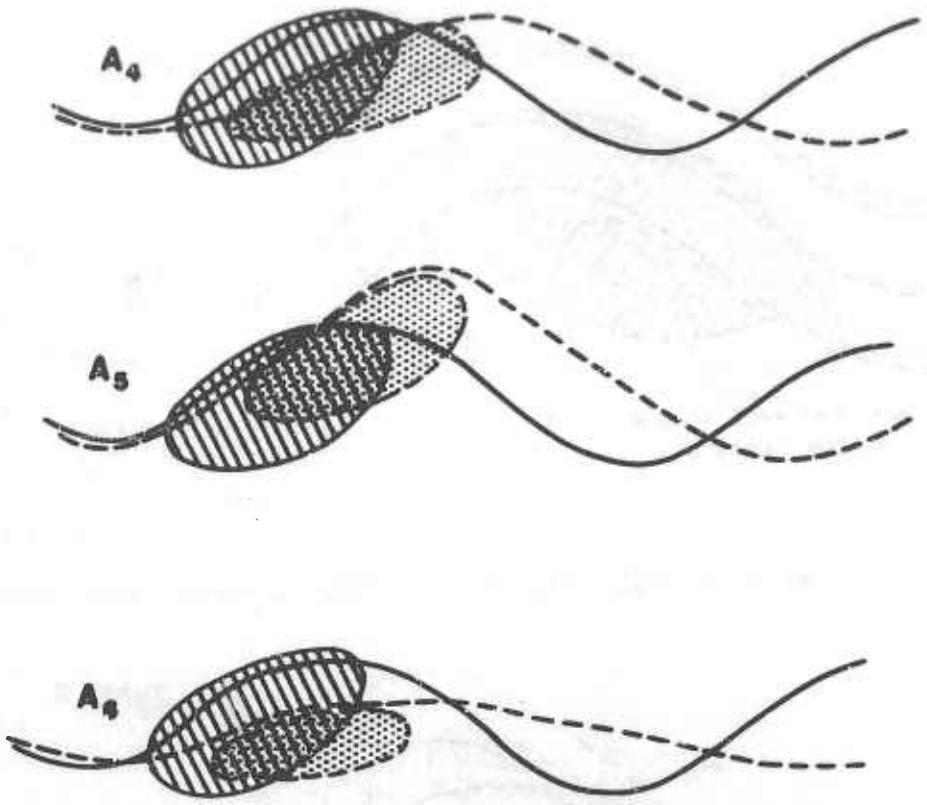

Figure 41b. Rules A4, A5, A6. (For legend, see Figure 41a.)

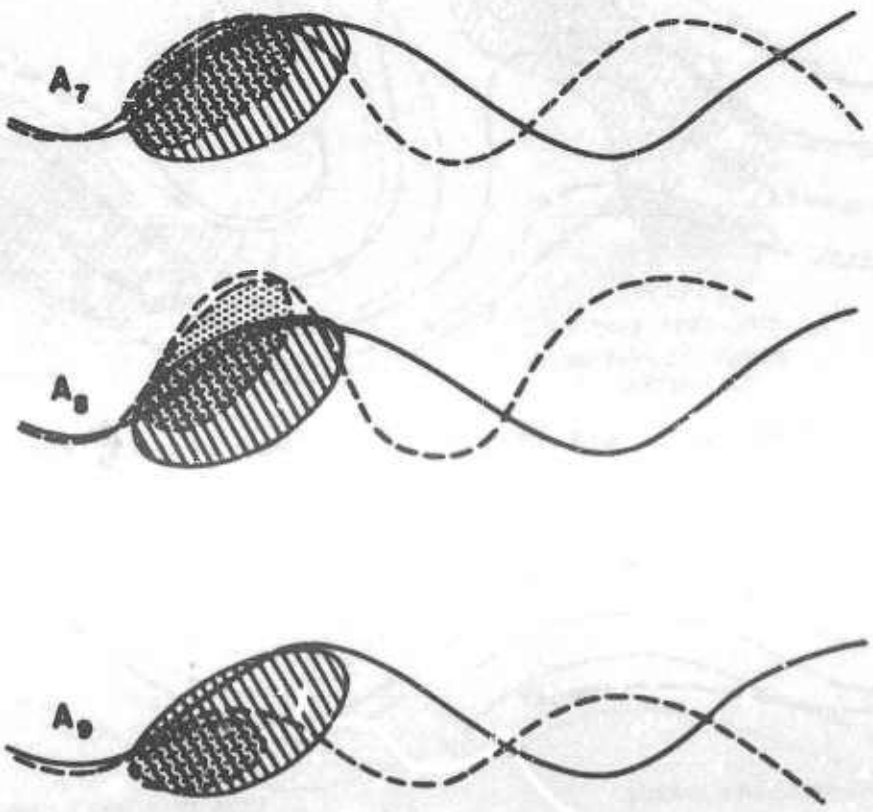

Figure 41c. Rules A7, A8, A9. (For legend, see Figure 41a.)

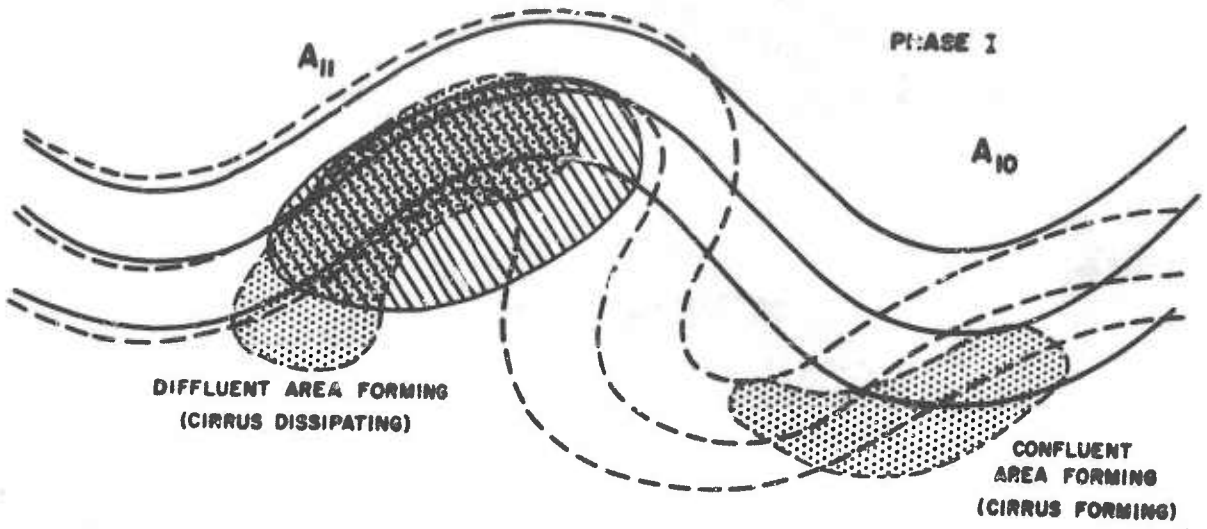

Figure 41d. Rules A10, A11 (Phase I). (For legend, see Figure 41a.)

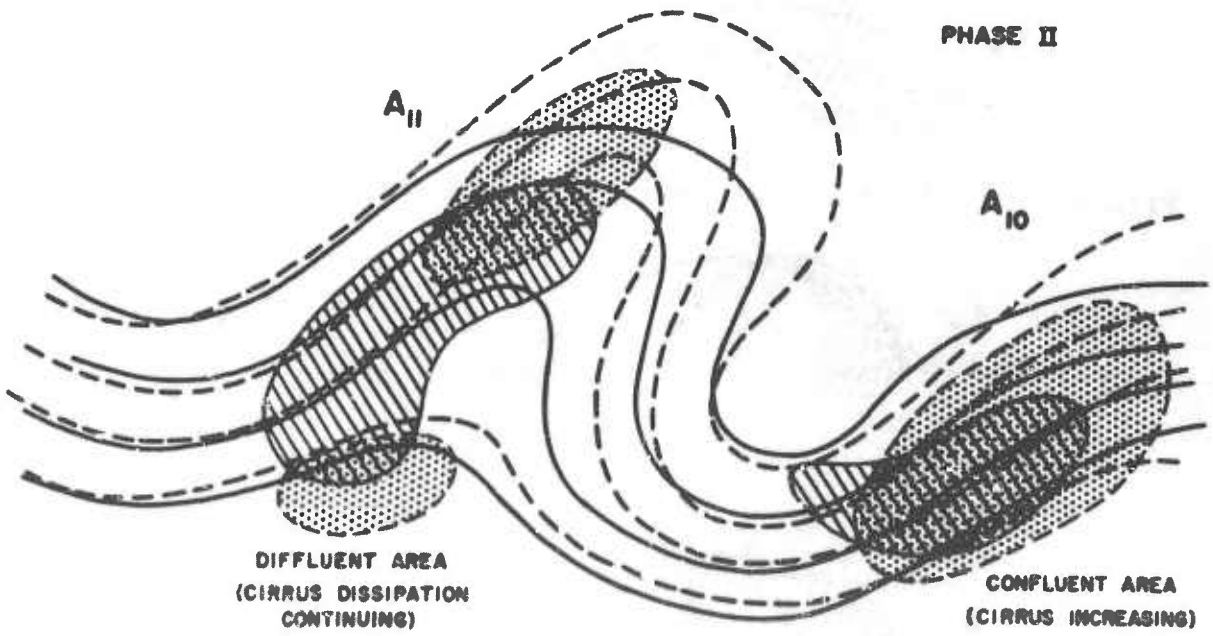

Figure 41e. Rules A10, A11 (Phase II). (For legend, see Figure 41a.)

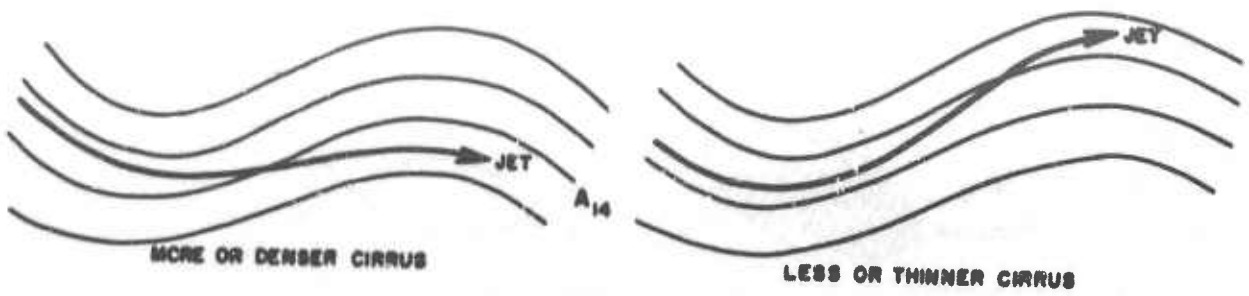

Figure 41f. Rule A14.

RULE C1. If straight-line or anticyclonic flow exists (at 300-200 mb) over the area downstream from a thunderstorm area, cirrus may appear the next day and advance ahead of the ridgeline.

RULE C2. If the contours over area downstream are cyclonically curved, cirrus may or may not appear. It is more likely to appear if the flow is weak.

4.3.3. Procedure for Determining Cirrus Heights.

4.3.3.1. Advective Cirrus. The height of the base and top of advective cirrus appears to have a close relationship to the vertical wind shear. Although no statistical evaluation has been yet determined, cirrus has been noted to be more prevalent with certain types of wind profiles. The height of the base and top can be determined with the use of wind profiles as shown in Figure 42.

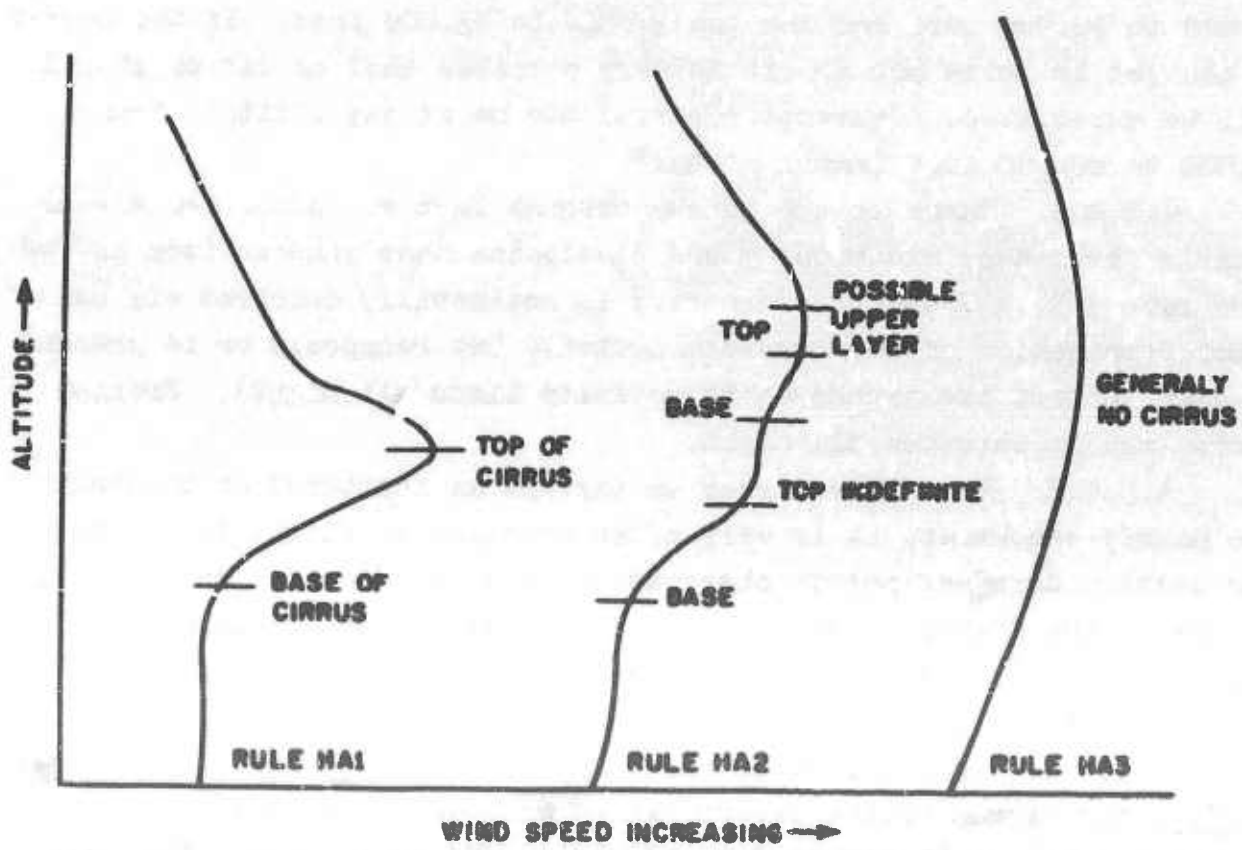

Figure 42. Models of Wind Profiles Illustrating Rules for Forecasting the Heights of Cirrus Layers (see Text).

RULE HA1. (Figure 42) The greater the wind shear between cirrus bases and tops, the greater the density, probability of occurrence, and

validity of this rule. [Compare, however, investigations by others, paragraph 4.1.12.]

RULE HA2. (Figure 42) Low density, but in layers, and the total distance from the base of the lowest layer to the top of the highest layer is greater.

RULE HA3. (Figure 42) No cirrus or very thin layers not visible from the ground and reducing horizontal visibility only slightly.

4.3.3.2. Convective Cirrus. There is no definite technique for determining the heights of convective cirrus, but the base may coincide with a good wind-shift or shear and the top will very often be near the tropical tropopause.

4.3.4. Further Notes.

4.3.4.1. It has been noticed that the bases of advective cirrus are higher than those of convective cirrus. Generally, the base is 33,000 to 39,000 feet and the top 37,000 to 43,000 feet. If the center of the jet is below 300 mb, it is very possible that no cirrus at all will be associated. Convective cirrus may be at any altitude from 25,000 to 60,000 feet (maybe higher).

4.3.4.2. There is a definite diurnal factor. Advective cirrus usually forms near mid-morning and dissipates near sundown [see, however, paragraph 3.3]. Thunderstorm cirrus is not usually observed six hours after termination of thunderstorm activity but reappears or is present at dawn (unless the thunderstorm activity lasts all night). Frontal cirrus may be observed all night.

4.3.4.3. Even when cirrus is carried as scattered or broken in the hourly sequences, it is very often overcast at flight level, but low density does not permit observation from the ground. This usually occurs in the fringe areas of the main cirrus region [compare paragraphs 2.1.6, 3.1, and 3.3]. When forecasting cirrus, it is safer to call it overcast, or overcast with thin spots.

4.3.4.4. An interesting example of the reverse use of the wind-profile for cirrus-height determination was made in a recent [1953] record-breaking B-47 flight from Limestone AFB to England. The crew was briefed on the principle of maximum winds being just at the top of the cloud deck. The crew was advised to seek out this level when winds were between 250° and 260°. The crew reported that this procedure gave them several additional knots tail wind and helped them to establish

the new record.

4.3.4.5. Contrail forecasting can be combined with the neph-chart. Areas conducive to cirrus formation are more likely to have contrails in the marginal case (90% to 100% humidity curves of the diagram in AWSM 105-100 Rev.).

4.4.0. An Approach to the Problem of Cirrus-Cloud Forecasting, by R. L. Hendrick [31].* Hendrick has attempted to devise a simple practical method of cirrus forecasting by combining the idea of thickness advection as an indirect indication of vertical motion with an indirect indication of moisture aloft, on a single chart something like the one suggested by Fletcher and Sartor [23]. The resulting "cirrus-indicator chart" is considered a forecasting aid which the forecaster may in turn improve upon subjectively. A limited test indicated the chart used by itself led to considerably better forecasts than those made without any special aid or method, but even so, the "skill" shown was rather low. The chart does not do well in summer nor for scattered high-level cirrus. The parameters used in the chart are themselves difficult to predict accurately, which rather critically affects the location of the cirrus — no-cirrus dividing line and hence the accuracy in predicting the percentage area of the prognostic map which will have cirrus. Hendrick's report follows:

4.4.1. Introduction. Observations of the United States during the colder seasons show that cirrus clouds occur at all elevations between 20,000 and 40,000 feet, with warmer conditions and lower latitudes favoring the higher levels. The average height of cirrus appears to be approximately 30,000 feet.

Fletcher and Sartor [23], French and Johannessen [24] [and paragraph 4.2], Endlich [20], Sawyer and Ilett [54], Schwerdtfeger [57], and Reed and Plagge [52] are among those who have reported on studies relating various synoptic parameters to cirrus-cloud formation. Southerly wind components, veering winds with height, 500-mb moisture, positive vorticity advection, positive temperature advection, the east side of upper troughs, and the southerly side of westerly jet streams have shown varying degrees of apparent relationship with cirrus-cloud formation.

---

* Reprinted with permission of Sandia Corporation.

It is the purpose of this study to investigate a combination of parameters which may be related to cirrus-cloud formation in such a way as to offer further possibilities for forecasting improvement.

4.4.2. Selection of Parameters. Upward motion and high relative humidity at the cirrus levels are the properties directly related to cirrus-cloud formation. Unfortunately, direct, accurate measurements of these properties are not possible.

Investigations have shown cirrus clouds to be associated with southerly wind components, veering wind with height, the east side of upper troughs, or the west side of upper ridges. These associations suggest a relationship between cirrus clouds and warm-air advection at the cirrus levels. Empirical evidence indicates that the effect on local temperature change attributed to horizontal temperature advection is ordinarily reduced by vertical motion, or upward motion is usually associated with warm-air advection. A further check on the validity of this relationship at the 300-mb level was made and it was found to be true in 72% of 240 cases studied. However, the average of two 12-hour advection values was used as the mean over the 12-hour periods, and this could lead to some error. Although little confidence can be placed in the figure of 72%, the result does substantially indicate the previously-stated relationship between temperature advection and vertical motion.

In this study, the sign of the geostrophic advection of the 400- to 300-mb thickness on the 400-mb surface was selected as a parameter which should be related to vertical motion and cirrus-cloud formation. The use of thickness advection rather than temperature advection at a particular level allows a study of mean advection through a substantial layer in the cirrus region and also permits a more accurate analysis.

Temperatures in the 400- to 300-mb layer do not permit accurate relative-humidity measurements. However, if any moisture is detected at these levels, it usually signifies a condition of near saturation. The presence of any measurable moisture above the 400-mb level was selected as a second parameter related to cirrus-cloud formation.

The two parameters selected for study, the sign of the 400- to 300-mb thickness advection and the presence of measurable moisture above 400 mb, are presumedly related to the properties necessary for cirrus-cloud formation, namely, vertical motion and high relative humidity at the cirrus levels.

4.4.3. Cirrus-Cloud and Parameter Data at Albuquerque, New Mexico. The parameters described above were measured at Albuquerque, New Mexico, for each 12-hour sounding period over the months of March, April, October, November, and December 1953. Observed cirrus cloudiness for the same period at Albuquerque was recorded using a 5-hour average of tenths of cirrus coverage centered at the 0300Z and 1500Z upper-air soundings. Two-tenths or more average cirrus coverage was considered a "cirrus case" and less than 0.2 average coverage a "no-cirrus case." The cirrus and no-cirrus cases were then compared with the signs of the two parameters. Table VI shows the results of these data. The cases of observed cirrus definitely favor the combination of positive advection and measurable moisture above 400 mb.

TABLE VI

Albuquerque Cirrus and Upper-Air Parameter Data

Observed	M- A-	M+ A-	M- A+	M+ A+
Cirrus	5	9	15	42
No Cirrus	116	30	51	14

M+ = moisture above 400 mb
M- = no moisture above 400 mb
A+ = positive 400- to 300-mb thickness advection
A- = negative 400- to 300-mb thickness advection

Table VII is the tetrachoric table (see Brooks and Carruthers, "Statistical Methods in Meteorology") of this same data. The combination of positive advection and measurable moisture is considered as indicating cirrus while all other combinations of parameter signs are considered as indicating no cirrus. The correspondence between the indicator data and the observed data is 8[illegible]%. The tetrachoric correlation between indicated-cirrus and no-cirrus and observed-cirrus and no-cirrus cases was computed to be r_t = +0.8[illegible].

TABLE VII

Tetrachoric Table of Albuquerque Cirrus and Upper-Air Parameter Data.

Parameter Signs	Observed		
	Cirrus	No Cirrus	Total
M+ A+	42 (14)	14 (42)	56
M- A-			
M+ A-			
M- A+	29 (57)	197 (169)	226
Total	71	211	282

Indicated and observed correspondence = 85%
r_t = 40.84
( ) = distribution expected if no relation exists between parameter signs and observed cirrus
M+ = moisture above 400 mb
M- = no moisture above 400 mb
A+ = positive 400- to 300-mb thickness advection
A- = negative 400- to 300-mb thickness advection

4.4.4. Cirrus-Indicator Chart. In order to combine the advection and moisture parameters in such a way as to facilitate their testing and possible forecast use over a large area, a cirrus-indicator chart was prepared. At each upper-air station over western United States, 400-mb heights, 400-mb and 25,000-ft winds, 400- to 300-mb thickness values, and the lowest pressure at which any moisture is measurable were plotted on an ordinary weather chart; 400-mb contour analysis and 400- to 300-mb thickness analysis were then completed. Areas of positive thickness advection were then outlined. As an aid to advection analysis, plus signs were plotted by each station showing veering winds from 400 to 300 mb or from 25,000 to 30,000 feet, and negative signs were plotted by stations showing backing winds. Areas of moisture above 400 mb were then outlined. Cirrus clouds were considered indicated wherever areas of moisture above 400 mb coincided with areas of positive thickness advection. All other areas were considered as indicating no cirrus.

4.4.5. Test of the Cirrus-Indicator Chart. Current data, beginning 18 October 1954, and running through 4 February 1955, were used in

testing th cirrus-indicator chart. The 1500Z chart for each of the five weekd was prepared. The area analyzed covered the area of the United Sta west of a line from Green Bay, Wisconsin to Houston, Texas and tended to Ships N and P. Observed cirrus clouds at 111 stations, few or less equally spaced over western United States, were plotted on separate chart. The 1530Z Schedule A observations were used for ob served cirrus data. Scattered or more clouds at or above 20,000 feet were considered cirrus cases. The comparisons between indicated-cir and no-cirrus and observed-cirrus and no-cirrus cases are shown in Tables VIII and IX.

Table VIII shows the distribution of observed cirrus and no-cirrus cases with all combinations of parameter signs.

TABLE VIII

Parameter and Observed-Cirrus Data for Cirrus-Indicator Chart Test.

Observed	Parameter Signs			
	M- A-	M+ A-	M- A+	M+ A+
Cirrus	280	349	398	1497
No Cirrus	1825	378	1383	399

M- = moisture above 400 mb
M+ = no moisture above 400 mb
A- = positive 400- to 300-mb thickness advection
A+ = negative 400- to 300-mb thickness advection

Table XX is the tetrachoric table for this same data. The correspondence between the indicator-chart data and the observed data is 78%. The tetrachoric correlation was computed to be $r_t = +0.78$. An examination of Figure 46 shows 628 more cases of observed cirrus than indicated cirrus. The observed cirrus column shows that 41% of the observed cirrus was not indicated. The average daily area of indicated cirrus for the 76-day test period was 29% while the average daily area of observed cirrus was 39%. In these cases the percentage of area is considered to be the same as the percentage of stations. The correlation coefficient between daily areal percentages of indicated and observed cirrus was computed to be $r = +0.71$. It appears that while indicated- and observed-cirrus areas are closely correlated, the indicated-

cirrus areas are consistently smaller than the observed-cirrus areas, this being the major discrepancy between the cirrus-indicator and observed-cirrus charts.

26 of the 111 cirrus-observation stations were radiosonde stations. It might be argued that the cirrus-indicator chart would be more accurately analyzed at these stations. This is obviously true for the moisture parameter. The correspondence between indicated-cirrus and no-cirrus and observed-cirrus and no-cirrus cases for these 26 radiosonde stations was 76%, not significantly different than the 78% for the entire data.

TABLE IX

Tetrachoric Table of Cirrus-Indicator Chart Test Data

Indicated	Observed		
	Cirrus	No Cirrus	Total
Cirrus	1497 (735)	399 (1161)	1896
No Cirrus	1027 (1789)	3586 (2824)	4613
Total	2524	3985	6509

Indicated and observed correspondence = 78%
r_t = +0.78
( ) = distribution expected if no relation exists between indicated and observed cirrus

Figure 43 shows the percentage of cirrus occurrence over the area studied. It is evident that cirrus occurs more frequently over the more northerly regions.

Figure 44 shows the percentage agreement between indicated-cirrus and no-cirrus and observed-cirrus and no-cirrus cases for each station. The values vary from a low of 60% at Lander, Wyoming, to a high of 91% at Daggett, California.

Figures 45 and 46 show the percentage agreement for cirrus and no-cirrus cases, respectively. Geographical variations in Figures 44, 45, and 46 are not considered significant.

Figures 47 through 50 are a sequence of cirrus-indicator charts and the accompanying observed-cirrus charts. Two independent cirrus-cloud areas are evident, one moving rapidly through a ridge over the

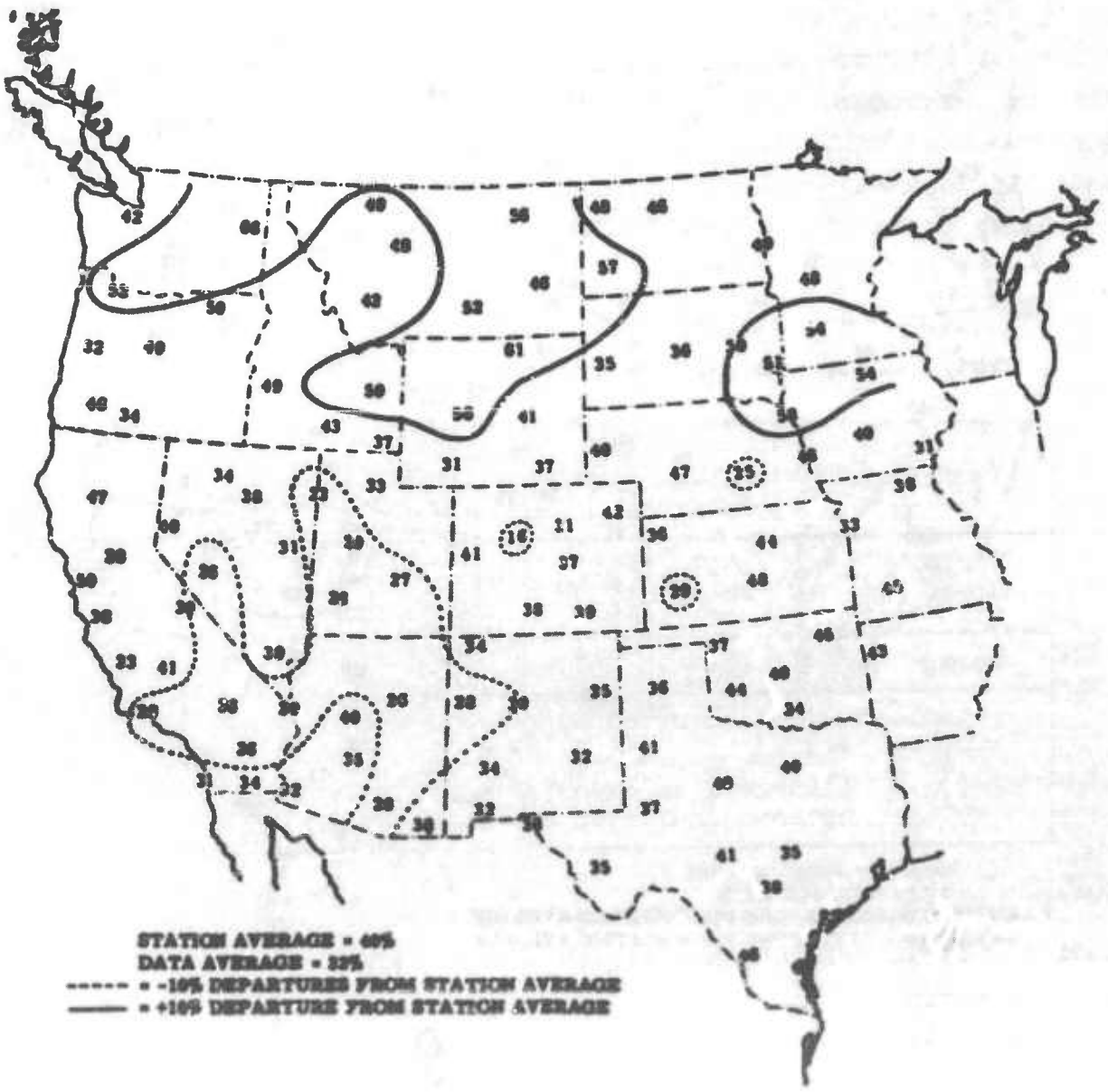

Figure 43. Percentage of Total Observations With Scattered or More Clouds at or Above 20,000 Feet.

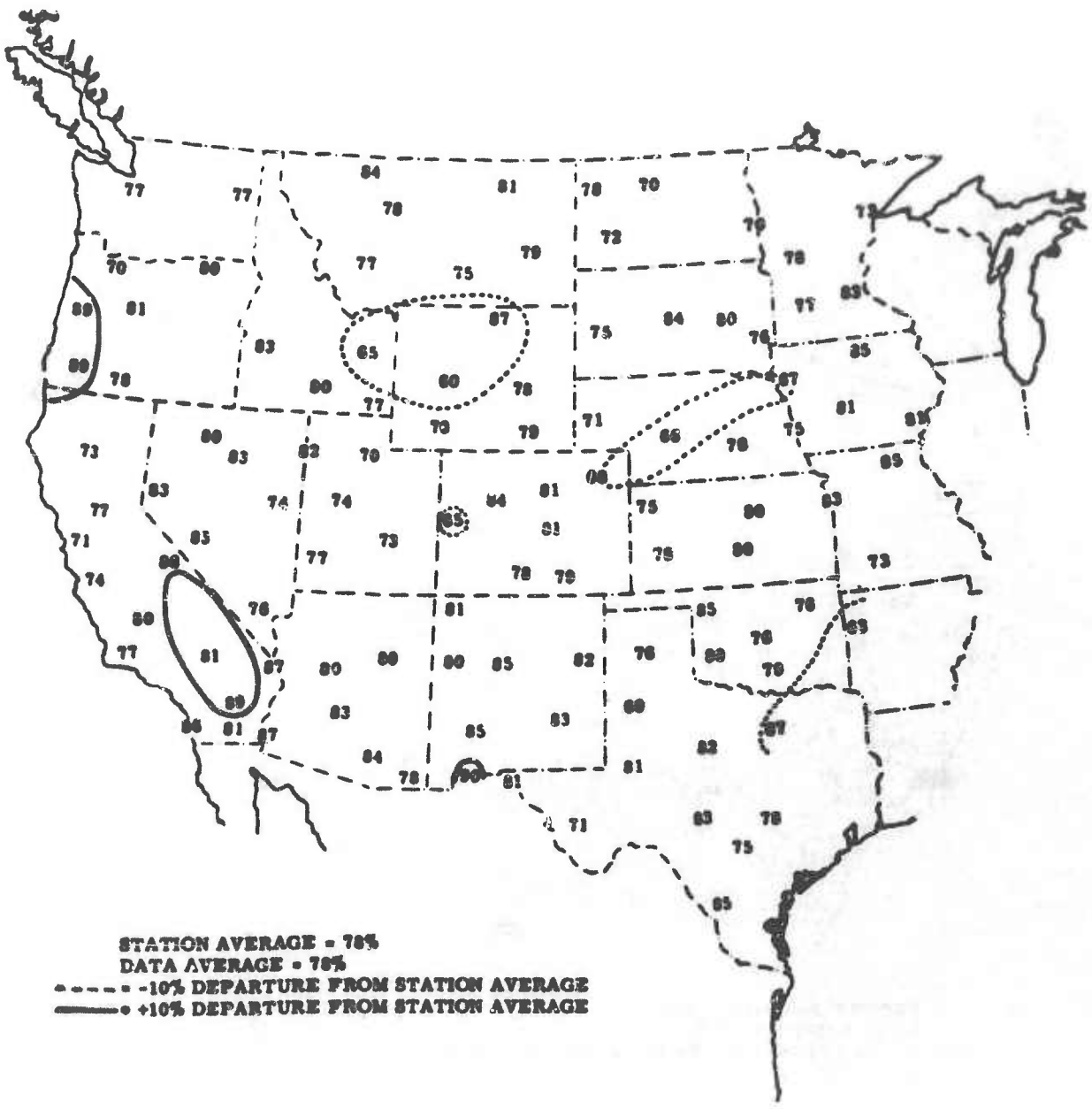

Figure 44. Percentage Agreement of Each Station Between Indicated and Observed Conditions.

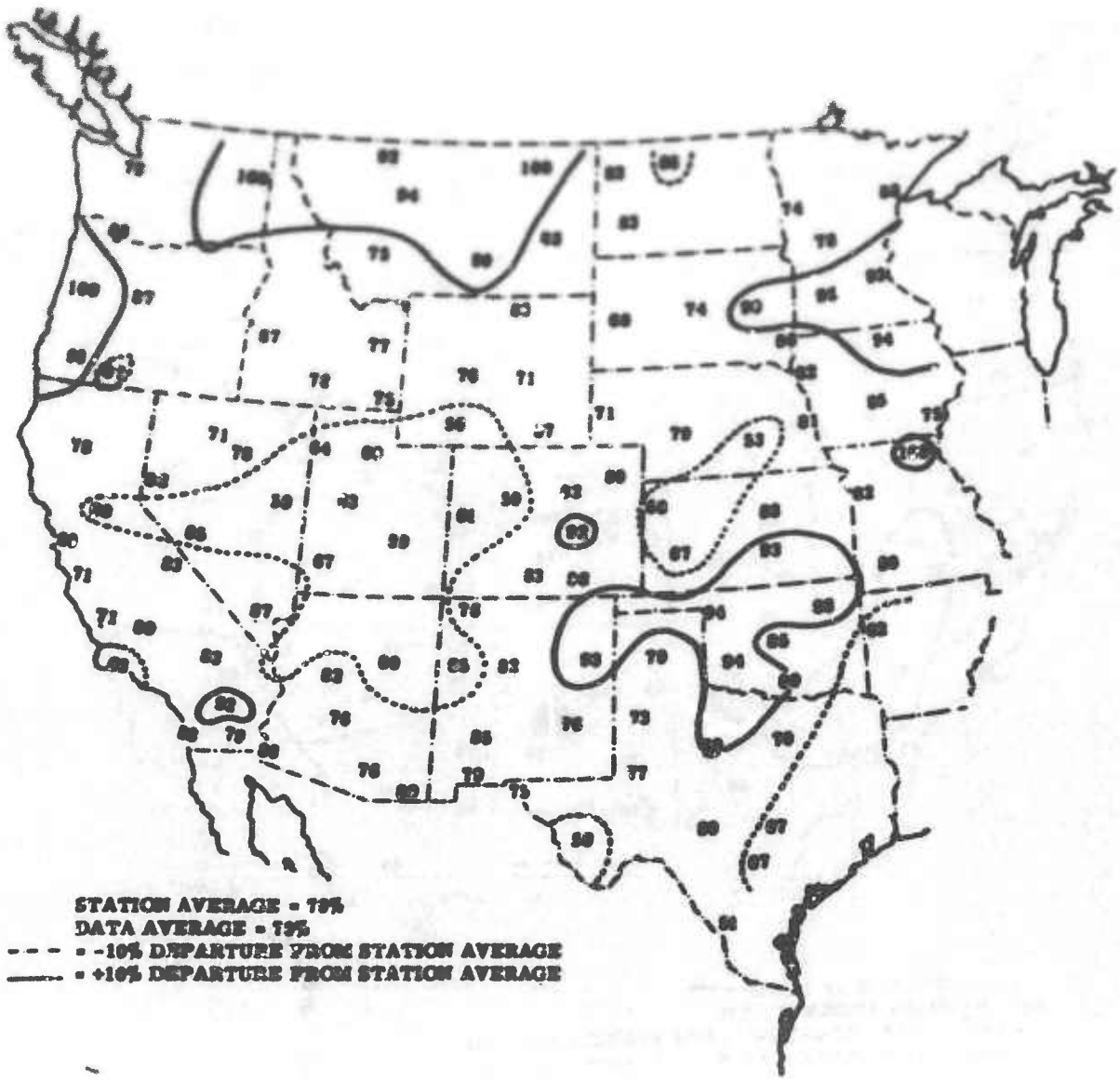

Figure 45. Percentage of Observed Cirrus for All Indicated-Cirrus Cases.

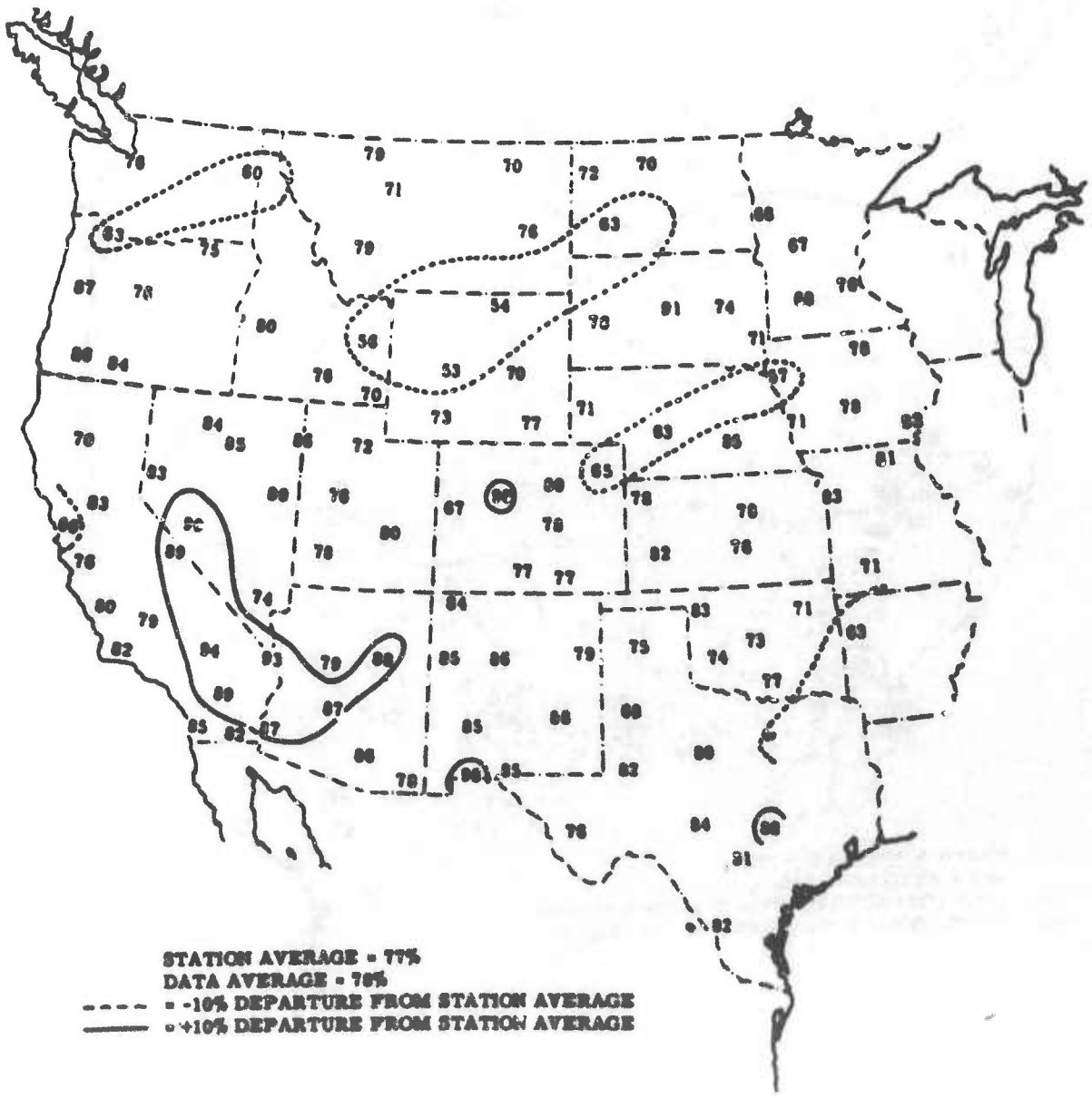

Figure 46. Percentage of Observed No-Cirrus for All Indicated No-Cirrus Cases.

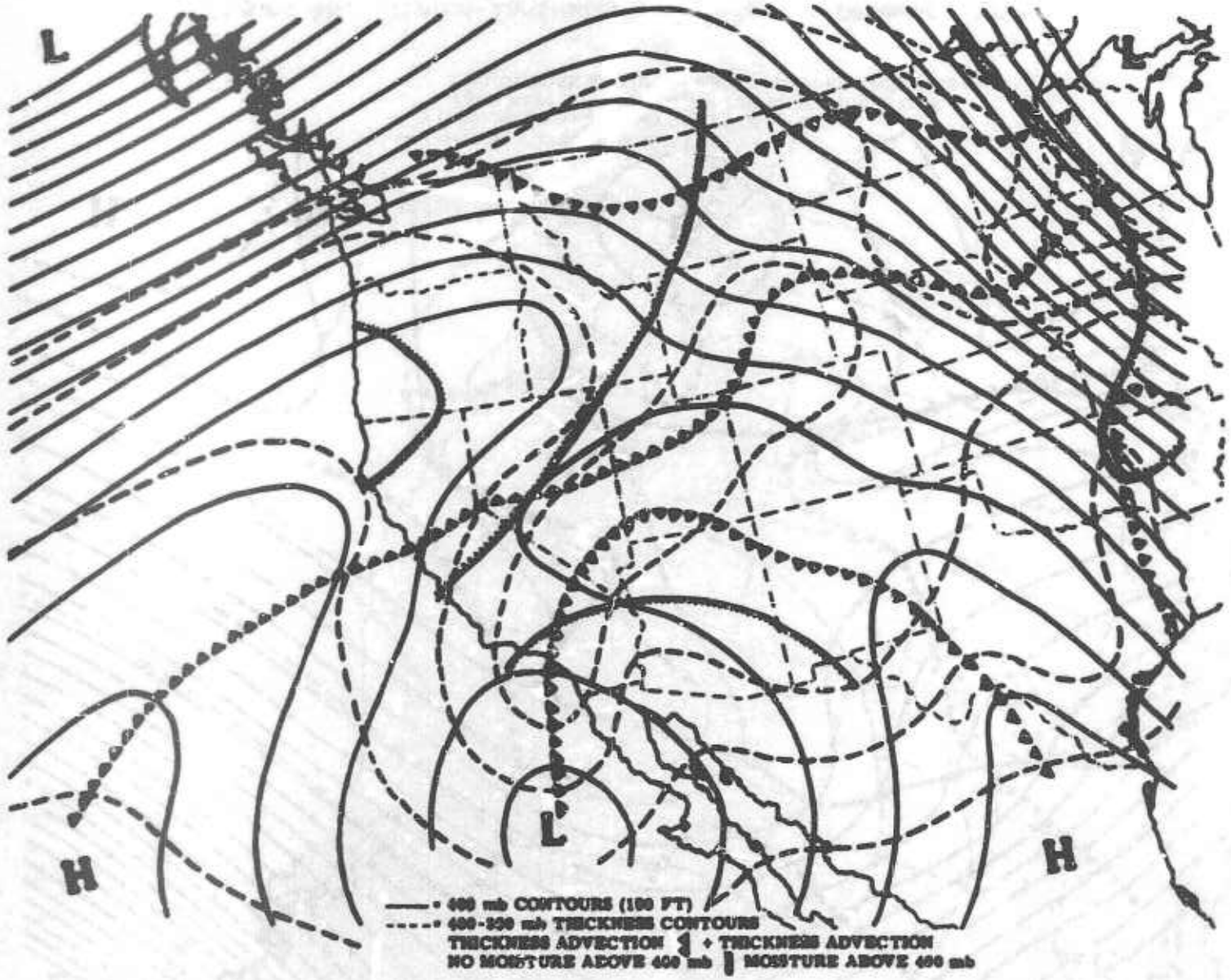

Figure 47. Cirrus-Indicator Chart for 20 December 1954.

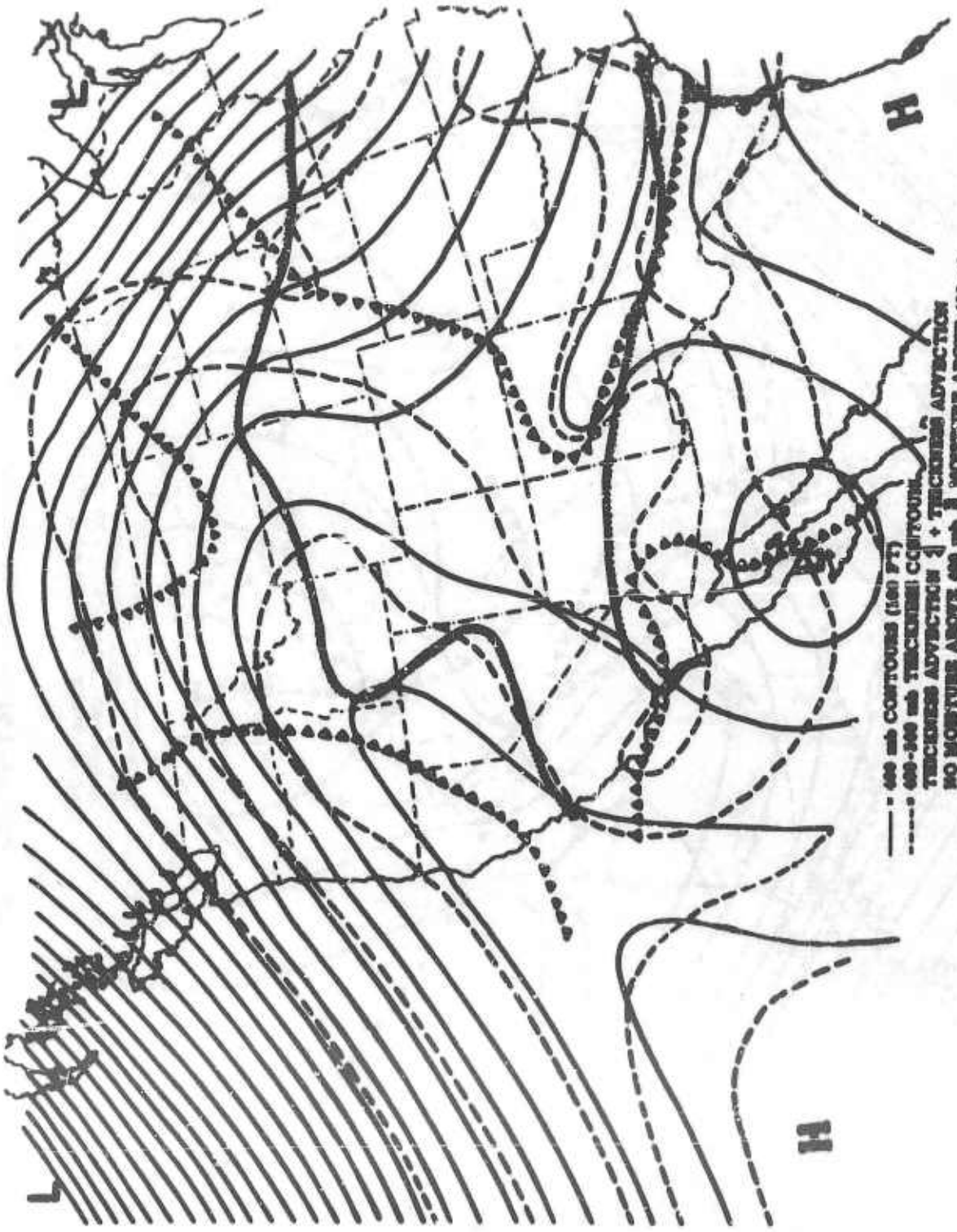

Figure 48. Cirrus-Indicator Chart for 21 December 1954.

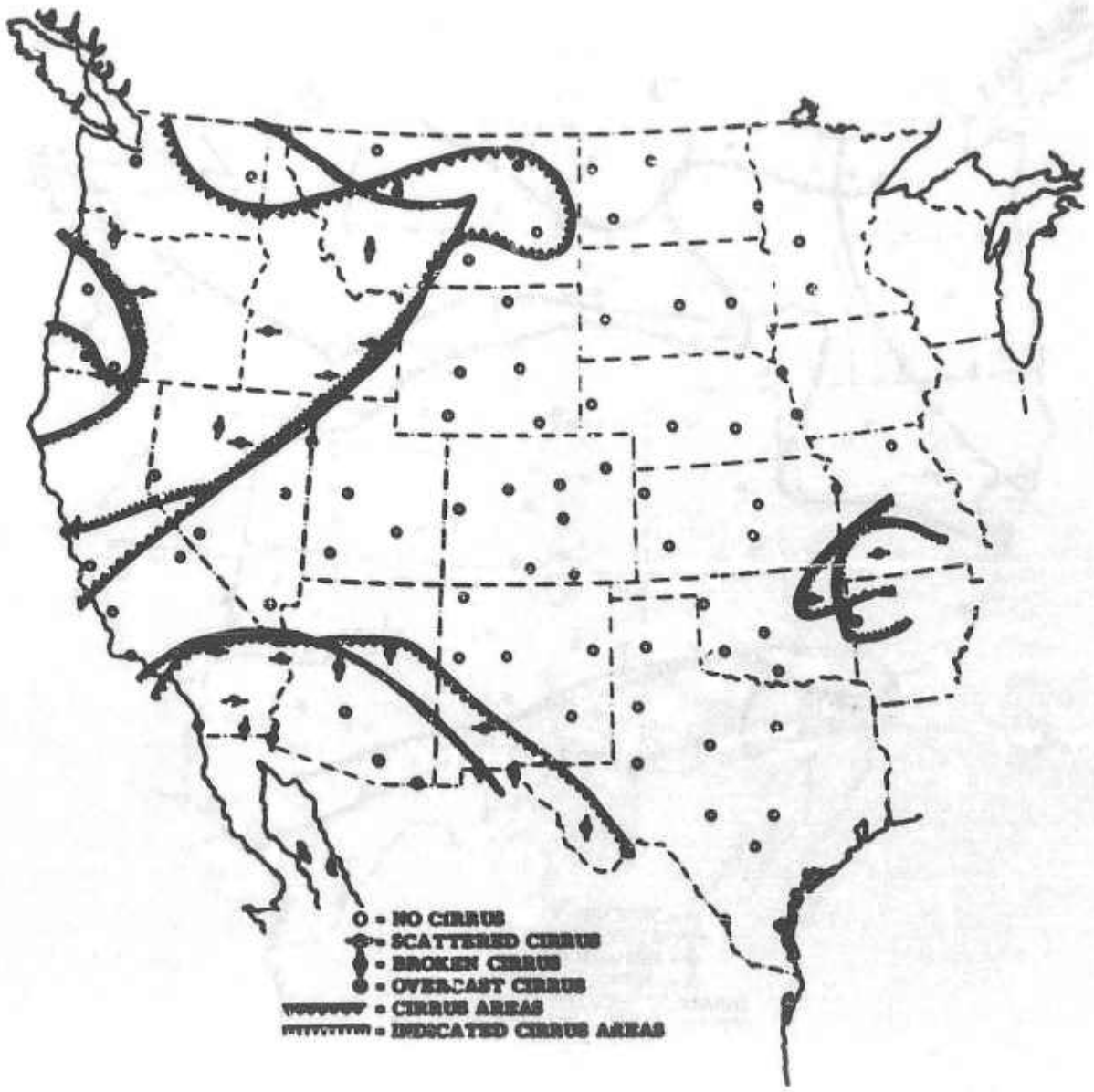

Figure 49. Observed-Cirrus Chart for 20 December 1954.

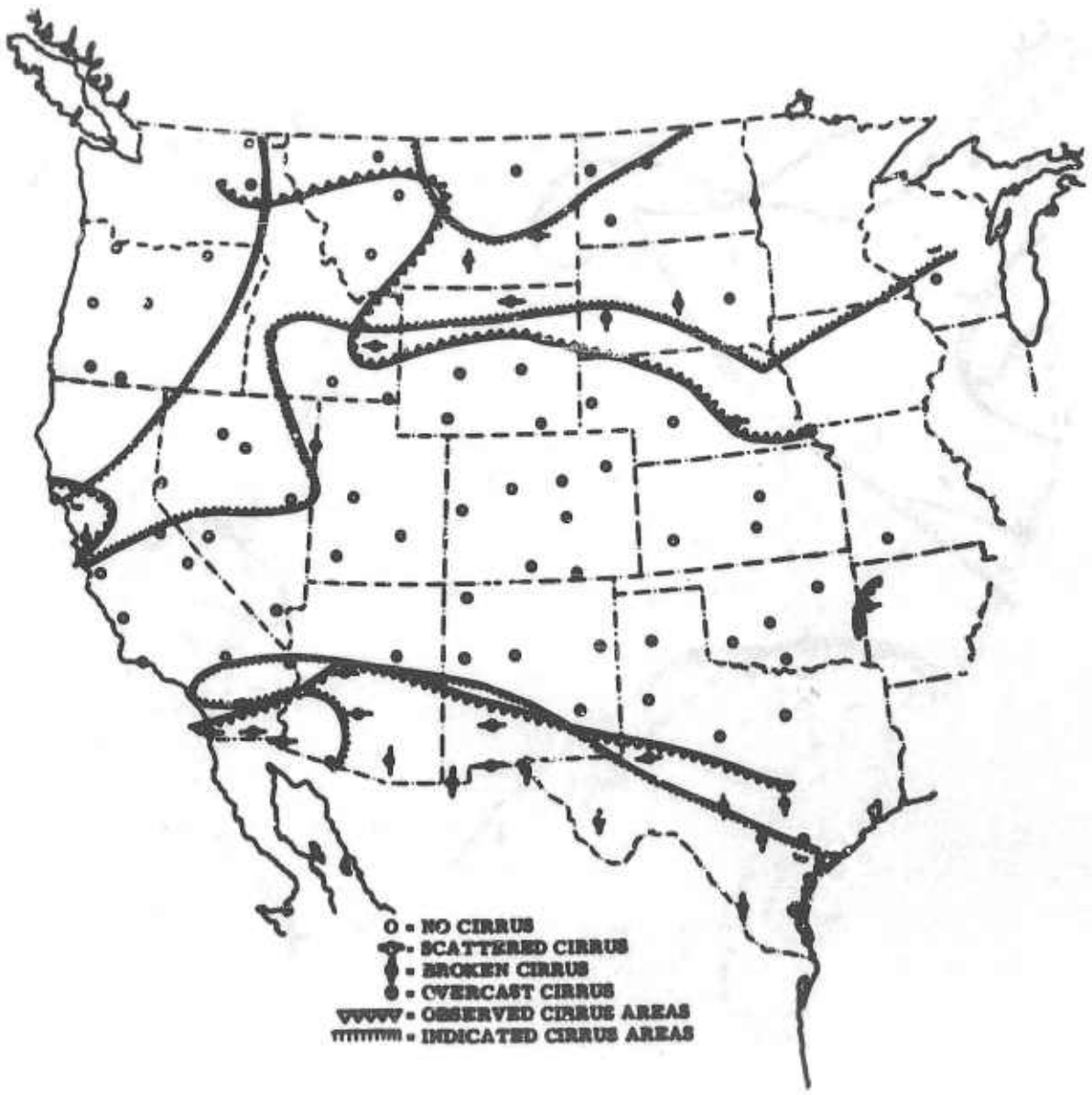

Figure 50. Observed-Cirrus Chart for 21 December 1954.

northern states and the other moving very slowly ahead of a cutoff low in the far southwest. The correspondence between indicated-cirrus and no-cirrus and observed-cirrus and no-cirrus cases for these two days was 84%, 6% above the average for the entire period.

The cirrus-indicator-chart-test results show the chart to be a fairly re able indicator of existing cirrus and no-cirrus areas over the period and region studied. There is no reason to assume this reliability would not hold throughout the colder seasons between 25° and 50° north latitude.

4.4.6. Errors and Limitations. The degree of correspondence between indicated-cirrus and no-cirrus and between observed-cirrus and no-cirrus areas is about as high as could be expected when errors and limitations are considered. Some degree of analysis error in the cirrus-indicator chart is unavoidable. Relatively minor errors in the 400-mb contour analysis and in the 400- to 300-mb thickness analysis can lead to substantial errors in the positive and negative thickness advection areas. Measurable moisture above 400 mb is a discontinuous space-variable and therefore subject to analysis error. Minor errors in the radiosonde data are often undetected and can lead to analysis errors. All clouds reported at or above 20,000 feet above the ground were considered to be cirrus. The possibilities for errors in the observed-cirrus charts are apparent.

The parameters studied are restricted by definition to the 400- to 300-mb layer. The ability of the parameters to indicate cirrus which is forming outside of this layer is uncertain. An example of the fixed-layer limitation is given by the 57 cases of observed cirrus which occurred in positive thickness-advection areas but with no moisture reported above 400 mb because the -40°C isotherm was below the 400-mb surface. Minus 40°C is the lowest temperature at which moisture can be recorded. In these cases, it was impossible for the moisture parameter to function in its fixed layer.

Many cases of very high and thin cirrus were observed when no moisture was reported above the 600-mb level. In these cases, the cirrus may have been forming well above the parameter layer in temperatures too cold to record moisture.

The cirrus-indicator chart cannot be analyzed in sufficient detail to detect cirrus patches that form in an association with local advection or convection processes. These small-scale areas of cirrus are

usually reported as scattered and are seldom indicated. The data show scattered cirrus to be less reliably indicated than broken or overcast cirrus. Scattered cirrus accounted for 33% of all observed-cirrus cases, and accounted for 44% of the cirrus cases not indicated by the cirrus-indicator chart.

In spite of the inability of the cirrus-indicator chart to detect unusually high-level cirrus, very cold-temperature cirrus, and scattered patches of localized cirrus, and regardless of the observational and analysis uncertainties of both the observed-cirrus and cirrus-indicator charts, the data nevertheless indicates the cirrus-indicator chart to be a fairly reliable indicator of existing cirrus and no-cirrus areas.

4.4.7. Use of the Cirrus-Indicator Chart as a Forecasting Aid. During the cirrus-indicator-chart-test period, 24-hour forecasts of cirrus coverage over the western United States were prepared by this writer. The cirrus-indicator chart was used as the principle forecast aid. The total forecast data showed 63% accuracy.

Table X shows the tetrachoric table for the entire forecast data.

Table XIa shows the forecast results for the four stations of San Diego, El Centro, and Thermal, California and Yuma, Arizona. The accuracy for these four stations was 67%. These four stations were examined separately in order to make a comparison with 24-hour forecasts made by the Sandia Corporation Meteorology Section for the Salton Sea Test Base without the aid of cirrus-indicator charts.

Table XIb shows the results of the Salton Sea Forecasts. The accuracy was 53%.

The Salton Sea forecasts, made without reference to cirrus-indicator charts, called for cirrus 60% of the time while cirrus was observed but 22% of the time. At the selected four stations in the same area, cirrus was forecasted, using the indicator chart, to occur 38% of the time and was observed 31% of the time.

It appears that the use of the cirrus-indicator chart as a forecasting aid leads to some improvement in forecasting accuracy. A substantial improvement in accuracy was not anticipated because of the difficulties in prediction of the parameters selected. It is believed quite significantly that the use of the cirrus-indicator chart as a forecast aid leads to forecasts which properly apportion the percentage of cirrus both in time and space. The correlation coefficient between the daily percentages of predicted- and observed-cirrus areas was

computed to be r = +0.39. The principal forecasting difficulty is in the proper location of the cirrus and no-cirrus areas. This relates to the difficulty of predicting positive- and negative-advection areas.

TABLE X

Tetrachoric Table for Entire Forecast Test Data

Forecast	Observed		
	Cirrus	No Cirrus	Total
Cirrus	836 (620)	720 (936)	1556
No Cirrus	694 (910)	1590 (1374)	2284
Total	1530	2310	3840

Verification = 63%
r_t = +0.54
() = distribution expected if no relation exists between forecast and observed cirrus

TABLE XIa

Forecast Results for SDV, ELC, TRM, and YUM, Using Cirrus-Indicator Chart as a Forecast Aid.

Forecast	Observed	
	Cirrus	No Cirrus
Cirrus	29	33
No Cirrus	21	80
Verification = 67%		

TABLE XIb

Forecast Results for SSTB, Without Use of Cirrus-Indicator Chart.

Forecast	Observed	
	Cirrus	No Cirrus
Cirrus	16	40
No Cirrus	4	33
Verification = 53%		

43179O O - 57 - 9

4.5.0. An Objective Method of Local Forecasting of Cirrostratus Clouds, by H. Appleman. In connection with the Air Weather Service program for wider use of objective forecasting techniques, Mr. H. Appleman at the Directorate of Scientific Services, Hqs AWS, made a pilot investigation in 1953-54 to explore the feasibility of cirrus forecasting by such an approach. Two parameters were selected as indirect indicators of vertical motion and humidity and scattergrams prepared for one year's data from Fairbanks (Alaska), Caribou (Maine), Liverpool, Wiesbaden, and Port Lyautey. The results were not too encouraging in the respect that the relationships found varied much with season and locality – which brings into question the universality of application of the parameters chosen. Although a moderate degree of "correlation" was shown, the forecasting value was not tested on independent data. From a composite of all the scattergrams it was judged that the parameters $\Delta 24\ H_{300}$ and $\Delta 24\ T_{300}$ were most universally significant and that an additional test of these on independent data at one station would be desirable, including a test on no-cirrus days also. This was done for Fairbanks and the results are reported below. The bias of having to use for data only days without obscurations preventing observation of cirrus is one that seriously limits the validity of studies of this type using surface cloud observations. Therefore, aircraft cloud observations should be sought if at all possible. This bias probably accounts for some of the unexplainable and illogical apparent correlations found in the Appleman scattergrams.

The detailed report of Appleman containing the original scattergrams and tables for all the stations listed above is not reproduced here because the results of the further test on Fairbanks data indicated the original parameters were not as predictive as some combinations of them. The Fairbanks test report given below is sufficient to show the method and sort of results to be expected.

4.5.1. Introduction. An unpublished report entitled "An Investigation Into the Possibility of Forecasting Cirrostratus Clouds by Objective Methods" evaluated various meteorological parameters for use in forecasting cirrustratus clouds over five widely separated geographical areas for all four seasons of one year, 1951. The places tested were Fairbanks, Caribou, Liverpool, Wiesbaden, and Port Lyautey.

Accurate high-cloud data for purposes of constructing and testing a forecast study are difficult to obtain. The only routine cirrus

observations available are those made by the surface observer in the hourly observation (recorded on the WBAN-10 form, e.g.). In cases of lower broken or overcast cloud layers the presence of upper clouds immediately becomes questionable. Nighttime observations of high clouds also are unreliable. Hence, any resulting correlations are biased toward usage during the daytime and when low or middle clouds are absent or scattered. To reduce this bias the questionable cases were individually analyzed by a professional meteorologist and as often as possible placed in the proper group. However, in certain areas and seasons the questionable cases still outnumbered those known.

The number of hours of combined broken or overcast cirrostratus was counted for each calendar day, based on local time. If less than three hours occurred, the day was defined as "non-cirrus" (N); if three to five hours, "partial cirrus" (P); and if six or more hours, "cirrus" (C). The upper-air data were obtained for 0300Z on the forecast date. Where 24-hour changes were used, the value at 0300Z the day preceding was subtracted from the value at 0300Z of the forecast day.

Graphs were plotted on the duration of cirrostratus (i.e., N, P, or C) as a function of the 24-hour change in temperature at 300 mb ($\Delta_{24}T_3$), the 24-hour change in height at 300 mb ($\Delta_{24}H_3$), the mean lapse-rate between 500 mb and 300 mb (T_3-T_5), and the height at 300 mb (H_3), each parameter being used separately. Scatter diagrams were plotted of the duration of cirrostratus as a function of $\Delta_{24}H_3$ vs $\Delta_{24}T_3$, T_3-T_5 vs $\Delta_{24}T_3$, and T_3-T_5 vs $\Delta_{24}H_3$, two parameters being used on each graph. The data were separated by season and station. Thus, four graphs and three scatter diagrams were drawn for each station for each season.

Lines of best fit were drawn on the scatter diagrams visually separating the data into two areas, one containing as many cirrus (C) and partial-cirrus (P) cases as possible, the other containing chiefly non-cirrus (N) cases. If either two C or two N areas were defined on one graph, the total values of N, C, or P for both areas were combined.

If the parameters used had been directly associated with the occurrence of cirrus, the best-fit lines would have been simple. However, since the parameters available were only indirectly related to cirrus formation, the lines were somewhat complex. Also, they tended

to vary between stations and to a lesser extent between seasons for a single station. In order to increase the probability that the curves will fit future independent data, their shapes were kept as simple as possible and not distorted to pick up or omit individual cases. In most cases, for the same parameters, the curves were of the same general shape for the various seasons and stations, though rather differently placed on the graph.

Skill scores (see AWSM 105-40) were calculated for each scatter diagram. These skill scores could be considered as giving only a rough index as to the significance of the parameters. The more complex the curve, the less weight could be given to the score. It was pointed out in the original report that additional data were needed to locate the lines of demarcation accurately. Also, it was indicated that before being used operationally, the graphs must be checked using independent data. Such a check with a larger sample of independent data has since been made on the summertime graphs for Fairbanks (Ladd AFB), Alaska. The results are presented below.

4.5.2. Results of Fairbanks Summer Test. The three graphs which appeared most successful for forecasting cirrostratus at Fairbanks in the original study (based on data from the summer of 1951) were each based on three parameters: $\Delta_{24}H_3$ vs $\Delta_{24}T_3$, $\Delta_{24}T_3$ vs T_3-T_5, and $\Delta_{24}H_3$ vs T_3-T_5. The results obtained from the first set of parameters in the original study are shown in Figure 51. In the cirrus (C) area there are 27 cases of cirrus and 11 of no cirrus; in the no-cirrus (N) area the values are 5 and 23 respectively. This gives a total of 50 correct cases out of 66, giving a "forecast accuracy" of 76% and skill score of 0.48 (see AWSM 105-40).

Using the same line of demarcation, the results of the new study, based on the data from the summers of 1952-53, are shown in Figure 52. In order to increase the validity of the test, cases of doubtful data were omitted. This was practicable because of the greater quantity of data available. Altogether, 42 quite clear-cut cases of cirrus and 18 of no-cirrus were found. The C-Area on the graph included 32 cases of cirrus, 9 of no-cirrus; the N-Area, 10 and 9. This gives a forecasting accuracy of 68% and skill score of 0.26.

Figure 53 combines the data from the two studies using the original line of demarcation. The C-Area contains 59 cases of cirrus, 20 of no cirrus; the N-Area, 15 and 32. This gives a forecasting accuracy of 72% and a skill score of 0.41. It is possible that slightly greater

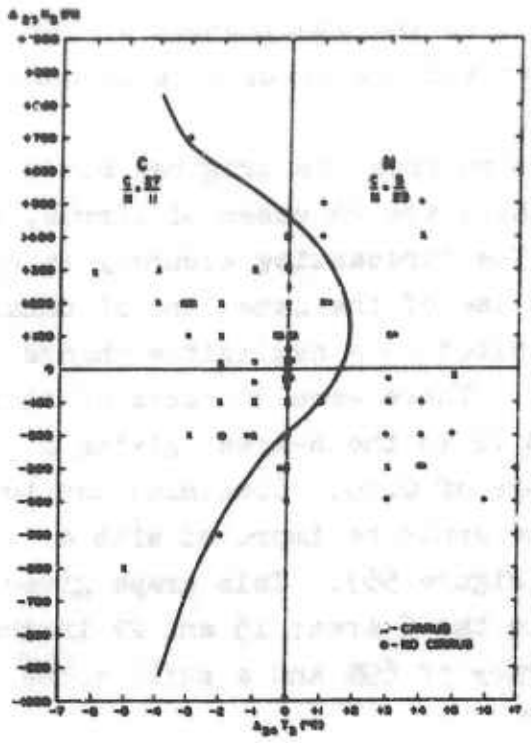

Figure 51.

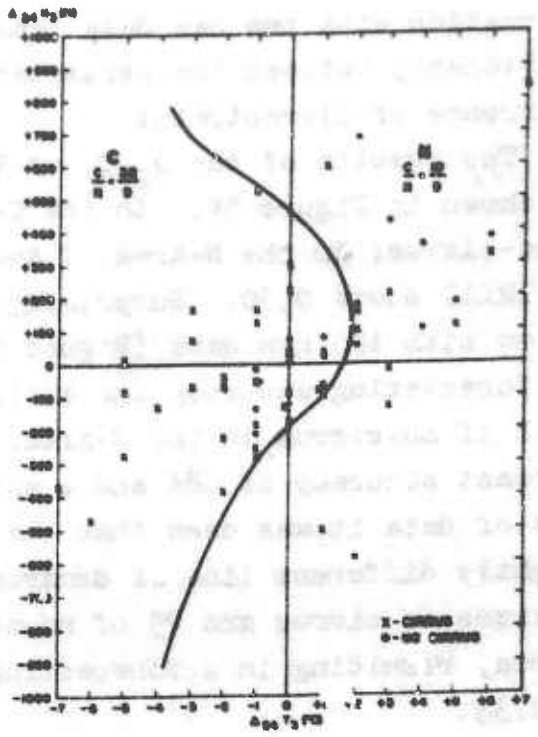

Figure 52.

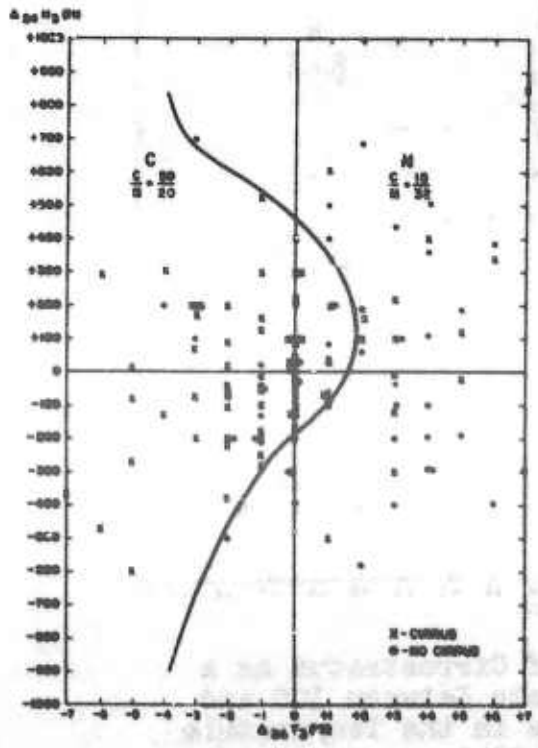

Figure 53.

Figure 51. The Occurrence of Cirrostratus as a Function of the 24-Hour Change in the Temperature and Height at 300 mb, Fairbanks, Summer 1951.

Figure 52. The Occurrence of Cirrostratus as a Function of the 24-Hour Change in the Temperature and Height at 300 mb, Fairbanks, Summer 1952, 1953.

Figure 53. The Occurrence of Cirrostratus as a Function of the 24-Hour Change in the Temperature and Height at 300 mb, Fairbanks, Summer 1951, 1952, 1953.

accuracies could be obtained in Figures 52 and 53 using new lines of demarcation. The fact that skill was shown using the original line of demarcation with the new data lends weight to the genuineness of the relationship between the parameters tested and the occurrence or non-occurrence of cirrostratus.

The results of the $\Delta_{24}T_3$ vs T_3-T_5 graph from the original study are shown in Figure 54. In the C-Area there are 26 cases of cirrus, 16 of no-cirrus; in the N-Area, 7 and 17. The forecasting accuracy is 65% the skill score 0.30. Surprisingly, the use of the same line of demarcation with the new data (Figure 55) resulted in a negligible change in the forecasting accuracy and skill score. There were 30 cases of cirrus and 7 of no-cirrus in the C-Area; 13 and 12 in the N-Area, giving a forecast accuracy of 68% and a skill score of 0.30. Combining the two sets of data it was seen that the results could be improved with a slightly different line of demarcation (Figure 56). This graph gives 61 cases of cirrus and 25 of no-cirrus in the C-Area; 15 and 27 in the N-Area, resulting in a forecasting accuracy of 69% and a skill score of 0.33.

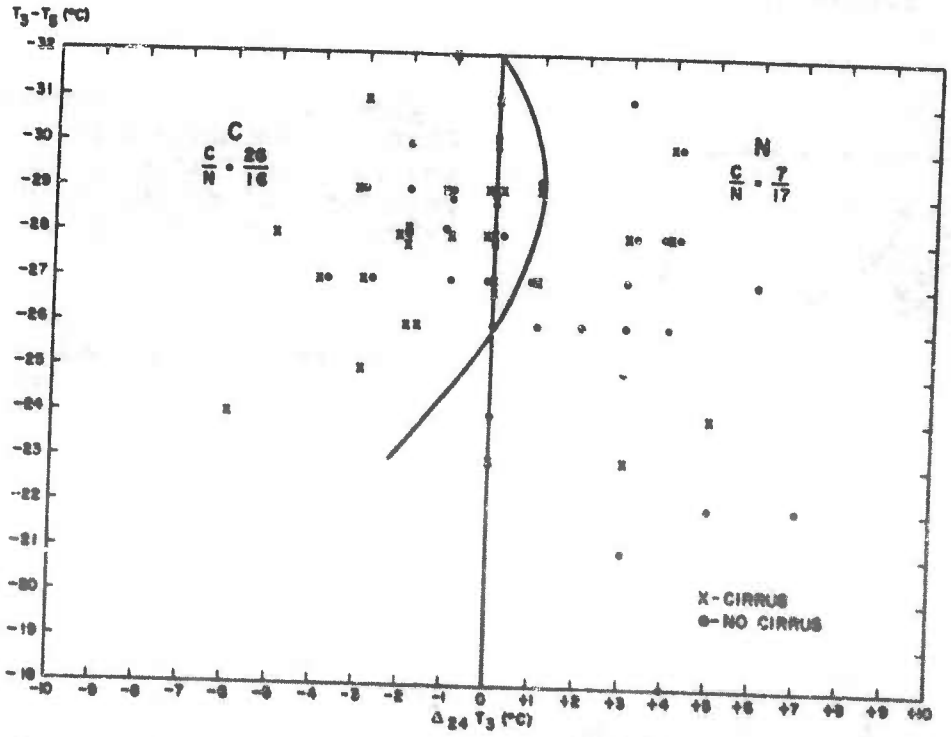

Figure 54. The Occurrence of Cirrostratus as a Function of the Mean Lapse Rate Between 300 and 500 mb and the 24-Hour Change in the Temperature at 300 mb, Fairbanks, Summer 1951.

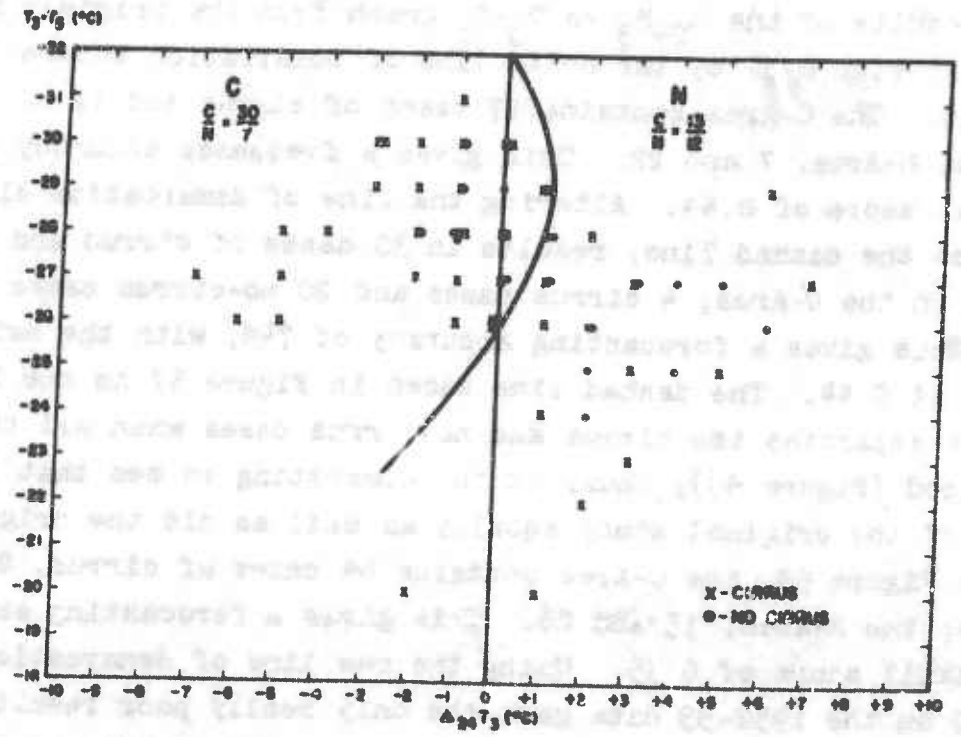

Figure 55. The Occurrence of Cirrostratus as a Function of the Mean Lapse Rate Between 300 and 500 mb and the 24-Hour Change in the 300-mb Temperature, Fairbanks, Summer 1952, 1953.

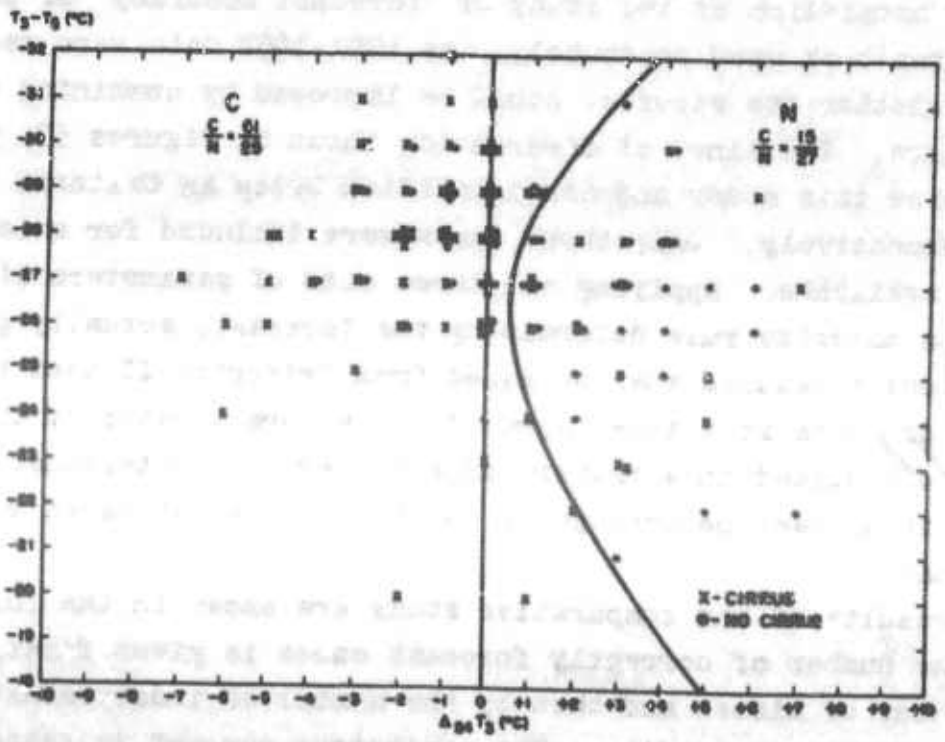

Figure 56. The Occurrence of Cirrostratus as a Function of the Mean Lapse Rate Between 300 and 500 mb and the 24-Hour Change in the 300-mb Temperature, Fairbanks, Summer 1951, 1952, 1953.

The results of the $\Delta_{24}H_3$ vs T_3-T_5 graph from the original study are shown in Figure 57 by the solid line of demarcation between the C- and N-Areas. The C-Area contains 27 cases of cirrus and 12 of no-cirrus; the N-Area, 7 and 22. This gives a frequency accuracy of 72% and a skill score of 0.44. Altering the line of demarcation slightly, as shown by the dashed line, results in 30 cases of cirrus and 14 of no-cirrus in the C'-Area; 4 cirrus cases and 20 no-cirrus cases in the N'-Area. This gives a forecasting accuracy of 74%, with the skill score remaining at 0.44. The dashed line shown in Figure 57 is the line which best separates the cirrus and no-cirrus cases when all the data are combined (Figure 59); thus, it is interesting to see that it fits the data of the original study equally as well as did the original line. In Figure 59, the C-Area contains 64 cases of cirrus, 26 of no cirrus; the N-Area, 13 and 26. This gives a forecasting accuracy of 70% and skill score of 0.35. Using the new line of demarcation from Figure 59 on the 1952-53 data gave the only really poor results of the entire test (Figure 58). Here the C-Area contains 34 cases of cirrus, 12 of no cirrus; the N-Area, 9 and 6. This gives a forecasting accuracy of 66% and a skill score of 0.13.

After completion of the study of "forecast accuracy" of the three sets of parameters used separately, the 1951-1952 data were used to determine whether the accuracy could be improved by combining the sets of parameters. The lines of demarcation shown in Figures 53, 56, and 59 were used for this study and are identified below as Criteria I, II, and III respectively. Only those cases were included for which all data were available. Applying all three sets of parameters simultaneously, with majority rule determining the forecast, actually gave slightly poorer results than obtained from Criterion II used by itself. Using two criteria at a time improved the accuracy ratio of the C-Area. However, it resulted in a rather large number of indeterminate cases, and hence in a lower percentage of correctly forecast cases when based on the total.

The results of the comparative study are shown in the following Table. The number of correctly forecast cases is given first, followed by the number of misses and then by the number of indeterminate cases for the two-criteria studies. The percentage correct is based on the total number of cases (60) followed in parentheses by the percentage correct after eliminating the indeterminate cases.

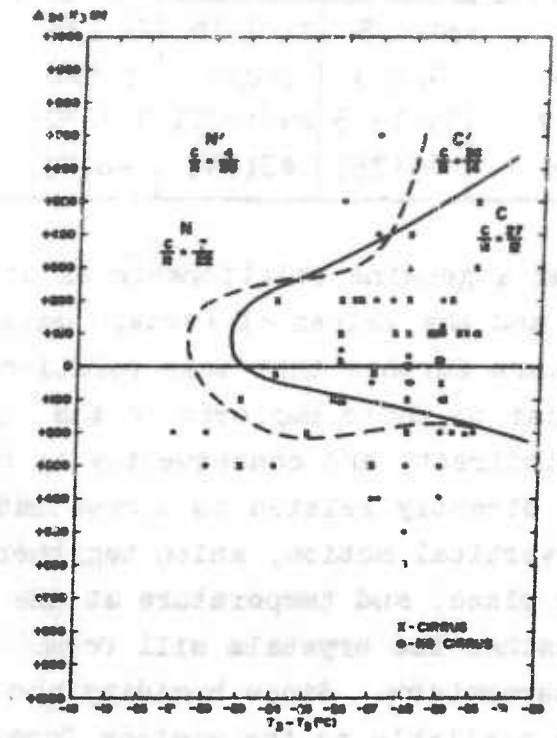

Figure 57.

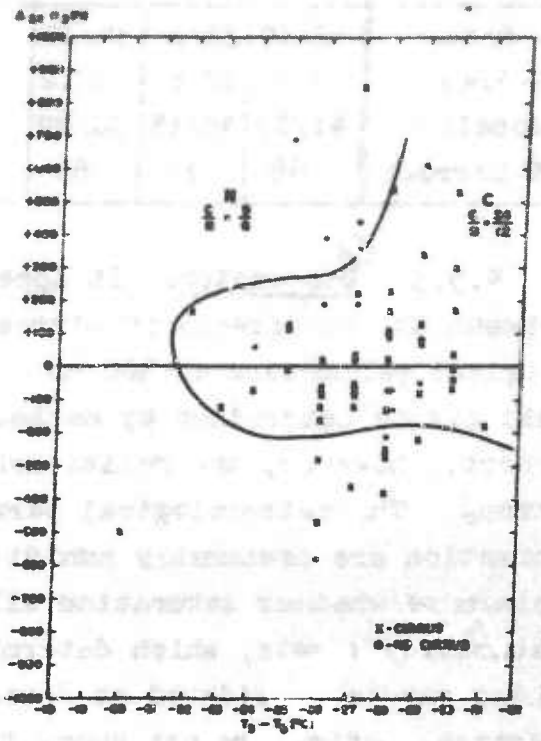

Figure 58.

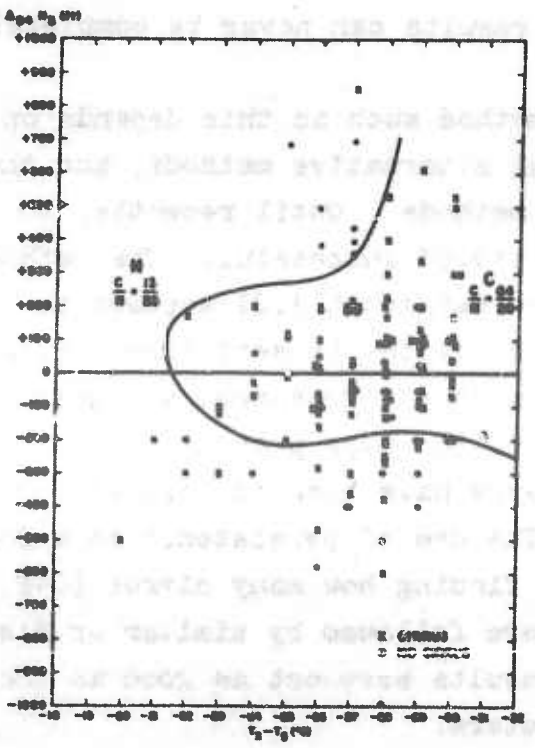

Figure 59.

Figure 57. The Occurrence of Cirrostratus as a Function of the Mean Lapse Rate Between 300 and 500 mb and the 24-Hour Change in the 300-mb Height, Fairbanks, Summer 1951.

Figure 58. The Occurrence of Cirrostratus as a Function of the Mean Lapse Rate Between 300 and 500 mb and the 24-Hour Change in the 300-mb Height, Fairbanks, Summer 1952, 1953.

Figure 59. The Occurrence of Cirrostratus as a Function of the Mean Lapse Rate Between 300 and 500 mb and the 24-Hour Change in the 300-mb Height, Fairbanks, Summer 1951, 1952, 1953.

Criterion	I	II	III	I & II & III	I & II	I & III	II & III
C-Area	32/10	33/9	32/10	34/8	30/7/5	24/2/16	24/1/17
N-Area	9/9	12/6	6/12	9/9	9/5/3	5/8/5	5/5/8
Totals	41/19	45/15	38/22	43/17	39/13/8	29/10/21	29/6/25
% Correct	68	75	63	72	65(75)	48(74)	48(83)

4.5.3. Discussion. It appears that a genuine relationship exists between the occurrence of cirrostratus and the values of certain meteorological parameters at 300 mb. It appears further that this relationship can be determined by methods similar to those employed in the first report. However, the relationship is indirect, and consequently is not strong. The meteorological parameters directly related to cirrostratus formation are presumably humidity and vertical motion, which together determine whether saturation will take place, and temperature at the saturation levels, which determines whether ice crystals will form. These may be considered as "primary" parameters. Since humidity and vertical motion are not among the data available to the weather forecaster, it is necessary to resort to "secondary" parameters which might be associated with the primary parameters. Such was done in these studies. Unfortunately, the secondary and primary parameters do not have a one-to-one relationship, so the results can never be completely satisfactory.

The value to the forecaster of a method such as this depends on its accuracy, the existence of practical alternative methods, and the comparative ease-of-use of the various methods. Until recently, no method of forecasting cirrostratus had proved successful. The method developed by French and Johannessen (see paragraph 4.2) appears to offer the greatest opportunity of success at the present time. Such a method, however, is perhaps not easy for some forecasters and detachments to use, whereas an objective aid of the type presented here can be applied by anyone, once the basic graphs have been constructed.

4.5.4. Persistence Forecasting. The use of persistence as a forecasting tool was tested by Appleman by finding how many cirrus (C+P) and non-cirrus (N) days at Fairbanks were followed by similar or dissimilar days (see Table below). The results were not as good as those obtained by using meteorological parameters.

Today	Tomorrow							
	Summer		Fall		Winter		Spring	
	C+P	N	C+P	N	C+P	N	C+P	N
C+P	27	11	6	8	3	7	14	12
N	11	18	11	13	7	23	13	33

4.6. Suggestions for Further Study. It seems obvious from present knowledge that the fully satisfactory solution of the cirrus forecasting problem awaits the provision of routine humidity soundings to at least the tropopause, and perhaps vertical displacement charts in addition. The following topics should be given particular attention, either because they seem to be promising or because they have not yet been given any adequate trial:

1. How does cirrus show up in the radiosoundings?
2. Upper-level humidity indications from radiosondes and from lower-level parameters (paragraph 4.1.15).
3. Use of nephanalysis, especially of aircraft and radar observations, combined with other techniques.
4. Wind-profile form and cirrus — test of Gayikian's idea (paragraph 4.1.12).
5. Trajectories and cirrus occurrence.
6. Development of cirrus states of sky (see paragraph 2.1.4) and models for their successions in various synoptic conditions (see paragraph 3.5).

It is of great importance to all approaches that better and more extensive cirrus observations be obtained; without them data for study will be inadequate and likewise data for verification or test of hypotheses. The wider use of aircraft and radar [50] observations (preferably by photography) for this purpose should be pressed (see paragraph 3.3.2 and 3.3.3).

5.0. Summary and Conclusions.

Cirrus (or "cirriform") clouds are conventionally divided into three genera: cirrus (proper), cirrostratus, and cirrocumulus. The latter is a relatively rare cloud and may be ignored for practical purposes. Cirrus proper (detached fine or patchy cirrus) does not usually create a serious operational problem. Cirrostratus and extensive cirrus

haze, however, are troublesome in high-level jet operations, for aerial photography, interception, rocket tracking, and guided-missile navigation systems, etc. Therefore, some requirement for cirrus forecasting exists. No universally applicable nor highly successful forecasting methods have been found, though several methods have been advanced which seem to have some success, or promise of success, under certain conditions.

The WMO classification of cirrus forms used in present observational procedures makes distinctions based purely on the visual aspects of the clouds as seen from the ground. These forms unfortunately do not have a clear-cut relation to the physical constitution of the clouds nor to synoptic conditions associated with their formation. All types of cirrus (except perhaps some cirrocumulus) consist of small ice crystals of relatively elemental forms. But some middle-level clouds, such as altostratus, also often contain predominantly ice (or snow) particles. A few water drops can persist in cirrus, and some cases of light rime icing in cirrus are thus explained; even heavier ice may occur in anvils close to the top of the parent Cb.

The initial formation of cirrus normally requires that cooling take place to saturation with respect to water and to temperatures near -40°C. Under these conditions water droplets are first formed but most of them immediately freeze. The resulting crystals persist as long as the environmental humidity remains near ice-saturation; a deep ice-saturated layer usually exists just below the cirrus-formation level, which permits long cirrus streamers to descend (slowly) to lower levels and to persist for many hours (or even perhaps days) before evaporating. There is some evidence that the speed of the cooling and the kind and abundance of "freezing nuclei" may have an important effect on the form and occurrence of cirrus. Slow ascent (cooling) starts crystalization on specially favorable freezing nuclei at humidities substantially below saturation with respect to water; this is presumably the case in extensive cirrostratus associated with warm-front altostratus. If slow ascent occurs in air having insufficient freezing nuclei, a widespread haze may result which even at -30° to -40°C is predominantly of water drops. In the case of more rapid cooling (ascent) there is a tendency for the first condensation to contain a higher proportion of water drops, leading to a "mixed cloud" (ice and water) which will convert to ice or snow in time. Presumably, dense cirrus, fine cirrus, cirrocumulus, and

anvil cirrus are of this rapid-ascent type; it has been suggested, for example, that fine cirrus (proper) is formed in shallow layers undergoing rapid convection due to advection of colder air at top of a shear layer. On the other hand, the fine cirrus and the cirrostratus are so often associated, and cirrostratus is so often reported by pilots as developing from the merging of fine cirrus streamers, that there is question whether the process of formation in cirrus and cirrostratus is essentially different. Nevertheless, the prevailing crystal types in cirrus and cirrostratus seem to differ, though this may not be universal or may merely represent different ages in a characteristic cirrus-evolution. The old hypothesis that all cirrus is formed of "fallstreaks" is possibly worthy of re-examination in light of the above considerations.

Horizontal visibilities within extensive cirrostratus over middle latitudes are generally between 500 feet and two miles. But even thin cirrus haze, invisible from the ground, often reduces the visibility to three miles. Burton's empirical rule for forecasting the visibility has been successful for the Arctic cirrus and may work elsewhere.

The climatology of cirrus occurrence is unsatisfactory because the usual ground observations (in humid climates) miss more than 50% of the true frequency or amount, and aircraft observations are very scarce.

The aircraft observations available provide some data on the heights of cirrus, data which are valuable to forecasters as an aid in forecasting cirrus heights and for climatological estimates in operations planning. In mid-latitudes, the top of most extensive and thick cirrus layers is at or within several thousand feet of the polar-tropopause height; only some patchy cirrus is found between the equivalent polar-tropopause height and the tropical (high) tropopause. A small percentage of cirrus cases (including even sometimes extensive cirrostratus) is observed in the lower stratosphere above the polar tropopause, up to 50,000 feet, but mainly below the level of the jet-stream core. The cirrus of the equatorial zone also generally extends to the tropopause. There is a general tendency for the mean height of the bases to increase from high to low latitudes more or less parallel to the mean tropopause height, ranging from 7.5 km at 70°-80° Latitude to 11 or 12 km around the equator. The thickness of individual cirrus layers (the clouds are often multi-layered) is most frequently about 250 m in mid-latitudes; some cases, however, range up to 3000 m or more,

the average for cirrus-affected zones (solid, or multi-layers taken together) being about 2000 m. The mean thickness of the cirrus-affected zone tends to increase from high to low latitudes. In polar continental regions in winter, cirrus virtually comes down to the ground. In mid-latitudes and tropics there is little seasonal variation in mean-cirrus heights.

Radar cloud-detection sets appear to promise much more complete cirrus observations than possible from visual observers.

A cirrus-forecasting method, whether empirical or with a physical hypothesis, should exploit what is already known about cirrus in relation to other forecastable parameters. A considerable number of such parameters have been tried in the course of past studies, in addition to pure extrapolation of the movement of cirrus-cloud ("neph") systems. Except for the use of the surface-pressure pattern, these are all upper-air parameters. Most of them were tried or chosen on the generally accepted hypothesis that cirrus, like other clouds, form where there is sufficient large-scale vertical motion and the initial humidity is relatively high. Since routine direct observations or evaluations of these two parameters at high levels are not feasible at present, the objective has been to find accessible parameters which provide satisfactory indirect indications of vertical motion and/or humidity at high levels. For vertical motion, the vorticity advection at 300 mb appears to be the most promising and objective indicator, at least until such time as suitable vertical-motion or vertical-displacement charts can be provided by NWP methods. The use of qualitative estimates of the vorticity advection on the 300-mb chart is recommended as the best and easiest aid in cirrus forecasting. However, without also considering the humidity, an accurate estimate of the vertical-motion field by itself is likely to forecast the "no-cirrus" area much more accurately than the cirrus area. Changes in humidity are reasonably well indicated by present United States, Canadian, British, French, Swiss, and West German radiosondes down to -60°C, or even colder, but at the lower temperatures the indicated values are not usually transmitted (in the United States and Canada, at least). Results of several studies suggest transmission of these humidities might serve as a valuable adjunct to the vertical-motion field in cirrus forecasting; this is being investigated. Wind-direction aloft and the humidity measured at levels well below the cirrus have been proposed as indirect indicators of 300-mb

humidity, but they have not been thoroughly tried. Most of the various parameters chosen in the more empirical procedures which have been used or proposed for cirrus forecasting can be given a rational interpretation as having indirect relations to humidity or vertical motion. For example, the models of frontal, pressure, contour, and wind patterns associated with cirrus are in this category. Such methods are very subjective and depend on considerable experience for success. But other hypotheses, such as a relation of the temperature, or the lapse-rate, or the wind shear, to cirrus occurrence or height, do not seem to find much convincing statistical support nor a clearly defensible physical basis. Statistical techniques for local cirrus forecasting tried thus far have not been too encouraging, but with better data and more experience with other techniques further trials of this sort should be worthwhile.

Several approaches to practical cirrus forecasting are recommended for further investigation, clarification, and testing:

a. How does cirrus show up in the temperature soundings (temperature and lapse rate)?

b. Use of upper-level humidity indications from radiosondes.

c. Use of nephanalysis of aircraft and radar observations.

d. Relation of vertical-wind profile to cirrus.

e. Trajectories and cirrus occurrence.

f. Development of cirrus states-of-sky on an operational-criteria basis.

g. Development of models of the succession of cirrus skies for various synoptic conditions (especially for the tropics and sparse-data regions).

Accelerated basic research on cirrus physics in relation to cirrus forms and synoptic conditions will be essential if very accurate and detailed cirrus forecasts should become necessary. For less critical and more generalized cirrus forecasting, adequate results should be obtainable, once routine cirrus observations by radar and aircraft and regular humidity soundings to the tropopause become available.

APPENDIX A

STUDY OF CIRRUS CLIMATOLOGY FROM DATA TAKEN ON PROJECT CLOUD TRAIL

A1.0. Description of Project.

Project CLOUD TRAIL was established within the Air Defense Command in conjunction with Air Weather Service to collect high-level weather information from jet aircraft. The aircraft were to accumulate sufficient data to serve as a basis for improved methods of forecasting contrails, cirrus clouds, haze, and turbulence at the heights of jet-aircraft operation. To obtain these data, the observational phase of the Project ran from 1 December 1954 to 15 December 1955. During this period 36 fighter-interceptor squadrons based in the United States collected data over 23 upper-air sounding stations. The procedure employed was as follows:

a. Each day from approximately one hour before to two hours after 1530Z, two aircraft were vectored to a point 25,000 feet above an upper-air sounding station. The aircraft then climbed to the maximum altitude obtainable, maintaining position within 30 miles of the station.

b. The wingman observed whether or not the lead aircraft produced exhaust trails and whether they were continuous or intermittent, pronounced or faint, including bases and tops of layers in which the trails formed.

c. The aircraft attempted to penetrate all cirrus and haze layers, avoiding holes in the cloud layers. The leadman estimated the coverage of each such layer in tenths as well as the measured heights of cirrus and haze bases and tops actually penetrated. During the climb he also reported whether or not turbulence was encountered and its intensity, giving the bases and tops of each layer.

A2.0. Cloud Observations.

One set of observations made by Project CLOUD TRAIL aircraft dealt with the bases and tops of high-cloud layers as measured by actual penetrations. Since the aircraft ascents were made over radiosonde stations, accurate temperature measurements were available for all reported heights. Only clouds at 25,000 feet and above were tabulated; most of these were cirrus but some altostratus was undoubtedly included.

A statistical summary of this cloud data, as obtained from the aircraft and radiosonde measurements and prepared under supervision of H. Appleman and Lt. Col. C. A. Spohn, is shown in the Tables below. The data were tabulated separately by season, latitude, and cloud coverage. Latitude effect was studied by dividing the stations into a northern (N) and southern (S) group, then combining them (US). (The southern stations were, with exception of Norfolk and Washington, all in the Southwest.) The dividing line used was 39°N. Coverage also was broken down into two groups: scattered (1/10 - 5/10), and broken, including overcast, (6/10 - 10/10).

A2.1. The Tables A1 - A4 give the summaries by season, and Table A5 for the year. The rows inclosed in boxes are the ranges where the majority or all of the cases were at temperatures warmer than -30°C, and thus probably include many altostratus clouds. This happened chiefly in the spring, summer, and autumn. The basis for this opinion will be found in a comparison of these Tables with Table A6, which gives the distribution of temperatures observed on all flight days of Project CLOUD TRAIL. (The standard and mean deviations of the heights with reference to the mean heights in these Tables are discussed in AWS TR 105-110A.)

The seasons were defined as follows:

Winter: December-February
Spring: March-May
Summer: June-August
Autumn: September-November

With regard to the data on thickness, there were a few cases in each season in which the observers reported the cloud present in two layers.

Table A7 gives the mean values for the data in Tables A1-5.

A2.2. In as much as the data in the preceding Tables (A1-7) include a certain proportion of cases of middle clouds, the conclusions that might be drawn from the tabulations cannot be regarded as applying strictly to cirrus clouds, except perhaps in the winter season. A separate tabulation (Tables A8-9) was therefore made of those cases when the temperature of the cloud base was -40°C or lower, the range in which the clouds are indubitably cirrus. This tabulation may be of some interest to cloud physicists but cannot be of much climatological or operational value because there are so many cirrus cases excluded –

433730 O - 57 - 10

i.e., those that occur in the range -30° to -40°C.

A2.3. For many practical purposes it is desired to know what is the probability of encountering cloud at various fixed altitudes, regions, seasons, etc. Tables A10-12 provide such information for northeast, northwest, and southwest United States, tabulated from the Project Cloud-Trail data by 1000-ft height intervals. The columns headed F give the number of flights reaching the respective heights, columns headed C give the number of cases of cloud (probably all cirrus above 28,0C feet) encountered on the flights at each height, and columns headed % give the corresponding percentage frequencies of clouds (C/F). Tabulations by individual months were originally prepared, but the small number of cases made it desirable to group by seasons.

TABLE A1

Distribution of Observed Values of Cloud Height, Thickness, and Temperature.

WINTER

	Number of Cases and Cumulative Percentages: (1/10 - 5/10 Coverage)						Number of Cases and Cumulative Percentages: (6/10 - 10/10 Coverage)					
	N		S		US		N		S		US	
Height (1000's ft)	No.	%	No.	%	No.	%	No.	%	No.	%	No.	%
25-28	18	(29)	7	(25)	25	(27)	28	(53)	9	(35)	37	(47)
29-32	25	(68)	9	(53)	34	(63)	20	(91)	12	(81)	32	(87)
33-36	13	(89)	7	(77)	20	(85)	2	(94)	5	(100)	7	(96)
37-40	6	(98)	5	(93)	11	(97)	3	(100)	--		3	(100)
> 40	1	(100)	2	(100)	3	(100)	--		--		--	
Thickness (100's ft)												
< 5	13	(22)	5	(19)	18	(21)	7	(14)	0	(0)	7	(10)
6-15	20	(56)	9	(52)	29	(55)	12	(38)	2	(9)	14	(29)
16-25	13	(78)	6	(74)	19	(77)	6	(50)	6	(36)	12	(46)
26-35	5	(86)	5	(93)	10	(88)	8	(66)	4	(55)	12	(63)
36-45	4	(93)	0	(93)	4	(93)	3	(72)	3	(68)	6	(71)
46-55	1	(95)	1	(96)	2	(95)	6	(84)	2	(77)	8	(82)
56-65	2	(98)	0	(96)	2	(98)	0	(84)	1	(82)	1	(83)
66-75	0	(98)	0	(96)	0	(98)	4	(92)	3	(95)	7	(93)
> 75	1	(100)	1	(100)	2	(100)	4	(100)	1	(100)	5	(100)
Temperature (°C)												
-31/35	2	(4)	1	(4)	3	(4)	2	(4)	1	(5)	3	(5)
-36/40	2	(7)	4	(20)	6	(11)	8	(22)	3	(19)	11	(21)
-41/45	14	(33)	2	(28)	16	(32)	10	(44)	8	(57)	18	(48)
-46/50	10	(52)	7	(56)	17	(53)	12	(71)	5	(81)	17	(74)
-51/55	15	(80)	3	(68)	18	(76)	7	(87)	3	(95)	10	(89)
-56/60	7	(93)	4	(84)	11	(90)	4	(96)	1	(100)	5	(97)
-61/65	3	(98)	3	(96)	6	(97)	1	(98)	--		1	(99)
< -66	1	(100)	1	(100)	2	(100)	1	(100)	--		1	(100)

TABLE A2

Distribution of Observed Values of Cloud Height, Thickness, and Temperature.

SPRING

	Number of Cases and Cumulative Percentages: (1/10 - 5/10 Coverage)						Number of Cases and Cumulative Percentages: (6/10 - 10/10 Coverage)					
	N		S		US		N		S		US	
Height (1000's ft)	No.	%	No.	%	No.	%	No.	%	No.	%	No.	%
25-28	32	(33)	7	(22)	39	(30)	25	(40)	10	(45)	35	(42)
29-32	38	(72)	15	(69)	53	(71)	16	(66)	6	(73)	22	(68)
33-36	20	(93)	7	(91)	27	(92)	16	(92)	4	(91)	20	(92)
37-40	2	(95)	2	(97)	4	(96)	5	(100)	2	(100)	7	(100)
> 40	5	(100)	1	(100)	6	(100)	--		--		--	
Thickness (100's ft)												
≤ 5	13	(14)	6	(19)	19	(15)	2	(3)	0	(0)	2	(2)
6-15	26	(42)	7	(41)	33	(41)	7	(15)	3	(14)	10	(15)
16-25	14	(56)	6	(59)	20	(57)	10	(32)	4	(33)	14	(32)
26-35	14	(71)	4	(72)	18	(71)	11	(50)	3	(48)	14	(49)
36-45	3	(75)	1	(75)	4	(75)	5	(58)	2	(57)	7	(58)
46-55	10	(85)	4	(88)	14	(86)	5	(67)	3	(71)	8	(68)
56-65	4	(89)	0	(88)	4	(89)	6	(77)	1	(76)	7	(77)
66-75	1	(90)	0	(88)	1	(90)	3	(82)	0	(76)	3	(80)
> 75	9	(100)	4	(100)	13	(100)	11	(100)	5	(100)	16	(100)
Temperature (°C)												
-35	5	(6)	2	(8)	7	(6)	11	(20)	4	(19)	15	(19)
-36/40	16	(25)	3	(21)	19	(23)	7	(32)	7	(52)	14	(38)
-41/45	14	(40)	6	(46)	20	(41)	10	(50)	3	(67)	13	(55)
-46/50	25	(69)	6	(71)	31	(69)	12	(71)	3	(81)	15	(74)
-51/55	14	(85)	4	(88)	18	(86)	9	(88)	2	(91)	11	(88)
-56/60	11	(98)	1	(92)	12	(96)	6	(98)	1	(95)	7	(97)
-61/65	2	(100)	2	(100)	4	(100)	1	(100)	1	(100)	2	(100)
≤ -66	--		--		--		--		--		--	

TABLE A3

Distribution of Observed Values of Cloud Height, Thickness, and Temperature.

SUMMER

	Number of Cases and Cumulative Percentages: (1/10 - 5/10 Coverage)						Number of Cases and Cumulative Percentages: (6/10 - 10/10 Coverage)					
	N		S		US		N		S		US	
Height (1000's ft)	No.	%	No.	%	No.	%	No.	%	No.	%	No.	%
25-28	25	(20)	9	(39)	34	(23)	13	(36)	0		13	(32)
29-32	38	(50)	10	(82)	48	(55)	10	(64)	3		13	(65)
33-36	28	(72)	3	(95)	31	(75)	5	(78)	0		5	(78)
37-40	25	(91)	1	(100)	26	(92)	6	(94)	0		6	(92)
> 40	11	(100)	--		11	(100)	2	(100)	1		3	(100)
Thickness (100's ft)												
≤ 5	16	(13)	4	(18)	20	(14)	0	(0)	0		0	(0)
6-15	38	(43)	5	(41)	43	(43)	2	(6)	1		3	(8)
16-25	31	(68)	3	(54)	34	(66)	4	(17)	0		4	(18)
26-35	11	(76)	3	(68)	14	(75)	7	(37)	0		7	(36)
36-45	12	(85)	3	(82)	15	(85)	1	(40)	0		1	(38)
46-55	4	(89)	1	(86)	5	(88)	3	(48)	1		4	(49)
56-65	6	(93)	0	(86)	6	(92)	5	(63)	0		5	(61)
66-75	1	(94)	1	(91)	2	(94)	1	(66)	0		1	(64)
> 75	7	(100)	2	(100)	9	(100)	12	(100)	2		14	(100)
Temperature (°C)												
≥ -30	13	(10)	5	(22)	18	(12)	7	(20)	0		7	(18)
-31/35	16	(23)	8	(56)	24	(28)	8	(43)	1		9	(41)
-36/40	19	(38)	3	(69)	22	(43)	9	(68)	2		11	(66)
-41/45	17	(51)	4	(87)	21	(57)	1	(71)	0		1	(72)
-46/50	20	(67)	1	(91)	21	(70)	3	(80)	0		3	(79)
-51/55	17	(80)	1	(95)	18	(82)	1	(83)	0		1	(82)
-56/60	14	(91)	1	(100)	15	(92)	4	(94)	0		4	(92)
≤ -61	11	(100)	--		11	(100)	2	(100)	1		3	(100)

TABLE A4

Distribution of Observed Values of Cloud Height, Thickness, and Temperature.

AUTUMN

	Number of Cases and Cumulative Percentages: (1/10 - 5/10 Coverage)						Number of Cases and Cumulative Percentages: (6/10 - 10/10 Coverage)					
	N		S		US		N		S		US	
Height (1000's ft)	No.	%	No.	%	No.	%	No.	%	No.	%	No.	%
25-28	20	(55)	4	(31)	24	(30)	17	(47)	4	(40)	21	(46)
29-32	30	(76)	7	(85)	37	(77)	10	(75)	5	(90)	15	(78)
33-36	12	(94)	1	(92)	13	(94)	7	(94)	1	(100)	8	(96)
37-40	3	(98)	0	(92)	3	(97)	2	(100)	--		2	(100)
> 40	1	(100)	1	(100)	2	(100)	--		--		--	
No. of Cases	66		13		79		36		10		46	

Thickness (100's ft)

< 5	7	(11)	3	(23)	10	(13)	5	(14)	0	(0)	5	(11)
6-15	18	(38)	2	(38)	20	(38)	4	(25)	2	(20)	6	(24)
16-25	17	(64)	1	(46)	18	(61)	4	(36)	1	(30)	5	(35)
26-35	3	(68)	0	(46)	3	(65)	4	(47)	1	(40)	5	(46)
36-45	7	(79)	0	(46)	7	(74)	5	(61)	1	(50)	6	(59)
46-55	5	(86)	3	(69)	8	(84)	5	(75)	4	(90)	9	(78)
56-65	3	(91)	1	(77)	4	(90)	2	(81)	0	(90)	2	(83)
66-75	2	(94)	0	(77)	2	(91)	1	(83)	0	(90)	1	(85)
> 75	4	(100)	3	(100)	7	(100)	6	(100)	1	(100)	7	(100)
No. of Cases	66		13		79		36		10		46	

Temperature (°C)

> -30	2	(3)	0	(0)	2	(3)	2	(6)	1	(10)	3	(7)
-31/35	11	(17)	3	(23)	14	(20)	5	(19)	2	(30)	7	(22)
-36/40	14	(41)	6	(69)	20	(46)	11	(50)	5	(80)	16	(57)
-41/45	14	(62)	1	(77)	15	(63)	7	(69)	1	(90)	8	(74)
-46/50	15	(85)	1	(85)	16	(85)	5	(83)	1	(100)	6	(87)
-51/55	6	(94)	1	(92)	7	(94)	5	(97)	--		5	(98)
-56/60	3	(98)	0	(92)	3	(97)	0	(97)	--		0	(98)
< -60	1	(100)	1	(100)	2	(100)	1	(100)	--		1	(100)
No. of Cases	66		13		79		36		10		46	

TABLE A5

Distribution of Observed Values of Cloud-Base Height, Thickness, and Base Temperature.

YEAR

	Number of Cases and Cumulative Percentages: (1/10 - 5/10 Coverage)						Number of Cases and Cumulative Percentages: (6/10 - 10/10 Coverage)					
	N		S		US		N		S		US	
Height (1000's ft)	No.	%	No.	%	No.	%	No.	%	No.	%	No.	%
25-28	95	(27)	27	(28)	122	(27)	83	(44)	23	(37)	106	(42)
29-32	131	(64)	41	(70)	172	(65)	56	(74)	26	(79)	82	(75)
33-36	73	(85)	18	(88)	91	(85)	30	(90)	10	(95)	40	(91)
37-40	36	(95)	8	(96)	44	(95)	16	(99)	2	(98)	18	(98)
> 40	18	(100)	4	(100)	22	(100)	2	(100)	1	(100)	3	(100)
No. of Cases	353		98		454		187		62		249	
Thickness (100's ft)												
≤ 5	49	(14)	18	(19)	67	(15)	14	(8)	0	(0)	14	(6)
6-15	102	(44)	23	(44)	125	(43)	25	(23)	8	(14)	33	(20)
16-25	75	(65)	16	(61)	91	(64)	24	(36)	11	(33)	35	(35)
26-35	33	(75)	12	(73)	45	(74)	30	(53)	8	(47)	38	(51)
36-45	26	(83)	4	(78)	30	(81)	14	(61)	6	(57)	20	(59)
46-55	20	(88)	9	(88)	29	(88)	19	(71)	10	(75)	29	(71)
56-65	15	(92)	1	(88)	16	(92)	13	(78)	2	(79)	15	(77)
66-75	4	(94)	1	(89)	5	(93)	9	(82)	3	(84)	12	(82)
> 75	21	(100)	10	(100)	31	(100)	33	(100)	9	(100)	42	(100)
No. of Cases	345		94		439		181		57		238	
Temperature (°C)												
≥ -30	15	(4)	5	(6)	20	(5)	9	(5)	1	(2)	10	(4)
-31/35	34	(15)	14	(22)	48	(16)	26	(20)	8	(16)	34	(19)
-36/40	51	(30)	15	(41)	67	(32)	35	(41)	17	(46)	52	(42)
-41/45	59	(48)	13	(56)	72	(49)	28	(57)	12	(68)	40	(61)
-46/50	70	(69)	15	(74)	85	(70)	32	(76)	9	(84)	41	(79)
-51/55	52	(84)	9	(84)	61	(84)	22	(88)	5	(93)	27	(90)
-56/60	35	(95)	6	(91)	41	(94)	14	(96)	2	(96)	16	(97)
≤ -61	18	(100)	7	(100)	25	(100)	6	(100)	2	(100)	8	(100)
No. of Cases	334		85		419		172		56		228	

TABLE A6

Relative Frequency (%) of Temperatures for Selected-Altitude Intervals from All Project-Cloud-Trail Ascents.

WINTER

Height (100's ft)	Temperature in °C									
	< -60°	-55° to -60°	-50° to -55°	-45° to -50°	-40° to -45°	-35° to -40°	-30° to -35°	> -30°	Mean Temp.	No. Cases
405 to 465	16.7	34.0	31.2	16.8	1.3				54.9	629
365 to 405	25.6	26.3	23.6	20.1	4.1	0.3			55.5	653
325 to 365	3.5	36.0	39.5	16.4	3.6	0.9			53.3	658
285 to 325		3.8	30.5	46.2	17.0	2.0	0.5		48.3	653
245 to 285		0.2	3.1	13.1	35.7	38.8	9.3	0.8	40.4	605

SPRING

405 to 465	26.6	41.2	24.3	7.8	0.2				56.9	580
365 to 405	29.4	39.1	19.9	10.0	1.5				56.7	649
325 to 365	1.2	32.7	49.5	14.9	1.8				53.4	673
285 to 325		1.3	14.6	48.5	30.5	5.0			46.3	678
245 to 285			0.3	7.7	19.4	46.9	23.5	2.1	37.9	659

SUMMER

405 to 465	45.4	35.6	14.3	4.5	0.2				58.6	595
365 to 405	1.8	33.8	54.8	8.5	1.1				53.8	615
325 to 365		0.8	21.6	43.4	34.1				46.9	624
285 to 325			0.2	7.7	25.4	39.5	27.2		33.2	622
245 to 285					0.3	9.1	30.7	59.9	30.0	593

FALL

405 to 465	41.5	40.8	15.2	2.5					58.6	564
365 to 405	9.3	39.7	41.5	9.2	0.3				54.9	590
325 to 365		6.8	42.4	39.9	10.8	0.2			49.8	592
285 to 325		0.2	2.5	20.1	46.6	25.8	4.7		42.0	596
245 to 285			0.3	1.2	6.8	24.7	45.1	21.8	33.5	586

Mean Temperature of All Flights and Levels Was: -48.5°

TABLE A7

Seasonal Mean Values of Cloud Base Height, Thickness, and Base Temperature.

WINTER

	1/10 - 5/10 Coverage			6/10 - 10/10 Coverage		
	N - US 39°N	S - US 39°N	US	N - US 39°N	S - US 39°N	US
Height (ft)	31,080	32,810	31,640	28,920	30,470	29,430
Thickness (ft)	1,850	1,930	1,170	3,120	3,960	3,380
Temperature (°C)	-49	-50	-50	-47	-45	-46

SPRING

Height (ft)	30,630	31,380	30,820	30,300	29,640	30,120
Thickness (ft)	3,000	3,390	3,100	4,470	4,750	4,550
Temperature (°C)	-47	-46	-47	-45	-43	-44

SUMMER

Height (ft)	33,190	29,650	32,650	31,290	33,000	31,460
Thickness (ft)	2,600	2,830	2,640	5,970	6,120	5,990
Temperature (°C)	-45	-35	-43	-40	-43	-41

AUTUMN

Height (ft)	30,410	31,020	30,510	30,160	28,750	29,850
Thickness (ft)	2,790	4,090	3,000	4,120	3,920	4,080
Temperature (°C)	-42.8	-41.5	-42.6	-42.0	-37.7	-41.1
No. of Cases*	66	13	79	36	10	46

YEAR

Height (ft)	31,590	31,330	31,540	30,070	30,060	30,070
Thickness (ft)	2,620	3,030	2,710	4,320	4,400	4,340
Temperature (°C)	-45.7	-43.6	-45.3	-43.9	-42.6	-43.6
No. of Cases*	353	98	451	187	62	249

* Number of cases for which height values were available.

TABLE A8

Distribution of Observed Values for All Clouds Having Base Temperature -40°C or Colder, Project Cloud Trail.

Height (1000's ft)	Winter		Spring		Summer		Fall	
	N	S	N	S	N	S	N	S
	No. %	No. %	No. %	No. %	No. %	No. %	No. %	No. %
25-28	34 (36)	6 (12)	21 (17)	3 (9)	1 (1)	1 (13)	8 (14)	2 (20)
29-32	37 (75)	24 (60)	51 (60)	16 (59)	19 (21)	2 (38)	25 (57)	5 (70)
33-36	15 (91)	11 (82)	39 (92)	7 (81)	30 (53)	3 (75)	19 (90)	2 (90)
37-40	6 (97)	6 (94)	5 (97)	6(100)	31 (86)	1 (88)	5 (98)	0 (90)
> 40	3(100)	3(100)	4(100)	--	13(100)	1(100)	1(100)	1(100)
No. of Cases	95	50	120	32	94	8	58	10
Median	30,000	32,400	32,300	34,000	36,600	34,500	32,400	31,000

Thic'ness (100's ft)

≤ 5	14 (16)	4 (10)	11 (9)	3 (9)	11 (12)	1 (13)	10 (17)	0 (0)
6-15	26 (44)	7 (27)	28 (34)	6 (28)	31 (46)	1 (25)	16 (45)	2 (20)
16-25	20 (67)	13 (59)	19 (50)	2 (34)	24 (72)	1 (38)	14 (69)	1 (30)
26-35	10 (78)	6 (73)	21 (68)	9 (63)	8 (80)	2 (63)	3 (74)	1 (40)
36-45	6 (84)	4 (83)	6 (73)	4 (75)	7 (88)	2 (88)	6 (84)	0 (40)
46-55	5 (90)	3 (90)	12 (83)	4 (88)	4 (92)	0 (88)	5 (93)	2 (60)
56-65	2 (92)	3 (98)	5 (88)	1 (91)	2 (95)	0 (88)	1 (95)	0 (60)
66-75	3 (96)	1(100)	2 (89)	0 (91)	0 (95)	1(100)	1 (97)	0 (60)
> 75	4(100)	--	12(100)	3(100)	5(100)	--	2(100)	4(100)
No. of Cases	90	41	116	32	92	8	58	10
Median	1,700	2,100	2,500	3,100	1,600	3,000	1,700	4,500

Temperature (°C)

-40/45	29 (31)	13 (26)	33 (27)	11 (35)	21 (22)	4 (50)	23 (40)	6 (60)
-46/50	21 (53)	17 (60)	41 (62)	6 (55)	23 (47)	1 (63)	19 (72)	2 (80)
-51/55	26 (80)	7 (74)	24 (82)	8 (81)	19 (67)	1 (75)	11 (91)	1 (90)
-56/60	12 (93)	7 (88)	18 (97)	3 (90)	18 (86)	2(100)	3 (97)	0 (90)
-61/65	5 (98)	5 (98)	4(100)	3(100)	11 (98)	--	2(100)	1(100)
≤ -66	2(100)	1(100)	--	--	2(100)	--	--	--
No. of Cases	95	50	120	31	94	8	58	10
Median	-49.6	-48.7	-48.7	-49.2	-50.7	-45.0	-46.5	-44.0

TABLE A9

Mean Seasonal Values of Base Heights and Thicknesses of Cirrus Clouds with Base Temperatures -40°C or Colder, Project Cloud Trail.

WINTER

	North	South	U. S.*
Height (ft) Thickness (ft)	30,500 2,560	32,810 2,730	31,650 2,640
No. of Cases	95	50	

SPRING

Height (ft) Thickness (ft)	31,900 3,230	32,400 3,570	32,150 3,400
No. of Cases	120	32	

SUMMER

Height (ft) Thickness (ft)	36,000 2,340	33,900 3,120	34,950 2,730
No. of Cases	94	8**	

AUTUMN

Height (ft) Thickness (ft)	32,000 2,450	32,500 5,200	32,250 3,825
No. of Cases	58	10**	

* U. S. values are simple arithmetic averages of the mean values for the North and South.

** The values in these columns must be considered particularly doubtful because of the few cases involved.

TABLE A10

High-Cloud Frequency Over Northeastern United States.

(Stations: Rome, St.-Ste.-Marie, Washington, Mt. Clemens, Nantucket, Norfolk, Pittsburgh, Buffalo, Caribou, Dayton, Hempstead.)

Height	Winter			Spring			Summer			Fall			Year		
	F[1]	C[2]	%[3]	F	C	%	F	C	%	F	C	%	F	C	%
25,000	339	24	7.1	428	31	7.2	390	6	1.5	407	3	0.7	1564	64	4.1
26,000	332	33	10.0	427	41	9.6	386	16	4.1	405	8	1.9	1550	98	6.3
27,000	327	38	11.6	426	45	10.6	386	26	6.7	404	12	2.9	1543	121	7.8
28,000	326	38	11.7	423	47	11.1	384	31	8.1	402	24	5.9	1535	140	9.1
29,000	324	39	12.0	421	51	12.1	380	32	8.5	400	25	6.2	1525	147	9.6
30,000	317	41	12.9	419	63	15.0	374	42	11.2	397	35	9.1	1507	181	12.0
31,000	219	40	13.7	412	72	17.4	363	47	12.9	389	36	9.3	1455	195	13.4
32,000	284	36	12.7	407	70	17.2	359	46	12.8	386	40	10.4	1436	192	13.4
33,000	274	38	13.9	398	68	17.1	353	46	13.0	383	38	9.8	1408	190	13.5
34,000	263	32	12.2	377	72	19.1	348	50	14.4	375	32	8.5	1363	186	13.7
35,000	255	19	7.5	365	69	18.9	342	51	14.8	362	31	8.5	1324	170	12.8
36,000	226	13	5.8	333	57	17.1	324	44	13.6	344	29	8.4	1227	143	11.7
37,000	207	13	6.3	312	39	12.5	319	41	12.9	334	25	7.5	1172	118	10.1
38,000	186	7	3.8	290	35	12.1	315	42	13.9	324	18	5.6	1115	102	9.1
39,000	161	4	2.5	261	31	11.8	292	30	10.3	312	13	4.1	1026	78	7.6
40,000	129	1	0.8	218	21	9.6	276	35	12.7	300	11	3.7	923	68	7.4
41,000	89	1	1.1	171	16	9.4	231	27	11.7	259	5	1.9	750	49	6.5
42,000	69	1	1.4	140	8	5.5	202	22	10.9	231	1	0.5	642	32	5.0
43,000	57	0	0	105	5	4.8	182	20	11.1	204	0	0	548	25	4.6
44,000	48	0	0	81	3	3.7	151	14	9.3	180	0	0	460	17	3.7
45,000	31	0	0	48	0	0	104	11	10.6	125	0	0	308	11	3.6
Total	4,535	418	9.2	6,462	844	13.1	6,461	679	10.5	6,923	386	5.6	24,381	2,327	9.5

1 F = number of flights reaching respective height.

2 C = number of cases of high cloud reported.

3 % = percentage of flights reporting high cloud.

Underscored values are the maxima.

TABLE A11

High-Cloud Frequency Over Northwestern United States

(Stations: Rapid City, Spokane, Great Falls, Portland, Sands Point, St. Cloud.)

Height	Winter			Spring			Summer			Fall			Year		
	F[1]	C[2]	%[3]	F	C	%	F	C	%	F	C	%	F	C	%
25,000	169	33	20	196	7	4	202	4	1.9	215	4	1.8	782	48	6.1
26,000	164	38	23	194	9	5	201	8	3.9	211	9	4.3	770	64	8.3
27,000	164	40	24	192	12	6	200	15	7.5	210	13	6.2	766	80	10.4
28,000	164	38	23	191	16	8	200	15	7.5	210	17	8.1	765	86	11.2
29,000	161	36	22	190	21	11	198	17	8.6	204	19	9.3	753	93	12.3
30,000	159	35	22	185	19	10	191	14	7.3	199	22	11	734	90	12.3
31,000	152	32	21	182	17	9	191	14	7.3	195	25	13	720	88	12.2
32,000	144	29	20	177	14	8	191	15	7.9	192	24	13	704	82	11.6
33,000	136	26	19	168	14	8	183	18	9.8	186	27	14	673	85	12.6
34,000	127	21	17	161	14	9	182	22	12.1	182	24	13	652	81	12.4
35,000	121	16	13	156	16	10	174	20	11.5	169	18	11	620	70	11.3
36,000	108	13	12	143	12	8	170	15	8.8	159	13	8	580	53	9.1
37,000	98	10	10	136	7	5	165	18	10.9	151	7	4.6	550	42	7.7
38,000	84	8	10	121	3	3	160	15	9.4	144	6	4.2	509	32	6.3
39,000	69	5	7	106	1	1	139	11	7.9	138	3	2.2	452	20	4.4
40,000	52	2	4	79	0	0	102	6	5.9	109	1	0.9	342	10	2.8
41,000	35	1	3	65	0	0	77	5	6.5	80	2	2.5	257	7	2.7
42,000	20	1	5	42	0	0	62	3	4.8	55	1	1.9	179	5	2.8
43,000	18	0	0	33	0	0	50	2	4.0	41	1	2.4	142	3	2.1
44,000	15	0	0	20	0	0	33	0	0	34	0	0	102	0	0
45,000	2	0	0	10	0	0	19	0	0	19	0	0	50	0	0
Total	2,162	384	18	2,747	182	7.2	3,090	237	13.0	3,103	236	7.3	11,102	1,039	9.4

[1] F = number of flights reaching respective height.

[2] C = number of cases of high cloud reported.

[3] % = percentage of flights reporting high cloud.

Underscored values are the maxima.

TABLE A12

High-Cloud Frequency Over Southwestern United States.
December 1954 – November 1955

(Stations: Albuquerque, Long Beach, Oakland, and Tucson.)

Height	Winter			Spring			Summer			Fall			Year		
	F[1]	C[2]	%[3]	F	C	%	F	C	%	F	C	%	F	C	%
25,000	166	10	6.0	203	8	3.9	190	1	0.5	183	1	0.5	742	20	2.7
26,000	165	15	9.1	203	8	3.9	190	4	2.1	182	1	0.6	740	28	3.8
27,000	165	19	11.5	202	10	5.0	190	5	2.6	182	2	1.2	739	36	4.9
28,000	163	17	10.4	202	10	5.0	190	4	2.1	182	3	1.6	737	34	4.6
29,000	163	19	11.7	202	10	5.0	190	4	2.1	182	6	3.3	737	39	5.3
30,000	161	22	13.7	201	15	7.5	190	7	3.7	182	7	3.8	734	51	6.9
31,000	160	25	15.6	201	15	7.5	188	9	4.8	181	7	3.8	730	56	7.7
32,000	159	23	14.5	200	14	7.0	188	10	5.3	180	9	5.0	727	56	7.7
33,000	158	23	14.6	198	14	7.1	188	10	5.3	180	8	4.4	724	55	7.6
34,000	154	19	12.3	196	16	8.2	188	9	5.3	180	6	3.3	718	50	7.0
35,000	151	18	11.9	192	13	6.8	187	7	4.7	174	5	2.9	704	43	6.1
36,000	141	18	12.8	186	13	6.8	185	5	3.6	169	3	1.8	681	39	5.7
37,000	135	12	8.9	182	11	6.0	184	3	2.7	163	2	1.2	664	28	4.2
38,000	127	8	6.3	175	9	5.1	174	3	1.6	160	2	1.3	636	22	3.4
39,000	118	7	5.9	166	8	4.8	171	3	1.7	155	2	1.3	610	20	3.3
40,000	110	8	7.2	146	6	4.1	153	2	1.8	144	0	0	553	16	2.9
41,000	100	4	4.0	127	5	3.9	131	1	1.3	130	0	0	488	10	2.1
42,000	92	3	3.3	116	3	2.6	122	1	0.8	113	0	0	443	7	1.6
43,000	80	1	1.3	105	3	2.9	116	0	0.8	94	0	0	395	4	1.0
44,000	64	0	0	84	3	3.5	99	0	0	76	0	0	323	3	0.9
45,000	39	0	0	45	2	4.4	64	0	0	48	0	0	196	2	1.0
Total	2,771	271	9.8	3,532	196	5.5	3,478	88	2.5	3,240	64	1.9	13,021	619	4.7

[1] F = number of flights reaching respective height.
[2] C = number of cases of high cloud reported.
[3] % = percentage of flights reporting high cloud.
Underscored values are the maxima.

REFERENCES

[1] (Anon), Local Forecast Studies, Holloman AFB, 1943-1954, (on file in Hqs AWS, or available from ASTIA by No. AD 3206).

[2] (Anon), "Cirrus Forecasting," Local Forecast Study, Smoky Hill AAB, circa May 1945, 1 page, typescript, (on file in Hqs AWS or available from ASTIA by No. AD 79124).

[3] (Anon), "Study of Background Radiation and High Altitude Weather," North American Aviation, Inc., NAA Report AL-2084; also issued as WADC Tech. Report 54-581, 101 pp., December 1954, (review of literature). (AD 54347)

[4] (Anon), "Very High Cloud Layer, August 10, 1951," Met. Mag., pp. 365-366, December 1951.

[5] Barrett, E. W., Herndon, L. R. Jr., and Carter, H. J., "Some Measurements of the Distribution of Water Vapor in the Stratosphere," Tellus, Vol. 2, No. 4, pp. 302-311, November 1950.

[6] Barrett, E. W., Herndon, L. R. Jr., and Carter, H. J., "A Preliminary Notion of Measurement of Water Vapor Content in the Middle Stratosphere," Jn. Met., Vol. 6, No. 5, pp. 367-368, October 1949.

[7] Bannon, J. K., "An Analysis of Humidity in the Upper Troposphere and Lower Stratosphere," MRP 563, May 1950. (ASTIA, ATI-88400)

[8] Bannon, J. K., Frith, R., and Shellard, H. C., "Humidity of the Upper Troposphere and Lower Stratosphere Over Southern England," Geophysical Memoirs, No. 88, Met. Off., London, 1952.

[9] Best, A. C., "Ice Accretion in Cirrus Cloud," MRP 730, May 1952.

[10] Brooks, C. F., "A Cloud Cross-Section of a Winter Cyclone," Mo. Wea. Rev., Vol. 48, pp. 26-28, 1920; Cunningham, R. M., "Some Observations of Natural Precipitation Processes," Bull. Amer. Met. Soc., Vol. 32, November 1951, pp. 334-343; University of Arizona, Inst. of Atmos. Physics, Progress Report No. 2, November 1955.

[11] Brooks, C. F., "The Use of Clouds in Forecasting," Compendium of Meteorology, pp. 1167-1178, 1951.

[12] Clodman, J., "The Distribution of Cirriform Cloud," Met. Div., Dept. Transport., Canada, CIR-2737, TEC 227, 10 pp. 3 January 1956; also Mo. Wea. Rev., Feb. 1957, pp. 37-41.

[13] Cole, A. E., "(Uncl) Cloudiness Above 20,000 Feet," AF Surveys In Geophysics, No. 64, AF Cambridge Research Center, January 1955. (SECRET)

[14] Conover, J. H., and Wollaston, S. H., "Cloud Systems of a Winter Cyclone," Jn. Met., Vol. 6, No. 4, pp. 249-260, August 1949.

[15] Day, G. J., "The Occurrence of Ice Crystals in the Free Atmosphere," Met. Mag., Vol. 83, pp. 230-231, August 1954.

[16] Deppermann, C. E., "Cirrus Stripes and Typhoons," Bull. Amer. Met. Soc., Vol. 29, No. 4, pp. 166-174, April 1948.

[17] Dobson, G. M. B., and Brewer, A. W., "Water Vapor in the Upper Air," Compendium of Meteorology, pp. 311-319, 1951.

[18] Durst, C. S., "High-Level Cloud in the Tropics," MRP 727, May 1952.

[19] Dwyer, W. M., and Hannay, A. K., "Cloud Forms Associated With the Jet Stream," Austr. Met. Mag., No. 8, pp. 55-56, 1955.

[20] Endlich, Roy M., "A Study of Vertical Velocities in the Vicinity of Jet Streams," Jn. Met., Vol. 10, No. 6, pp. 407-415, December 1953; Sanders, F., "Relationships Between Vertical Motion and Indicators of Vertical Motion," Sci. Rept. #1, Contract AF 19(604)-1305, 10 pp. M.I.T., September 1951.

[21] Farquharson, J. S., "Cloud in the Stratosphere," Met. Mag., p. 341, November 1952.

[22] Fletcher, R. D., and Sartor, D., "Cirrus," Weatherwise, Vol. 5, No. 1, pp. 8-9, February 1952.

[23] (Fletcher, R. D., and Sartor, D.), "The Cirrus Forecasting Problem," AWS Tech. Rept. 105-81, November 1951.

[24] French, J. E., and Johannessen, K. R., "Forecasting High Clouds from High-Level Constant-Pressure Charts," Proc. Toronto Met. Conf. 1953, pp. 160-171.

[25] Frith, R., "Small-Scale Temperature and Humidity Patterns in the Free Air," MRP 402, 1948.

[26] Frost, Bernard C., "Flying in Jet-Stream Winds," Shell Aviation News, No. 186, December 1953; "More About the Jet Stream," Shell Aviation News, No. 195, pp. 14-18, September 1954.

[27] Gavikian, H., "A Method of Forecasting Cirrus Cloud," in: Forecasting Manual for SAC Operations, Hqs 1st Weather Group, pp. 194-207, September 1955.

[28] Gluckauf, E., "Notes on Upper Air Hygrometry — II. On the Humidity in the Stratosphere," Quart. Jn. Roy. Met., Vol. 71, pp. 110-114, January-April 1945.

[29] Grant, D. R., et al., "High-Level Cloud Photographs," Met. Mag., p. 229, August 1951.

[30] Haurwitz, B., "Insolation in Relation to Cloud Type," Jn. Met., Vol. 5, No. 3, pp. 110-113, June 1948.

[31] Hendrick, R. L., "An Approach to the Problem of Cirrus Cloud Forecasting," Research Rept. SC-3597 (TR), Eng. Res., Sandia Corp., 23 pp. February 1955.

[32] Hosler, C. L., "Ice Crystal Formation," Proc. Toronto Met. Conf. 1953, pp. 253-261.

[33] Howard, L., "On the Modification of Clouds . . .," Phil. Mag., Vol. 16, pp. 97-107, 344-357, 1803; Vol. 17, pp. 5-11, 1803.

[34] Hurst, G. W., "High-Level Cloud Photographs," Met. Mag., pp. 89-91, March 1951.

[35] Jacobs, L., "Dust Cloud in the Stratosphere," Met. Mag., Vol. 83, pp. 115-118, 1954.

[36] James, D. G., "Investigations Relating to Cirrus Cloud," MRP 933, September 1955; Met. Mag., No. 1,015, Vol. 86, pp. 1-12, January 1957.

[37] (Kampe, H. J. aufm), "Condensation and Sublimation in the Upper Troposphere," Translation of report of Deutsche Forschungsanstalt für Segelflug, Ainring, (F.B. Nr. 1491, ZWB), January 1942, available from ASTIA under ATI-10524. (See also ref. [82].)

[38] Kimachi, T., "Study on the Meteorological Elements of High Cloud," Jn. Met. Soc. of Japan, Vol. 30, No. 9, pp. 296-303, 1952. (Japanese, Engl. abstract, Eng. titles to Tables.)

[39] Krebs, H. D., and Doege, W., "Ein Beitrag zum Problem der Cirrusbewölkung," Meteorologische Rundschau, Vol. 9, No. 7-8, pp. 135-138, July-August 1956. (Transl. available in files of Hqs AWS.)

[40] Ludlam, F. H., "The Forms of Ice Clouds," Part I, Quart. Jn. Roy. Met. Soc., Vol. 74, pp. 39-56, January 1948; Part II, id. Vol. 82, pp. 257-265; Discussion, id. . . 127-129, January 1957.

[41] Ludlam, F. H., "The Physics of Ice Clouds and Mixed Clouds," in: Compendium of Meteorology, pp. 192-198, 1951.

[42] Ludlam, F. H., "Orographic Cirrus Clouds," Quart. Jn. Roy. Met. Soc., Vol. 78, pp. 554-562, October 1952; Kuettner, J. P., "Jet-Stream Project," Soaring, Vol. 19, No. 6, pp. 2-6, November-December 1955; Vol. 20, No. 1, January-February 1956.

[43] Malkus, J. S., and Ronne, C., "Concerning the Structure of Some Cumulus Clouds which Penetrate the High Tropical Troposphere," TR 27, Woods Hole Oceanogr. Instn., 1954; Palmer, C. E., "Final Report under Contract No. AF 19(604-546," UCLA, Inst. of Geophysics, 131 pp., June 1956.

[44] Mason, B. J., "The Nature of Ice-Forming Nuclei in the Atmosphere," Quart. Jn. Roy. Met. Soc., Vol. 76, pp. 59-74, January 1950.

[45] Murgatroyd, R. J., and Goldsmith, P., "Cirrus Cloud Over Southern England," MRP 833, September 1953; "High Cloud Over Southern England," Prof. Notes, No. 119, Met. Off., London, 1956.

[46] Murgatroyd, R. J., Goldsmith, P., and Hollings, W. E. H., "Some Recent Measurements of Humidity from Aircraft up to Heights of About 50,000 Feet Over Southern England," Quart. Jn. Roy. Met. Soc., Vol. 81, pp. 533-537, October 1955; Discussion, Id. Vol. 82, pp. 353-355; Helliwell, N. C., Mackenzie, J. K., and Xerley, M. J., "Further Observations. . .," MRP 976, April 1956.

[47] Murray, R., "The Upper Troposphere and Lower Stratosphere: An Examination of Observations Made by the MR Flight, Farnborough," MRP 813, May 1953.

[48] Murray, R., and Daniels, S., "Transverse Flow at Entrance and Exit to Jet Streams," Quart. Jn. Roy. Met. Soc., Vol. 79, pp. 236-241, April 1953.

[49] Palmer, H. P., "Natural Ice-Particle Nuclei," Quart. Jn. Roy. Met. Soc., Vol. 75, pp. 15-22, 1949; Murgatroyd, R. J., and Garrod, M. P., MRP 998, August 1956; University of Arizona, Inst. of Atmos. Physics, Progress Rept. No. 2, November 1955.

[50] Plank, V. G., Atlas, D., and Paulsen, W. H., "The Nature and Detectability of Clouds and Precipitation as Determined by 1.25-cm Radar," Jn. Met., Vol. 12, No. 4, pp. 359-378, August 1955; Boucher, R. J., Wexler, R., and Atlas, D., "Cloud and Precipitation Echoes on the APS-34 Vertical Beam Radar," Proc. 5th Weather Radar Conf., Sig. Corps. Eng. Lab., pp. 165-166, 1957.

[51] Rau, W., "Die Eiskeimbildung bei Temperaturen unter -30°C," Geofisica Pura e Applicata, Vol. 29, pp. 201-211, September-December 1954.

[52] Reed, J., and Flagge, H. J., "Some Aspects of Cirrus Forecasting at Salton Sea Test Base," Report No. SLD-6-29, Sandia Laboratory, 1949.

[53] Saito, S., and Narikawa, J., "Report on Cooperative Observations of High Clouds in West Japan," Jn. of Met. Research, Vol. 6, No. 8, pp. 299-314, November 1954, (Tokyo), (Japanese, with Engl. abstr. and titles to figs.)

[54] Sawyer, J. S., and Illet, B., "The Distribution of Medium and High Cloud Near the Jet Stream," MRP 633, April 1951. (ASTIA, ATI-113149)

[55] Sawyer, J. S., "The Distribution of Medium and High Cloud Near the Jet Stream," Met. Mag., Vol. 80, p. 277, 1951.

[56] Schaefer, V. J., "Cloud Forms of the Jet Stream," Tellus, Vol. 5, No. 1, pp. 27-31, February 1953; Schaefer, V. J., and Hubert, W. E., "A Case Study of Jet Stream Clouds," Tellus, Vol. 7, No. 3, pp. 301-307, August 1955; Barrows, J. S., Schaefer, V. J., and MacCready, "Project Skyfire . . .," Intermountain For. and Range Exp. Sta., Res. Paper No. 35, pp. 25-27, November 1954.

[57] Schwerdtfeger, W., "Über die höhen Wolken," Wissensch. Abhandl. Deutsch. Reichsamt für Wetterd., Vol. V, No. 1, 1938. (Transl. available from ASTIA, AD-64314.)

[58] Shellard, H. E., "Simultaneous Aircraft Soundings of Temperature and Frost Point," Met. Mag., Vol. 79, p. 355, 1950.

[59] Shellard, H. C., "Humidity of the Lower Stratosphere . . .," MRP 486, 1949.

[60] Soulage, G., "Sur la Constitution et l'activité Glacogène des noyeaux de Congélation Atmosphérique," C.R. Acad. Sci. Paris, Vol. 240, No. 22, pp. 2168-2170, June 1, 1955.

[61] Stevens, G. C., Fritz, S., and List, R. J., "Two Halo Displays Over Eastern U. S. in December 1948," Bull. Amer. Met. Soc., Vol. 31, No. 9, pp. 318-321, November 1950.

[62] Süring, R., "Photogrammetrische Wolkenforschung in Potsdam in dem Jahren 1900-1920," Veroff. Preuss. Met. Inst., Abhandlungen, Vol. VII, No. 3, 1922.

[63] Süring, R., Die Wolken, 2d ed., pp. 45, 46, 71, 103-115, Leipzig, 1941.

[64] Swingle, Donald M., "A Review of Operational Tests of Radar Cloud Detection Equipment," Proc. Conf. on Radio Meteorology, November 9-12, 1953, (Bur. Eng. Res., University of Texas, 1953), paper X-4, 2 pp.

[65] Weickmann, H., "The Ice Phase in the Atmosphere," (Translation of "Die Eisphase in der Atmosphäre," Volkenrode R and T, No. 716, February 1947), Roy. Acft. Establ., Farnborough, Library Translation No. 273, 94 pp. plus figs., September 1958, Ministry of Supply, London.

[66] Weickmann, H., "Formen und Bildung atmosphärische Kristalle," Beitr. Phys. der fr. Atmosph., Vol. 28, pp. 12-52, 1945.

[67] World Meteorological Organization, "International Cloud Atlas," 2 Vols., Geneva, 1956.

[68] Baer, F., "The Influence of Illumination on Cirrus Reports," Bull. Amer. Met. Soc., Vol. 37, No. 7, pp. 366-367, September 1956; University of Arizona, Inst. of Atmos. Physics, Progress Report No. 2, November 1955.

[69] Bundgaard, R. C., "Estimating Vorticity Advection," Bull. Amer. Met. Soc., Vol. 37, No. 9, pp. 465-472, November 1956.

[70] (Bundgaard, R. C.), "Forecasting Thunderstorm Icing," Project Track Sheep Techn. Comm. No. 1, 16 pp., July 1953. (Unpubl. MS. in files of Hqs Air Weather Service.)

[71] Endlich, Roy, and McLean, G. S., "Flight Aspects of Jet Streams," (abstract), Bull. Amer. Met. Soc., Vol. 37, No. 10, p. 539, 1956, (full article to appear later in Jn. Met., under title "The Structure of the Jet Stream Core").

[72] Findeisen, W., "Die kolloidmeteorologischen Vorgänge bei der Niederschlagsbildung," Met. Zeit., Vol. 55, No. 3, p. 129, 1938.

[73] Kampe, H. J. Aufm., and Weickman, H., "Particle-Size Distribution in Different Types of Cloud," Proc. 3d Radar-Weather Conf., McGill University, Paper B-9, September 1952.

[74] Moeller, M., "Beiträge zur Kenntnis der atmosphärische Wirbel und ihre Beziehungen zur Cirruswolke," Zeit. der Oesterr. Gesell. f. Met., Vol. 16, 1881, p. 241.

[75] Narayanan, M. V., and Manna, M. P., "Heights of Base of Clouds in India as Determined from Pilot Balloon Ascents," India Met. Dept. Sci. Notes, Vol. 3, No. 25, p. 77 ff., 1931.

[76] Nason, A. H., "A Study of the Formation of Nacreous Clouds," Bull. Amer. Met. Soc., Vol. 33, No. 4, p. 176, April 1952.

[77] Gayikian, H., "Play It by Eye," Combat Crew, Vol. VI, No. 9, pp. 26-29, March 1956.

[78] Stimmel, R. G., "Airplane-Charging Currents in an Active Thunderstorm," WADC Technical Note 56-450, October 1956.

[79] Hoecker, W. H. Jr., "Cloud Systems and Precipitation Processes in Pacific Coast Storms," Mo. Wea. Rev., pp. 425-426, December 1956.

[80] McLean, G. S., "Cloud Distributions in the Vicinity of Jet Streams," to appear in Bull. Amer. Met. Soc.

[81] Atlas, D., "Origin of 'Stalactites' in Precipitation Echoes," Proceedings 5th Radar Weather Conference and 139th National Meeting AMS, 12-15 September 1955, Sig. Corps. Eng. Lab., Ft. Monmouth, New Jersey, October 1956, pp. 321-324.

[82] Kampe, H. J. Aufm., "Humidity Conditions in Cirrus Clouds and Resulting Ice-Crystal Forms," Ber. d. Deut. Wetterd. U.S. Zone, No. 38, pp. 298-302, 1952. (Translation available from ASTIA, AD 119296.)

U. S. GOVERNMENT PRINTING OFFICE: 1957 O - 433736